Florida Institute of Technology
High Tech with a Human Touch™

Proof of Concept for Using Unmanned Aerial Vehicles for High Mast Pole and Bridge Inspections

Final Report

FDOT Contract Number: BDV28 TWO 977-02

Date Completed: June 30, 2015 (Reporting Period: June 2013 - June 2015)

TSER LABORATORY
Transportation Systems Engineering Research

Submitted by:

Luis Daniel Otero, Ph.D.

Florida Institute of Technology, Dept. of Engineering Systems

150 West University Blvd., Melbourne, FL 32901

(321) 674-7173, Email: lotero@fit.edu

Submitted to:

Florida Department of Transportation, Research Center

605 Suwannee St., MS 30, Tallahassee, FL 32399

Program Manager: Richard Kerr, P.E.

Disclaimer

The opinions, findings, and conclusions expressed in this publication are those of the authors and not necessarily those of the State of Florida Department of Transportation. Also, only general conclusions can be made regarding training time estimates for inspectors to safely operate small aerial vehicles due to the small sample size of the testers.

METRIC CONVERSION

SYMBOL	WHEN YOU KNOW	MULTIPLY BY	TO FIND	SYMBOL
LENGTH				
in	inches	25.4	millimeters	mm
ft	feet	0.305	meters	m
yd	yards	0.914	meters	m
mi	miles	1.61	kilometers	km
VOLUME				
fl oz	fluid ounces	29.57	milliliters	mL
gal	gallons	3.785	liters	L
ft^3	cubic feet	0.028	cubic meters	m^3
yd^3	cubic yards	0.765	cubic meters	m^3
NOTE: volumes greater than 1000 L shall be shown in m^3				
MASS				
oz	ounces	28.35	grams	g
lb	pounds	0.454	kilograms	kg
T	short tons (2000 lb)	0.907	megagrams (or "metric ton")	Mg (or "t")
TEMPERATURE (exact degrees)				
^oF	Fahrenheit	5 (F-32)/9 or (F-32)/1.8	Celsius	^oC

Technical Documentation Page

1. Report No.	2. Government Accession No.	3. Recipient's Catalog No.

4. Title and Subtitle	5. Report Date
Proof of Concept for Using Unmanned Aerial Vehicles for High Mast Pole and Bridge Inspections	*June 30, 2015*
	6. Performing Organization Code
7. Author(s) *Luis Daniel Otero, N. Gagliardo, D. Dalli, W-H Huang, and P. Cosentino*	8. Performing Organization Report No.
9. Performing Organization Name and Address *Florida Institute of Technology* *Department of Engineering Systems, College of Engineering* *150 W. University Blvd.* *Melbourne, FL 32901*	10. Work Unit No. (TRAIS) 11. Contract or Grant No. *BDV28-977-02*
12. Sponsoring Agency Name and Address *Florida Department of Transportation* *Research Center* *605 Suwannee Street, MS 30* *Tallahassee, FL 32399*	13. Type of Report and Period Covered *Draft Final Report* *May 2013 – June 2015* 14. Sponsoring Agency Code

15. Supplementary Notes

16. Abstract

Bridges and high mast luminaires (HMLs) are key components of transportation infrastructures. Effective inspection processes are crucial to maintain the structural integrity of these components. The most common approach for inspections is visual examination by trained and experienced inspectors. A proposed approach to assist inspectors during the visual inspection process is to use small unmanned aerial systems (sUAS) equipped with high-definition cameras to transmit video data of structural components in near real time. The use of sUAS as tools for structural inspections can significantly reduce costs and safety risks associated with inspectors and motorists, and improve the effectiveness and accuracy of structural health evaluations. Following a systems engineering approach, a proof-of-concept initial study was conducted to identify system limitations and gain insights into the expected usefulness of sUAS as tools for structural inspections. Extensive indoor controlled experiments using industrial fans were conducted to evaluate sUAS flight response in controlled wind conditions, to measure image quality in different flight scenarios, and to determine image quality in low-light conditions. Altitude, payload, and maneuverability tests were conducted to understand sUAS performance and limitation parameters related to their use for transportation infrastructure inspections. In full coordination with FDOT, limited field tests were conducted to collect image data of underside bridge sections and HMLs. The collected images were of similar quality than those collected by inspectors during previous inspections. In addition, a basic sUAS flight training program was developed, and a preliminary cost analysis was conducted to estimate the cost for using sUAS as tools during inspections. Preliminary results showed potential cost savings in man-hours by using an sUAS approach instead of conventional methods. Overall, results provided evidence that significant benefits can be obtained from using sUAS during bridge and HML inspections. However, there still exist gaps that need to be addressed in order to use these aerial systems safely and effectively in practice. Various future research areas are identified to close these gaps and increase the general understanding of sUAS for structural inspections.

17. Key Word	18. Distribution Statement
Bridge inspections, HML inspections, unmanned aerial systems, transportation systems engineering, sUAS, sUAV	*No restrictions.*

19. Security Classification (of this report)	20. Security Classification (of this page)	21. No. of Pages	22. Price
Unclassified	*Unclassified*	*150*	

Form DOT F 1700.7 (8-72) Reproduction of completed page authorized

Acknowledgements

This major research effort would not have been possible without the guidance and funding support provided by the Florida Department of Transportation (FDOT). In particular, special thanks to the Project Manager, Mr. Richard Kerr, and to the support provided by the following FDOT District 5 individuals: Mr. Chris Eckert, Mr. Ed Kestory, Mr. Ron Meade, Mr. Doug Shockley, Mr. Evan Vanderhoof, Mr. Ron Kneale, and Mr. Walter Loveless.

In addition, the following Florida Institute of Technology individuals contributed in one way or another to the development of this major research effort: Mr. Frank Kinney, Mr. John Politano, Mrs. Carolyn Lockyer, Dr. Muzaffar Shaikh, Ms. Arlene Grant, and Mrs. Judy Tryzbiak. Thank you for your support! Also, special thanks to Mr. Michael Gruenner for conducting some of the field test flight operations.

The contributions from the following Florida Institute of Technology graduate students were essential to this research project:

- Mr. Nicholas Gagliardo – Ph.D. Student in Systems Engineering
- Mr. Dennis Dalli – M.S. Student in Systems Engineering
- Mr. Wei-Hao Huang (Andrei) – M.S. Student in Systems Engineering

Other graduate students that contributed to this research effort to a lesser extent were:

- Mrs. Luz C. Ortega – Ph.D. Student in Systems Engineering
- Mr. Juan Avendano – Ph.D. Student in Systems Engineering

Executive Summary

Bridges and high mast luminaires (HMLs) are key components of transportation infrastructures. Effective inspection processes are crucial to maintain the structural integrity of these components. The most common approach for inspections is visual examination by trained and experienced inspectors. A proposed approach to assist inspectors during the visual inspection process is to use small unmanned aerial systems (sUAS) equipped with high-definition cameras to transmit video data of structural components in near real time. The use of sUAS as tools for structural inspections can significantly reduce costs and safety risks associated with inspectors and motorists, and improve the effectiveness and accuracy of structural health evaluations.

Following a systems engineering approach, a proof-of-concept initial study was conducted to identify system limitations and gain insights into the expected usefulness of sUAS as tools during structural inspections. Extensive indoor controlled experiments using industrial fans were conducted to evaluate sUAS flight response in controlled wind conditions, to measure image quality in different flight scenarios, and to determine image quality in low-light conditions. Results from these experiments provided evidence that support the potential ability to fly sUAS in high pressure zones, maintain safe flying proximity of 2-3 feet to a target, and the ability to detect crack sizes down to 0.02 inches. These findings, coupled with the ability to maintain adequate resolution under relatively low-light conditions, highlighted the high potential to use UAV systems to assist bridge and HML inspectors during field inspections.

Altitude, payload, and maneuverability tests were conducted to understand sUAS performance and limitation parameters related to their use for transportation infrastructure inspections. Altitude testing results showed that first person view (FPV) systems provide a pilot the capability to easily detect sUAV orientation up to at least 400ft vertically and 1,500ft horizontally. These tests also showed that the maximum vertical distance to reliably detect sUAV orientation is significantly limited (250ft for the hexa-copter) if relying only on the UAVs' LED lights. Payload testing results showed that carbon fiber propellers can increase flight time by 10 percent. These tests also resulted in a table that shows maximum flight times as a function of battery type, battery configuration, and payload weight. Maneuverability testing results showed that the sUAS could be properly operated by a skilled operator at a minimum clearance of 3ft from a target and with constant wind speeds of 15mph.

In full coordination with FDOT, limited field tests were conducted to collect image data of HMLs and underside bridge sections. Visual assessments of collected data (i.e., image and videos) by the research team and FDOT inspectors showed the potential benefits from using sUAV systems for structural inspection purposes. Images collected during field tests were of similar or better quality than those collected by FDOT inspectors during previous inspections.

In addition, a basic sUAS flight training program was developed to train inspectors in basic theory, operations, and maneuverability of sUAV systems. Using a base level sUAV with stabilization software, the time that it would take inspectors to safely operate sUAV systems in open space was estimated. Furthermore, a preliminary analysis to estimate the total cost for using sUAS systems during inspections was conducted. The cost parameters considered include operator, equipment, maintenance, repair, and video editing costs. Preliminary results showed potential cost savings in man-hours by using an sUAS approach to conduct visual bridge inspections instead of using conventional methods. These expected cost savings are mainly a function of reduced number of support staff on-site. It is assumed that cost savings from one or two inspections using an sUAS approach will cover initial equipment costs.

Overall, results provided evidence that significant benefits can be obtained from using sUAS during bridge and HML inspections. However, there still exist gaps that need to be addressed in order to use these aerial systems safely and effectively in practice. For example, media news have shown various incidences where malfunctions to sUAV flight controllers have resulted in the aerial systems going rogue and flying off from their operators (i.e., "flyaways"). Although major companies have claimed that this type of problem has been corrected, it should not have happened in the first place. Therefore, research is needed to overcome problems such as flyaways to significantly reduce mission failure risks and ensure public safety. A potential solution would be to develop safety-critical aerial systems for mission-specific applications, relying on robust systems engineering processes to eliminate risks. Other areas for future research include conducting field tests with the developed aerial systems to understand sUAS capabilities –and overall mission dynamics—when using them to collect image/video data of entire bridge spans, and to develop more accurate estimations regarding the duration of complete inspections using an sUAS. Another key area of future work is to develop and conduct mission-specific training programs to collect and analyze data for accurate estimation of training times. Proposed future research areas identified in this report would significantly increase the general understanding of sUAS capabilities and benefits from using them as tools during structural inspections, ultimately converting into reality the vision of using these complex systems for structural inspections.

TABLE OF CONTENTS

TABLE OF FIGURES

LIST OF TABLES

Abbreviations

ASCE	American Society of Civil Engineers
ATC	Air Traffic Control
ATO	Air Traffic Organization
CFI	Certified Flight Instructor
CFR	Code of Federal Regulations
COA	Certificate of Authorization or Waiver
CONOPS	Concept of Operations
CV	Columbia Village
ESC	Electronic Speed Controller
FAA	Federal Aviation Administration
FAR	Federal Aviation Regulations
FDMS	Federal Docket Management System
FPV	First Person View
FSDO	Flight Standards Disctrict Office
HD	High Definition
HML	High Mast Luminaire
HMLP	High Mast Lighting Poles
IFR	Instrument Flight Rules
IR	Infrared
LOA	Letter of Agreement
LiPo	Lithium Polymer
MFT	Maximum Flight Time
MOT	Maintenance of Traffic
MUAV	Micro Unmanned Aerial Vehicle
NAS	National Airspace
NDT	Non-Destructive Testing
NPRM	Notice of Proposed Rulemaking
PIC	Pilot in Command
RC	Radio Control
SAC	Special Airworthiness Certificate
SJ	Slip Joints
sUAS	Small Unmanned Aerial System
sUAV	Small Unmanned Aerial Vehicle
TDGT	Total Data Gathering Time
TSA	Transportation Security Administration
UAS	Unmanned Aerial System
UAV	Unmanned Aerial Vehicle
VLOS	Visual Line-of-Sight
VMC	Visual Meteorogical Conditions
VO	Visual Observer
VTOL or VTAL	Vertical Take-Off and Landing

CHAPTER 1

INTRODUCTION

1.1 OVERVIEW OF PROBLEM STATEMENT

A recent report from the American Society of Civil Engineers (ASCE) highlighted the current critical state of our nation's bridges [1]. This report stated that the average age of the nation's bridges –over 600,000—is 42 years. This statement means that many bridges have surpassed or are approaching their design life. Therefore, it is of critical importance to efficiently and reliably monitor the condition of our nation's bridges.

Researchers and practitioners agree that the most common approach for bridge inspections is visual examination by trained and experienced inspectors [2]. Although often complemented with other non-destructing testing (NDT) approaches, visual inspections have long been used as the primary technique to assess the structural health of bridges [3]. State agencies rely on these visual inspections to make key decisions about the health of structures–such as allocation of human resources and funds to maintain\repair structures—that significantly affect public safety and costs. For example, a study presented by the Michigan Department of Transportation described significant cost benefits achieved from various visual inspections of high mast luminaires (HML) that led to the creation of effective maintenance actions instead of the replacement of defective HML [4].

Preliminary research efforts at Florida Institute of Technology led to proposing a complex small unmanned aerial system (sUAS) that could potentially help inspectors during bridge and HML inspections. The envisioned system is composed of a small unmanned aerial vehicle (sUAV) system with a camera attached to it that will transmit near-real time images of a structure during an inspection. The objective of the sUAS is to assist structural inspectors during the visual inspection process. The use of sUAS as tools for structural inspections can significantly reduce costs, reduce safety risks associated with inspectors and motorists, and improve the effectiveness and accuracy of structural health evaluations.

As part of a robust systems engineering process, it was critical to conduct a proof-of-concept initial study to identify potential system limitations in order to develop an understanding of the expected usefulness of the system prior to incurring in additional costs (e.g., software development efforts). This proof of concept constituted the scope of this research project. Eventually, sensors and other equipment can be attached to a UAV platform to obtain various types of data; however, the visual inspection activity is currently an irreplaceable tool for structural inspections. The envisioned system would require software development activities related to image data transmission and the construction of server-side code for data management.

1.2 MOTIVATION FOR RESEARCH

The motivation to pursue this research effort resulted from three key factors. The first factor was related to the principal investigator's experience with UAS applications in both industry and academia. His experience includes large-scale UAS applications as a software/systems engineer for major defense corporations, and exposure to the development of complex sUAV systems for academic research purposes.

The second factor was related to the significant positive impact to society that can be gained from adopting a "continuous improvement" mentality to conduct applied research that relates the Systems Engineering field with processes to conduct structural/bridge inspections. Interactions between these two areas to develop/use complex sUAV systems for structural inspections are expected to produce fascinating results in terms of reducing inspection durations, improving safety of inspectors, and eliminating lane closures during routine inspections.

The third motivational factor was related to information provided by various news articles and reports (e.g., [5]) regarding the detrimental health of bridges, which highlighted the critical importance of routine bridge inspections. A preliminary review of the literature, as well as discussions with bridge inspectors and managers, made it clear that improving the visual inspection process could potentially result in significant positive value to society. These discussions and literature review effort ultimately led to the idea of using sUAV systems to assist bridge inspectors during the inspection process.

1.3 MAIN RESEARCH OBJECTIVE

The development of a complex aerial system to effectively and safely assist inspectors during the inspection process of bridge and HML structures is a major endeavor that must be carried out under a robust systems engineering process. The idea is to utilize proven systems engineering techniques and approaches to ensure the development of systems that adhere to quantifiable requirements –through a requirements engineering phase—and minimize risks. With this in mind, the main objective of this research project was to conduct a proof-of-concept initial study to identify potential system limitations in order to develop an understanding of the expected usefulness of the system prior to incurring in additional costs (e.g., software development efforts).

1.4 ORGANIZATION OF REPORT

This report is organized into 13 chapters. Chapter 2 presents a summary of literature review findings related to the use of small aerial systems for structural inspections. Chapter 3 presents federal requirements and guidelines to safely operate aerial systems in national airspace (NAS). Chapter 4 presents the systematic decision-making process followed to select key equipment and subsystems to carry out research tasks. Chapter 5 presents an initial demonstration to showcase the selected equipment. Chapters 6 and 7 present various controlled indoor experiments to understand system limitations. Examples include image quality tests under different vibration frequencies and low light scenarios. Chapters 8 and 9 present results from gathering image data from various structures and understanding the usefulness of such data for inspection purposes. Chapter 10 presents key maintenance procedures. Chapters 11 and 12 present experiments to estimate operator training times, and analyses to estimate inspection costs, respectively. Chapter 13 provides conclusions and future research areas.

CHAPTER 2

SUMMARY OF LITERATURE REVIEW FINDINGS

2.1 INTRODUCTION AND OBJECTIVES

Research related to the use of sUAS for structural inspections is relatively limited. This chapter presents a summary of the results obtained from a literature review effort that involved UAV platforms for structural inspections, UAV aircraft control, and different camera configurations. The following sections present a description of the general research method to conduct the literature review, followed by a description of key studies and a summary of findings.

2.2 RESEARCH METHOD

Following the guidelines proposed by [6], the literature review was structured into the following three stages: planning, conducting, and reporting. Based on these guidelines and the objective described in the introduction, research questions were developed along with a procedure to conduct a literature search to address them. The following research questions formed the basis for the literature review:

- **RQ1:** What are the potential benefits that the proposed system can provide to structural inspectors?
    - **Sub-question_RQ1-1:** What are the limitations of techniques currently used in practice for structural inspections of bridges and HML poles?
    - **Sub-question_RQ1-2:** What are the strengths and weaknesses of documented studies that employed similar systems (i.e., UAVs with attached cameras) to gather data for structural inspections (or for other goals that required high-definition images)?
    - **Sub-question_RQ1-3:** What logical correlation, if any, can be established between the results from documented studies (from Sub-question_RQ1-2) and the potential usefulness of the UAV system for bridge and HML inspections?
- **RQ2:** What is the current state of UAV aircraft control research?
- **RQ3:** What is the current state of research related to camera types and configurations that can be attached to small-scale UAVs for structural inspections?

Following a systematic literature review approach, the scope of the literature review effort was limited to research that involved UAV systems for structural inspections. Research studies that did not fit this general criterion were excluded from the literature review analysis. Examples of excluded topics are:

- Robotic approaches for structural inspections that did not involve UAVs
- Image processing and enhancement approaches for structural inspections

In addition, the research team only included relevant technical reports, academic conference papers, and journal papers. Information from sources such as newspaper articles and personal websites were excluded from the literature review effort.

2.3 UAV SYSTEMS FOR SURFACE STRUCTURAL INSPECTIONS

Table 2-1 presents a list of relevant studies related to the use of UAVs for monitoring or inspecting elements of transportation systems. This table shows a significant amount of studies related to understanding the capabilities and feasibility of using UAV systems for traffic monitoring and surveillance applications. However, *studies that involve UAVs for the specific purpose of bridge inspections are very scarce*, *and for inspection of HML are nonexistent*.

In [7], the authors described the design and implementation of an aerial bridge inspection system. The system consisted of a double helix ducted fan remote control aircraft (see Figure 2-1). The ducted fan approach not only served as a safe guard against collisions, but also slightly increased the aircraft's lift capacity. The aircraft was equipped with sensors and cameras for navigation and visual inspection purposes. The system design included structural shields –mostly composed of fiberglass—that gave the system the ability to be in close proximity with the structures being inspected. The main strength of this UAV system was that the ducted fans provided directional thrust as well as protection against nearby objects. A major design drawback of this system was that it required a power cord attached to the UAV for transferring of controls and electricity, which limited its applicability to only short-span bridge inspections. This design issue is a significant drawback given that inspection practices for long-span bridges often require the use of heavy machinery during bridge inspections, which involve maintenance of traffic (MOT) procedures that produce lengthy traffic interruptions and high costs. The results from this research project highlighted the need for a wireless UAV system for bridge inspections.

In [8], the authors described the potential benefits from using UAV systems to accurately define and monitor various highway issues using high-resolution imagery. Some of the key benefits from using UAV systems are fast collection of high definition images and the relatively small cost of acquiring images, thus making it possible to collect images on a regular short-term basis. The autonomous aerial aircraft used in this research is called AggieAir. This UAV is guided by satellite, follows a predetermined course, launches using a bungee (see Figure 2-2), and glides to the ground for a skid landing. A key objective of this research was to investigate the capability of the UAV system to monitor a highway construction project from its initial to completion phases. The authors concluded that many applications can potentially benefit from the relatively quick process of collecting and making images accessible for viewing. Examples of such applications include road construction and road damage, and inventorying roadway structures. The authors also concluded that the UAV system would be particularly beneficial for tasks that require immediate aerial images of roadways (e.g., roadways that are under construction). Furthermore, the authors stated that updating aerial images regularly on GIS databases could improve transportation-related decision-making. Finally, the authors emphasized on the potential cost savings that can be realized with effective image post-processing algorithms for classification.

Table 2-1 Relevant Work Using UAV Systems for Monitoring/Inspecting Transportation Systems

Title	Application	Reference
CALTRANS Bridge Inspection Aerial Robot	Bridge inspections	[7]
Evaluation and development of unmanned aircraft (UAV) for UDOT Needs	Monitoring state roadway structures	[8]
Use of Micro Unmanned Aerial Vehicles for Roadside Condition Assessment	Collect data for roadside infrastructure assets	[9]
The Use of Small Unmanned Aircraft by the Washington State Department of Transportation	Aerial roadway surveillance and avalanche control	[10]
Surface Transportation Surveillance from Unmanned Aerial Vehicles	Monitor freeway conditions, track vehicle movements, observe roadway network conditions, and monitor parking lot utilization	[11]
Use of Unmanned Aerial Vehicles in Traffic Surveillance and Traffic Management	Traffic monitoring	[12]
Lessons Learned: Application of Small UAV for Urban Highway Traffic Monitoring	Traffic Monitoring	[13]
A Survey of Unmanned Aerial Vehicles (UAVs) for Traffic Monitoring	Traffic monitoring	[14]
Statistical Profile Generation for Traffic Monitoring Using Real-Time UAV Based Video Data	Traffic monitoring	[15]
From Images to Traffic Behavior - A UAV Tracking and Monitoring Application	Traffic monitoring	[16]
Detecting and Counting Vehicles from Small Low-Cost UAV Images	Traffic monitoring	[17]
Quadcopter with Heterogeneous Sensors for Autonomous Bridge Inspection	Develop autonomous bridge inspection system	[18]
Develop a UAV Platform for Automated Bridge Inspection	Develop autonomous bridge inspection system	[19]
Evaluating the Use of Unmanned Aerial Vehicles for Transportation Purposes	Visual inspections of roadway assets; Traffic monitoring; LiDAR sensor for inspection of infrastructures; NDT on UAV platform for bridge inspections	[20]
Use of Unmanned Aerial Vehicles for AHTD Applications	Data collection for vehicle counts and vehicle classification	[21]

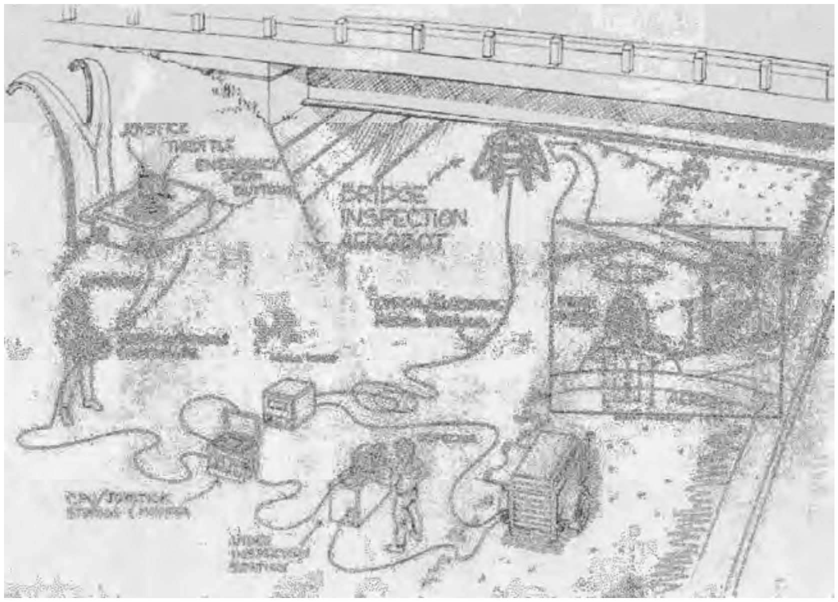

Figure 2-1 Schematic of Ducted Fan Inspection System [6]

Figure 2-2 AggieAir Aircraft[1]

In [9], the authors investigated the effectiveness of micro-UAVs (MUAVs) for collecting image data of roadside infrastructure assets. Three main conclusions were presented based on the results from three field experiments at different locations. First, wind was found to be the most restrictive weather condition. High quality images were constantly obtained during 0-5 mile per hour (mph) wind speeds. Wind speeds above 15 mph made the aircraft not operational. Second, when using the UAV system over rural highways or local streets with wind speeds of less than 10 mph, the condition ratings produced by the UAV system rater were matched to those assigned by field raters 84 percent of the time. Third, when using the UAV system over urban highways with wind speeds above 10 mph, the images produced by the UAV system were of low quality due to difficulty in operating the aerial vehicle. Overall, in low traffic volume and low wind speed conditions, the UAV system produced accurate results faster and arguably safer than conventional methods. The authors concluded with recommendations for future areas of research. One such area included investigating the applicability of using a UAV system to identify roadway segments that require detailed on-site investigation. Another area of future research was to

[1] Image source: http://www.suasnews.com/2012/04/14577/the-aggie-air-flying-circus/

further investigate possible relationships between flight altitude and image quality. Furthermore, the authors mentioned that research is needed to evaluate live data feed capabilities.

In [10], the authors evaluated the general capabilities of UAV systems as avalanche control tools on mountain slopes above highways. The researchers also evaluated the use of aerial systems to obtain images for traffic surveillance and data collection. The research team conducted two flight tests. For the first test, the team used a fixed wing aircraft known as BAT (see Figure 2-3). One of the objectives of this test was to evaluate the capability of this aircraft system to provide high-quality video data of roadways. The results were successful. The system was able to capture clear video roadway images, and individual vehicles were easily identified along the roadway. For the second test, the research team used a vertical takeoff and landing (VTOL) UAV. The researchers concluded that the UAV system was successful in flying along a road center-line to obtain clear images of traffic conditions. The authors also concluded that the system was very effective in supplementing routine avalanche control operations. Similar to [9], the authors found that the ability to control the aerial vehicles during bad weather conditions was a major issue. However, the main issue identified in this study was the lengthy process to obtain approval by the Federal Aviation Administration (FAA) to fly UAVs.

Figure 2-3 BAT UAV[2]

The process of obtaining FAA approval to fly UAVs in transited areas has been a major issue identified by various studies. For example, [11] conducted field experiments with UAV systems to monitor freeway conditions, track vehicle movements, and monitor parking lot utilization. The authors found strong indications that the use of aerial vehicles for such applications was effective and valuable, but key obstacles were the restrictive FAA guidelines. In another study, [12] investigated the capability of UAV systems for data collection, as well as for traffic and incident management. The authors concluded that UAVs provided a cost effective solution for traffic data collection and analysis, but that FAA regulations were a major restriction in making UAV systems effective tools for traffic management. In [13], the authors described key lessons learned from experimenting with a UAV system for urban highway traffic monitoring. The authors concluded that UAV systems were capable of providing real-time traffic data effectively, but FAA regulations posed a serious impediment for using UAV systems for these types of applications. A year later, [10] arrived at the same conclusion regarding FAA approval issues while experimenting with flying UAV systems near highways.

Most of the studies found in the literature dealt with the use of UAV systems for traffic monitoring applications. A very recent study presented the results of a literature review effort related to applications of UAV systems for traffic monitoring [14]. The scope of the review effort included research activities

[2] Image source: http://www.holdentechnology.com/autonomous/airvehicles.html

from academia and research centers. The researchers found that wireless connectivity and maneuverability are the most significant parameters that make UAVs more useful than other existing methods. The study also found that there is an ongoing strong research focus on application of different types of sensors (e.g., vision) and processing of incoming sensor data (in particular data coming from vision sensors). For example, [15] converted real-time visual data from a UAV system into traffic statistical profiles that were fed to existing traffic simulation models. The traffic profiles improved the calibration, accuracy, and traffic predictions of the models. In [16], the authors evaluated a system that processes image data to recognize traffic behavior of tracked vehicles in real-time. The research by [17] presented a vision-based algorithm to process data from a UAV system to detect and count vehicles. In [18] and [19], researchers developed a prototype quadcopter platform with hopes to expand it into an automated bridge inspection system for remote bridge inspections. In [20], researchers evaluated various of-the-shelve sUAV systems for bridge deck assessments, traffic monitoring, roadway asset detection, LiDAR and thermal data processing, and inspection in confined spaces (e.g., such as culverts and sub-pump stations). The study recommended the following areas for future sUAV research: traffic monitoring, crash scene imaging, slope stability assessment, aerial imaging for surveying, optimal methods to store and share UAV datasets, improved thermal imaging, and higher accuracy UAV positioning sensors. When evaluating the sUAV systems during bridge inspections, none of the aerial systems were flown within bays (i.e., between girders) because of the limited resolution and lack of detail obtained from the sUAV systems used.

The literature also described various relevant ongoing studies related to the use of UAVs for monitoring or inspecting elements of transportation systems. These ongoing studies show that there continues to be research interest in understanding the capabilities of UAV systems for traffic monitoring and structural visual inspections. For example, researchers in [21] are investigating the potential use for UAV systems to collect data related to vehicle counts, headway, queues, vehicle classification, and VisSim modeling calibration.

2.4 UAV AIRCRAFT CONTROL

Autonomous navigation of UAV systems is an active research area for transportation applications such as traffic monitoring and structural inspections (e.g., [19]). In [22], the authors presented a new approach for automatic navigation of a UAV near 3D structures. The researchers described how a UAV autopilot can be programmed to navigate using images from an optical camera as reference points. The authors described an algorithm that allows an autopilot to extract valuable location information from an image by means of analyzing the image saturation. The authors developed a dynamic model of the UAV hovering controls. Based on this mathematical model, vector forces and torques needed to control a UAV in hovering mode can be predicted. Using image data from a camera, analyses to obtain a UAV's position relative to obstacles can be developed. The UAV used in this research was a single-rotor helicopter (see Figure 2-4).

Another research area involves the use of optical data for UAV navigation. For example, the research presented in [23] describes the use of a UAV equipped with optical sensors to track a contour of a river during flight. This research considered real time image data processing by means of image saturation. The authors used predictive algorithms to estimate the upcoming contours of a river. After these data were processed, control algorithms were used to determine the necessary control inputs to guide the UAV along the detected contour of the river. A similar approach could be employed to program a UAV system to track the contour of concrete structures; therefore, following an autonomous search pattern and potentially eliminating navigational tasks from system operators.

Figure 2-4 Image Navigation System, Single Rotor Helicopter [22]

The study in [24] presented an approach based on control algorithms to improve the stability of a UAV during flight. The authors generated an analytical model of the hovering inputs and outputs of a UAV with different payloads, which allowed the prediction of parameters necessary to compensate for the weight in the aircraft controllers.

An interesting technique that could be applied for controlling a UAV over large distances was presented in [25]. The authors describe the development of an internet-based solution to the control and operation of aerial vehicles. Although not tested, the idea is to use global telecommunications and mobile internet devices for operators to control a UAV from remote locations. This approach could potentially allow longer distances between UAVs and their control system.

Although the literature presents various innovative techniques to improve the navigation and control of UAV systems, there are many commercially available UAV systems with built-in control algorithms that are suitable for various transportation related applications. These are typically open-source devices, which mean that their existing control algorithms can be upgraded relatively easy.

2.5 CAMERA CONFIGURATIONS

Although most of the research studies described in the previous sections of this document include optical cameras for image data collection, there are other studies that investigate with different types of cameras or techniques involving optical devices. For example, in [26] the authors described a UAV system equipped with a hyper-spectral camera to collect images of crop fields, and then used the obtained data to map different crop characteristics. This type of camera allows the identification of different features of a target such as heat signals, reflectivity, and humidity. Another example involves the use of interferometry [27], which involves taking a series of still camera shots of an object of interest with various light projections. These images go through a series of analyses to convert them into 3D maps. This method is lengthy and requires a high level of understanding of the methodology and equipment used.

2.6 SUMMARY OF FINDINGS

Following is a list of key findings that resulted from the literature review effort:

- The majority of studies related to understanding the capabilities and feasibility of using UAV systems for transportation systems are in the area of traffic monitoring.
- Studies that involve UAVs for the specific purpose of bridge inspections are very scarce, and for inspection of HML are nonexistent. This presents an opportunity to investigate the use of UAV systems for bridge and HML inspections.
- A common issue for using UAV systems in transportation applications was the ability to control the aerial vehicles, particularly in wind speeds higher than 15mph. This presents an opportunity to develop more effective approaches to UAV control and navigation.
- The process of obtaining FAA approval to fly UAVs in transited areas has been a major issue identified by various studies.
- Wireless connectivity and maneuverability are arguably the most significant parameters that make UAVs more useful than other existing methods. This presents an opportunity to better understand the maneuverability of UAV systems in other applications such as bridge inspection.
- There is high potential for cost savings in using effective image post-processing algorithms for classification. This presents an opportunity to apply image processing techniques for post data analyses.

Some of the items in the list above also represent unique opportunities for future investigation. In addition, the literature mentions that a potential key use for UAV technology is being able to collect extensive image data to inventory and classify highway (or transportation related) features. However, there is a lack of studies that experiment with UAV systems to actually collect and inventory such data. Therefore, there is a need for studies to collect image data from UAV systems and develop libraries that can eventually be used for post analyses via image processing algorithms. There is also a need to develop database applications for image data storage and management. Another potential limitation for transportation agencies is uncertainty about the reliability of UAV systems related to the costs of equipment replacement and the consequences of a crash, which present an opportunity to conduct reliability and cost estimation studies. Another opportunity for future research is to investigate possible relationships between flight altitude and image quality.

CHAPTER 3

INVESTIGATING LEGAL CONSIDERATIONS

3.1 INTRODUCTION

One of the tasks of this research project was to compile and evaluate relevant FAA rules and regulations regarding operations of sUAV systems for structural inspections of bridges and HML. FAA regulations for operating UAS in the National Airspace System (NAS) depend on the type of UAS operations (i.e., civil, public, or model aircraft). This chapter provides information on FAA regulations regarding public and civil operations. The chapter also provides information regarding sUAV operations around bird nests.

This document applies mainly to public UAS operations, given that UAS operations under the Florida Department of Transportation (FDOT) are classified as "public" according to the following definition provided in Title 14 of the Code of Federal Regulations (CFR) Section 1.1 [28]:

> "*Public aircraft means any of the following aircraft when not being used for a commercial purpose or to carry an individual other than a crewmember or qualified non-crewmember:*
>
> - *an aircraft used only for the United States Government;*
> - *an aircraft owned by the Government and operated by any person for purposes related to crew training, equipment development, or demonstration;*
> - *an aircraft owned and operated by the government of a State, the District of Columbia, or a territory or possession of the United States or a political subdivision of one of these governments;*
> - *an aircraft exclusively leased for at least 90 continuous days by the government of a State, the District of Columbia, or a territory or possession of the United States or a political subdivision of one of these governments.*"

Examples of public entities are Department of Defense and its military branches; other local, state, and federal government agencies; and state universities. The following regulations and documents are relevant concerning UAS operations for public entities:

- FAA JO 7610.4 [29]
- FAA UAPO Interim Operational Approval Guidance 08-01 [30]
- Federal Registry Entry "FAA-2006-25714" [31]
- FAA Order 8130.34 [32]

For public UAS operations, it is required to have a registered UAV and a Certificate of Authorization or Waiver (COA) to describe the operation of a particular UAS for a particular purpose and in a specific area. UAS public operations must also abide to several operational requirements. Figure 3-1 provides an overview of the three major requirement areas specified by the FAA for public UAS operations in NAS. The following sections provide a description of each of these three areas.

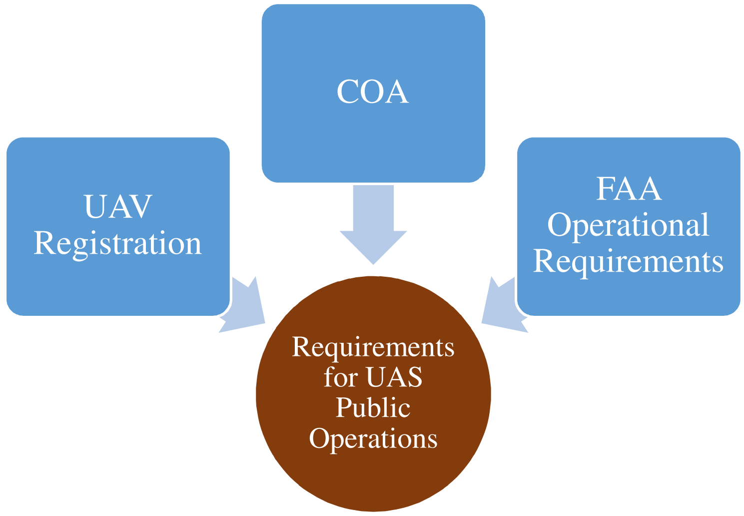

Figure 3-1 Overview of Requirements for UAS Public Operations

3.2 AIRCRAFT REGISTRATION

The FAA requires that UASs be registered prior to COA application [34]. Title 49 of U.S. Code Section 44101-44104 prohibits the operation of unregistered aircrafts for public operations and establishes the requirements for aircraft registration.

There are three main items required to successfully register a UAS. The first item required is a registration number, also known as N-Number because all aircraft registration numbers are prefixed by the letter "N". The registration number is an alphanumeric string composed of six symbols. The last two symbols may be alphabetical. The lowest possible number is N1, and a zero never precedes the first number. The following rules constitute acceptable N-Numbers:

- N1 through N99999, all symbols are numeric
- N1A through N9999Z, single alphabetical suffix
- N1AA through N999ZZ, double alphabetical suffix
- N1 to N99 are reserved for FAA internal use

If available, a registration number may be reserved for one year by using the FAA online N-number reservation request application. There is no reservation fee for government offices (a $10.00 reservation fee only applies to civil entities).

The second item required is an original Aircraft Registration Application form (AC Form 8050-1). Figure 3-2 shows a snapshot of the registration form. An original registration application form is required per aircraft (i.e., photocopies or computer generated copies of this form are not acceptable). Aircraft registration applications may be obtained from the Aircraft Registration Branch or a local FAA Flight Standards District Office (FSDO).

The third item required is evidence of ownership such as a bill of sale or affidavit of ownership. This document must be submitted to the Aircraft Registration Branch (AFS-750). The purchaser under a contract of conditional sale is considered the owner for the purpose of registration.

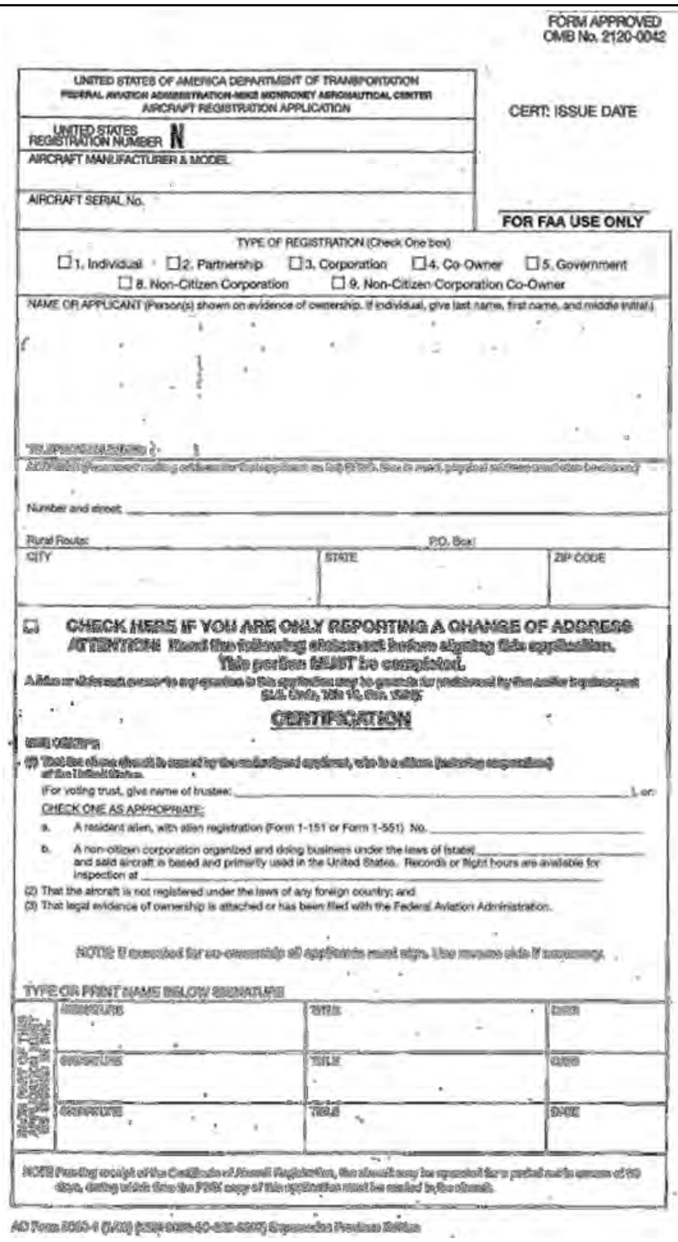

FORM APPROVED
OMB No. 2120-0042

UNITED STATES OF AMERICA DEPARTMENT OF TRANSPORTATION
FEDERAL AVIATION ADMINISTRATION-MIKE MONRONEY AERONAUTICAL CENTER
AIRCRAFT REGISTRATION APPLICATION

CERT. ISSUE DATE

UNITED STATES REGISTRATION NUMBER N

AIRCRAFT MANUFACTURER & MODEL

AIRCRAFT SERIAL No.

FOR FAA USE ONLY

TYPE OF REGISTRATION (Check One box)

☐ 1. Individual ☐ 2. Partnership ☐ 3. Corporation ☐ 4. Co-Owner ☐ 5. Government
☐ 8. Non-Citizen Corporation ☐ 9. Non-Citizen Corporation Co-Owner

NAME OF APPLICANT (Person(s) shown on evidence of ownership. If individual, give last name, first name, and middle initial.)

Number and street:

Rural Route: P.O. Box:

CITY	STATE	ZIP CODE

☐ CHECK HERE IF YOU ARE ONLY REPORTING A CHANGE OF ADDRESS

CERTIFICATION

(For voting trust, give name of trustee:), or:

CHECK ONE AS APPROPRIATE:

a. A resident alien, with alien registration (Form 1-151 or Form 1-551) No.

b. A non-citizen corporation organized and doing business under the laws of (state) and said aircraft is based and primarily used in the United States. Records or flight hours are available for inspection at

(2) That the aircraft is not registered under the laws of any foreign country; and
(3) That legal evidence of ownership is attached or has been filed with the Federal Aviation Administration.

TYPE OR PRINT NAME BELOW SIGNATURE

SIGNATURE	TITLE	DATE
SIGNATURE	TITLE	DATE
SIGNATURE	TITLE	DATE

Figure 3-2 Example of AC-8050-1 Form

An application for aircraft registration must be signed by the applicant, and include the typed/printed name of the applicant. Applications that do not include the printed or typed name of the signer will not be processed. A $5.00 registration fee payable to the FAA is required. Table 3-1 shows mailing addresses for completed applications.

3.3 Public COA General Information

A COA allows a public entity to safely use a defined block of airspace for a particular purpose. This permission to operate within the NAS may include restrictions such as flying only under visual flight rules (VFR) and only during daylight hours. Current UAS technology cannot fully comply with "see and avoid" rules that apply to all aircrafts; therefore, a visual *observer* (VO) or an accompanying "chase plane" must maintain visual contact with the UAS at all times. An observer must have unobstructed and direct line-of-sight to the UAS.

Table 3-1 Aircraft Registration Branch Mailing Addresses

U.S. Postal Service, Regular and Priority Mail:	Commercial Delivery Services:
FAA Aircraft Registration Branch, AFS-750 P.O. Box 25504 Oklahoma City, OK 73125-0504	FAA Aircraft Registration Branch, AFS-750 Registry Building Room 118 6425 South Denning Oklahoma City, OK 73169-6937

The objective of the FAA is to issue COAs with parameters that ensure levels of safety equivalent to manned aircrafts [35]. Typically, this entails not operating a registered *UAS* over populated areas and having an observer present during entire flight durations.

The FAA offers an online process for COA applications. During this process, the FAA conducts comprehensive operational and technical reviews. Provisions or limitations may be imposed by the FAA as part of the approval process to ensure that a UAS can operate safely with other users of the NAS. Following is a list of information that applicants are typically required to submit:

- Concept of Operations (CONOPS) or type of missions
- Launch/recovery/operation location(s)
- Operational altitudes
- Flight procedures
- Communications
- Emergency procedures, such as lost communication and training requirements
- Pilot in command (PIC), flight crew, and observer qualifications and training requirements

COAs are typically issued for up to two years. The FAA retains the full right to terminate a COA or limit its use if there are violations to the COA's terms and conditions. The COA process for public entities requires two steps: setting up an online account and filling out the COA application. The following subsections describe each component of the COA process.

3.3.1 Set up an Online Account

The COA application process is available online to streamline the process. An account is required to access the application system. To set up an account, applicants need to contact FAA's support desk by phone (201-580-7500) or email (oeaaa_helpdesk@cghtech.com) to provide required information such as [36]:

- Address and contact information
- Name and manufacturer of the UAS technology being considered
- Purpose for using the UAS technology (Concept of Operations)
- Level of aviation experience of the proponent (e.g., Does any member of the proponent organization holds a private or advanced FAA pilot certificate or an FAA Airman Medical Certificate?)

- Will the proponent be developing the UAS program “in house” or utilizing a third party to develop and/or implement its UAS program?
- A “declaration letter” from the Law Enforcement Agency’s (LEA) County or State Attorney General formally acknowledging that the proponent is recognized as a subdivision of the government of the State under Title 49 of the United States Code (USC) Section 40102 (a) 40141 (c) or (d) and that the proponent will operate its Unmanned Aircraft in accordance with 49 USC Section 40125 (b) (not for commercial purposes)

Once an account has been established, a public entity can move forward to complete the COA online application.

3.3.2 COA APPLICATION

The COA application process requires specific information regarding the aircraft to be used, the intended operator, and operation logistics (see Table 3-2). “The typical COA application approval process is completed within 60 days of receipt, provided there are no submittal errors, missing information, or safety or airspace issues” [35]. Released samples from current COA holders are available from FAA’s website [37].

The COA application requires the applicant to show that the aircraft to be used is airworthy. Airworthiness can be achieved either through FAA’s Certificate of Airworthiness process or by submitting an Airworthiness Statement. Examples of public entities that do not have an FAA Certificate of Airworthiness in their COA application are Cornell University, Miami-Dade Police Department and Texas Department of Public Safety [38].

3.4 FAA OPERATIONAL REQUIREMENTS FOR UAS

In order to obtain a COA, applicants must comply with all the rules and regulations established by the FAA. This section provides a summary of the necessary policies regarding safety evaluation and interoperability of UAS flight operations. The information is based on FAA UAPO “Interim Operational Approval Guidance 08-01” [30].

The FAA requires all aircrafts to operate safely and in harmony among all users of the NAS, including non-cooperative aircrafts (e.g., aircraft operated without a transponder), and other airborne operations not reliably identified by ATC radar (e.g., balloons, gliders, parachutists). Unless otherwise specifically authorized, any UAS must have a ground or airborne visual observer during flight. Of significant importance to the FAA is that any UAS flying in NAS must comply with the “see and avoid” procedures, as prescribed in Title 14 CFR Section 91.113. Risk mitigation for this issue is often achieved by using visual observers. Any other “see and avoid” strategies that do not rely on visual observers must provide system safety studies (i.e., hazard analysis, risk assessment, and level of risk documentation). The following subsections describe a set of guidelines for UAS operations.

Table 3-2 Procedural Requirements to Obtain a COA [37]

No.	Requirements for COA Application
1	Proponent Information
2	Point of Contact Information
3	Operational Description • Brief description of the program objectives and operational summary
4	Systems Description • Aircraft description, control station description, communication systems description, certified TSO components, image of the aircraft
5	Performance Characteristics • Cruise speed, operating altitudes, climb rate, descent rate, turn rate and launch/recovery procedure
6	Airworthiness • FAA certificate • Statement from proponent
7	Procedures • Applicant must include lost link/mission procedures, lost communication procedures and emergency procedures
8	Avionics/Equipment • Applicant must specify each UAS component
9	Lights • Applicant must indicate if the UAS have the following lights: landing, position/navigation, anti-collision and infrared (IR)
10	Spectrum Analysis Approval • Applicant must submit documents regarding the data link, control link, and operations utilizing radio control (RC) frequencies
11	Air Traffic Control (ATC) Communications • Transmitter/Receiver
12	Electronic Surveillance/Detection Capability
13	Visual Surveillance/Detection Capability
14	Aircraft Performance Recording
15	Flight Operations Area/Plan • The proposed areas must be plotted on an aeronautical chart, topographical map, or satellite image. The applicant must include latitude and longitude coordinates that identify the corners of the airspace boundary, the length of each side of the boundary, and the operating altitude
16	Flight Aircrew Qualifications
17	Special Circumstances
18	Preview Case
19	COA Status History

3.4.1 AIRSPACE CLASSES AND CONSIDERATIONS

Airspace is divided by classes according to Title 14 of the Code of Federal Regulations (14 CFR), Section 91. Regulations associated with different classes may vary depending on location. These classes are usually tailored to the needs of the airport and surrounding area. Hence, ceiling and radius rules may be different in various airports and zones. Descriptions for each class of airspace are outlined in Table 3-3.

Table 3-3 Airspace Classes

Class	Description
Class A	• Flight level of 18,000 to 60,000 feet • Filing of Instrument Flight Rules (IFR) Flight Plan • VOs are not required for this airspace class

Class B	• Surface to 10,000 feet
	• Radiuses vary per airport
	• Due to large amount of manned vehicles, UAS operations are not permitted
	• Operators can apply for special operations
	  o Public applicants must apply for Letter of Agreement (LOA)
	  o Civil applicants must state all segregation procedures into the operating limitations

Class C	• 4,000 feet above airport elevation • Radiuses vary per airport • Segregations procedures should be incorporated into the operating limitations
Class D	• 2500 feet above airport elevation • Radiuses vary per airport • Segregations procedures should be incorporated into the operating limitations
Class E	• Airspace that is not Class A, B, C, or D • Federal airway below 18,000 feet • Segregations procedures should be incorporated into the operating limitations
Class G	• Uncontrolled airspace • No IFR aircraft operation • Visual Flight Rules (VFR) aircraft allowed • Flight ceilings vary per area, usually 400 to 1,200 feet

3.4.2 DATA AND RECORDS COLLECTION

Development of policies and standards for UAS integration into NAS will be significantly affected by data collected from both public and private sectors. Data collections must follow Title 49 of the Code of Federal Regulations (49 CFR) under section 150.5 (Protection of Sensitive Security Information). Iterative UAS rule making and the implementation of future technologies can be supported by this database of records as a source of historical reference.

3.4.3 OBSERVER REQUIREMENT

A VO assists and supports a PIC to comply with the "see and avoid" procedures by scanning the area around the aircraft for potentially conflicting traffic. In addition, a VO assists the PIC with navigational awareness. The main responsibilities of a VO include:

- Assisting the PIC to ensure that the aircraft operates within visual line-of-sight limits

- Maintaining sufficient visual contact with the aircraft and the surrounding airspace to assist the PIC with:
    - Determining the UAS proximity to all other aviation activities and other hazards
    - Exercising effective control of the UAS
    - Complying with the 14 CFR section 91, General Operating and Flight Rules
    - Preventing any collision hazards
- Notifying the PIC of a possible loss of visual interaction or collision hazard
- May use binoculars, field glasses, night vision devices, or telephoto lenses if:
    - Only for augmentation of the observer's visual capability
    - Cannot be used as the primary means of visual contact
- During night operations, the VO must be in place 30 minutes prior to flight to ensure dark adaptation

Sequencing VOs or daisy-chaining of observers to increase visual operational range is not permitted unless previously approved by the FAA.

3.4.4 Air Traffic Control (ATC) Communications Requirements

A PIC must establish and maintain a direct two-way radio communication with ATC when:

- The aircraft is being operated in Class A or D airspace
- When required, during flight in Class E and G airspace
- The aircraft is being operated under IFR
- It is stipulated under the provisions of any issued COA or Special Airworthiness Certificate (SAC)

It is preferred that communications between the PIC and ATC be established through onboard radio equipment to provide a voice relay. A PIC must maintain immediate communication with a VO throughout communications with ATC.

3.4.5 Use of Electronic Devices

The use of electronic devices other than for UAS flight and operations is governed by section 91.21, Portable Electronic Devices, of the 14 CFR. Specifically, PIC to ATC communication is not allowed to be established by a cellular device as a primary form of communication, unless it is permitted under the Special Provisions of the COA.

3.4.6 Hazardous Materials, Expendable Storage, and Ejected Objects

UAS are permitted to have ejecting, spraying, and expendable storing capabilities, including hazard materials, which much undergo proper safety assessment and accident prevention procedure. The operation of these capabilities outside the restricted areas must comply with the 14 CFR section 91.15, Dropping Objects. Furthermore, procedures for material storages and loss of control link must be submitted to the FAA. The hazard materials must undergo similar procedures for authorization approval. If approved, this information will be listed in the special provision section of the COA or SAC.

3.4.7 Flight over Populated Areas

UAS operations over urban or populated areas are not allowed, unless the level of airworthiness is acceptable. UAS operation over populated areas may be approved in emergency situations if the proposed mitigation strategies are found to be acceptable.

3.4.8 Flight over Heavily Trafficked Roads or Open-Air Assembly of People

Operating a UAS over heavy trafficked or dense areas of people must be avoided, except where adequate level of airworthiness allows. If flying over these types of areas is required, proper safety measures must be taken. Safety is defined as the level of risks that it takes to perform an operation. Flights may still be permitted if an acceptable safety threshold is reached by reducing the risk level of operating procedures to offset the safety risk. The operation must show that risk of human injuries or damage of properties has been minimized along the UAS flight area. However, UAS flight/operation can be restricted if its performance specification negatively reflects on the performance of existing air traffic, established by the FAA and Air Traffic Organization (ATO).

3.4.9 Day/Night Operations

UAS operations outside of Class A airspace, restricted or warning areas designated for aviation use, or approved prohibited areas must be conducted during daylight hours. UAS operations during night hours may be authorized if an applicant demonstrates low level operational risks. An approved night time UAS operation requires all crewmembers to be present in the operational area 30 minutes prior to night flight for eye adaptation to dark conditions to ensure higher safety levels of operation.

3.4.10 Flights Below Class A Airspace

UAS operations performed beyond restricted, prohibited, sensitive security, or warning areas must be conducted in visual meteorological conditions (VMC) when using air or ground VOs. Additional requirements include:

- When a PIC is using IFR to fly the UAS, the PIC:
    - Must avoid flights through or around clouds
    - Is responsible for obtaining clearance from ATC with accordance to 14 CFR to perform this type of flight
- When a PIC is using VFR to fly the UAS, the following applies:
    - The PIC must avoid clouds with respect to 14 CFR section 91.155 (does not apply if flying in Class G airspace)
    - If operating in Class E, the in-flight visibility requirements are applicable and must be no less than three statute miles (SM)
- If using airborne VO’s in a chase aircraft, the in-flight visual requirement is five SM

3.4.11 UAS Autonomous Operations

FAA allows only UAS with direct pilot intervention capabilities to fly in the NAS when flights are inside restricted or warning areas designated for aviation use. This restriction does not apply when the UAS is operating under lost signal link or other similar phenomenon, which allow for certain built in recovery modes if the PIC is unable to control the UAS.

3.4.12 Operation Locations

Any UAS operational area should be located at least five miles away from any airport or heliport. The operational area includes takeoff and landing location of the UAS. In addition, a reasonable distance must be maintained from any objects, obstacles, and structures.

3.4.13 OPERATING UNDER INSTRUMENT FLIGHT PLAN (IFR)

While operating on an IFR, the following statements should be taken into consideration:

- An IFR flight plan must be submitted
- PIC must hold a current instrument rating
- All of the IFR operations and working equipment must be certified and described in the airworthiness statements
- PICs must have access to all of the navigation and chart databases
- PIC must gain clearance from ATC
- A direct two-way radio communication between PIC and ATC must be established and maintained
- Designate alternate communication capabilities with ATC for lost link and/or lost communication purposes which must be operational during all phases of flight
- Equip the UAS with a certified operating mode C transponder
- Any section of the flight throughout Class A airspace must be able to receive ATC radar services when possible
- Any flight beyond Class A, restricted, warned, or prohibited airspace must be clear of clouds
- PIC must gain clearance from ATC to diverge from Class A or restricted, warned, or prohibited airspace
- In accordance to 14 CFR section 91.3, the PIC is the final authority in the chain of commands and is responsible for the operation of the aircraft at all times
- Class A airspace does not required VOs unless stated in the COA or SAC

3.4.14 IN-FLIGHT EMERGENCIES

During emergency situations, the PIC must:

- Inform ATC of any in-flight emergencies
- Inform ATC of an aircraft accident as soon as possible
- Inform ATC of any loss of control link

3.5 AUTHORIZATION FOR CIVIL OPERATORS – GENERAL INFORMATION

Any aircraft operation in the NAS must have a certificated and registered aircraft, a licensed pilot, and operational approval [39]. Recently, there has been a high demand to expedite the integration of UAS into the NAS. Section 333 of the FAA Modernization and Reform Act of 2012 provides the legal flexibility for authorizing safe civil sUAS operations within the NAS. Specifically, this document grants the Secretary of Transportation the authority to determine whether an airworthiness certification is required for UAS operation in the NAS [40]. Section 333 applications are used to determine if UAS systems create potential hazards to users of the NAS or pose threats to national security. Some of the parameters that are used to evaluate Section 333 applications are proximity to airports and populated areas, and visual line of sight operations. These exemptions are granted in a case-by-case basis for certain UAS systems to perform commercial operations prior to the release of FAA's sUAS ruling.

The objective of Section 333 is to provide operators, who intend to operate safely and legally, a competitive advantage in industry. The exemption aims to discourage illegal operations and to improve overall safety. Additionally, Section 333 exemptions would simplify the process for private contractors to operate sUAS during field inspections for state departments of transportation. To date, 64 petitions under Section 333 have been granted for various types of applications (e.g., agricultural applications, aerial photography, film industry, and structural inspections). Structural inspections include inspections of oil and gas platforms, bridges, roof, towers, railroad infrastructure, and wind turbine blades.

The term “civil operations” refer to UAS operations for non-governmental purposes –excluding operating a UAS for recreation or hobby. Private contractors to departments of transportation fall under this category. The following subsections outline instructions for requesting FAA authorization for civil entities to conduct UAS operations (see Figure 3-3) [41]. Petitions must be submitted 120 days before the needed date for the exemption to take effect. Similar to the public COA, the average review time for the process is 60 days, depending on the complexity of the operation.

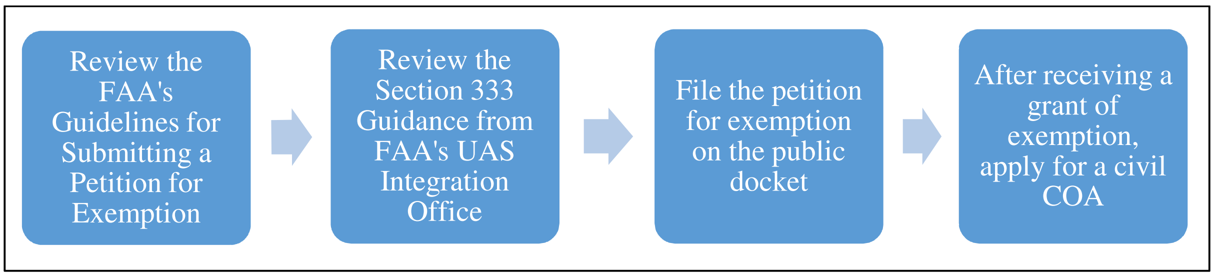

Figure 3-3 Instructions for Petitioning for Exemption under Section 333

3.5.1 Reviewing the FAA’s Guidelines for Submitting a Petition for Exemption

According to Title 14 CFR Part 11.81, a petition for exemption must include the following information [42]:

- Name and mailing address of application; other information such as fax number, telephone number and email address may be included as well
- The specific section(s) of Title 14 CFR from which the application seeks exemption
- The extent of relief the applicant seeks and the respective reasons
- Description of how the applicant’s request benefit the public as a whole
- Reasons why the exemption would not adversely affect safety or how the exemption would provide a level of safety, at least equal to the existing rule
- A summary to be published in the Federal Register that outlines the rule that the applicant seeks exemption from, and a brief description of the exemption the applicant seeks
- Any additional information, view or arguments to support the applicant’s request
- If applicable, the reason in which the application would like to exercise the exemption outside the United States

It is recommended that the petition for exemption be submitted electronically. Electronic submissions for exemptions may be made through the Federal Docket Management System (FDMS) web site at http://www.regulations.gov. Approved exemptions are typically granted for up to two years. Extensions for granted exemptions are allowed if requested at least 120 days before the expiration date. If the conditions and reasons in regards to public interest and safety remain unchanged, they must be stated in the extension request. The process for submitting petitions electronically can be found in [43].

3.5.2 REVIEWING THE SECTION 333 GUIDANCE FROM FAA'S UAS INTEGRATION OFFICE

The specific information that petitioners should submit to request FAA authorization for UAS operations in the NAS is documented in [44]. Section 333 provides the limited statutory flexibility to Title 49 United States Code (USC) Sections 44704 and 44711 in regards to airworthiness certification; however, it does not provide the same flexibility in regards to other sections of Title 49 USC or Federal Aviation Regulations (FAR). As an example, Title 49 USC Section 44711 requires all aircraft to be registered according to Part 47, where identification markings must be provided in accordance to Part 45, Subpart C [44]. Additionally, Part 36 prescribes that all aircrafts require noise certifications and testing. If an airworthiness certificate is determined not to be required, then noise certifications and testing are not required.

It must be noted that Section 333 does not provide any legal flexibility for the statutory requirement that PICs must possess an airman certificate under Part 44711. A PIC must have the appropriate airman certificate as written in Title 14 CFR Part 81 and the respective medicate certificate as outlined in Title 14 CFR Part 67. Since the Transportation Security Administration (TSA) carries out security screenings of certificated airman, a PIC with airman certificates would meet the statutory requirement of Section 333, in which operations do not comprise a national security threat [44].

The FAA provides specific guidelines to be considered when evaluating petitions under Section 333 [44]. These guidelines are specific to UAS platforms, PICs, and UAS operations. In addition, petitioners shall include a request for exemptions to regulations with which they are not able to fully comply. There are three main types of regulations that are considered for exemptions. The first one relates to airworthiness certificates (Part 21). The second one relates to certification for pilots, light and ground instructors (Part 61). The third one relates to general operating and flight rules (Part 91) [45], [46], [47]. Note that unless otherwise authorized or exempted, civil operators are required to comply with the rest of the FARs.

3.5.3 APPLYING FOR CIVIL COA

Civil COA applications can be made after approval of the petition. COA applications must include information described in [41]. Required information includes an exemption number (corresponding to the Federal Register Docket ID for the application's petition for exemption), and a registration number (aircrafts must be registered with the FAA).

The intention of the COA process is to ensure that the appropriate FAA ATC facilities are aware of the proposed UAS operations and resolved any airspace conflicts, if applicable. Furthermore, the COA application and petition for exemption must both be submitted under the same name or company name. Note that the public and civil portals are different. The civil COA portal can be found under the following link: https://oeaaa.faa.gov/oeaaa/external/uas/portal.jsp. Before starting the COA application, the applicant must register for an account in the system.

3.6 FUTURE LEGISLATION – PROPOSED PART 107

FAA recently released a *notice of proposed rulemaking* (NPRM) document for Part 107, which describes regulations for UAS operations. The proposed regulations specify that an sUAS must weigh less than 55 pounds, and a micro-UAS less than 4.4 pounds. These regulations would also allow the non-hobby and non-recreational operations of sUAS in the NAS. Furthermore, it outlines the equipment necessary for safe and efficient sUAS operations. The allowed operations listed under the proposed framework include bridge inspections, aerial photography, wildlife nesting evaluations, antenna inspections, research and development, educational and academic applications, crop monitoring and power-line and pipeline inspections [33]. The proposed regulations are currently under public commenting. The following subsections provide a summary of the major provisions indicated in the proposed Part 107 highlighted by the NPRM.

3.6.1 OPERATIONAL LIMITATIONS

There are various key operational limitations when operating an sUAS [48]. An sUAS must weigh less than 55lbs (25kg) and must only be operated within the parameters of visual line-of-sight (VLOS). An sUAS must remain within the VLOS of the operator or visual observer. Within the VLOS, an sUAS must be close enough to the operator to be visible without any visual aids. Therefore, first-person view cameras will not satisfy the “see-and-avoid” requirement; however, they can be used alongside anything that satisfies the requirement. Operations are restricted to daylight-only activities. Furthermore, under the proposed ruling, operations may use a VO. No person may be the operator or VO for more than one UAS operation at one time. The sUAS may not be operated over people that are not directly involved in the operation itself. Other operational constraints include a maximum speed of 100 mph, maximum altitude of 500 feet above ground level, and maximum weather visibility of three miles from the control station. Operators must always yield right-of-way to other manned and unmanned aircraft. There shall be no operations in Class A airspace (i.e., 18,000 feet and above). Operations in airspace classes B, C, D and E are allowed only with ATC permission. Operations in class G airspace are possible without ATC permission.

3.6.2 OPERATOR CERTIFICATIONS AND RESPONSIBILITIES

Operator certifications and responsibilities are important to decrease the chances of mission failures [48]. An sUAS pilot (i.e., “operator”) is required and responsible for preflight inspections and overall maintenance of the sUAS. The pilot decides if the sUAS is safe for operation. System checks must include inspection of the sUAS and ground control equipment. Upon request, operators must make the sUAS available for inspection or testing, and provide the associated documents/records required to be kept under the proposed rule. The following list provides some of the requirements for sUAS operators under the proposed ruling from the FAA:

- Be at least 17 years old
- Be vetted by the TSA
- Pass an initial aeronautical knowledge test at an FAA-approved knowledge testing center
- Obtain an unmanned aircraft operator certificate with a small UAS rating (never expires)
- Pass a recurrent aeronautical knowledge test every 24 months

Furthermore, the operator is responsible for reporting any accidents that resulted in any injury to a person or any damage to property other than the sUAS.

3.6.3 AIRCRAFT MARKINGS

Under the proposed ruling, aircraft registration and markings are required. If an sUAS is too small to display the markings provided by FAA, then the aircraft is required to display markings in the largest practical manner. However, an FAA airworthiness certification is not required.

3.6.4 sUAS AND MICRO-UAS DISTINCTIONS

The proposed rule defines a new category of UAS called "micro-UAS". Micro-UAS flights are allowed on Class G airspace over people not involved in the operation. This would also require the airman to self-certify that they are familiar with required aeronautical knowledge. Micro-UAS must weigh less than 4.4lbs, and not fly over 400 feet. Table 3-4 describes differences between sUAS and micro-UAS aircrafts for various provisions [49]. These provisions allow the operation of micro-UAS with less legal considerations for various applications.

3.7 WILDLIFE CONCERNS

There are no published guidelines regarding rules and procedures in flying any UAS near or around bird nests. However, there are certain regulations concerning injuring protected species. In general, operators must avoid flying sUAS around wildlife to avoid damages to equipment, possible injuries to people, damages to infrastructure, and injuries to wildlife. According to Florida Statute 379.411, it is unlawful to intentionally wound or kill any endangered species. This law includes protection of eggs and nests of birds. Anyone who violates this statute is guilty of a felony of the third degree [50].

Table 3-5 provides designated categories for protected species according to threat levels [51]. Table 3-6 provides a list of bird types that are protected according to the Florida Fish and Wildlife Conservation Commission [51]. As shown in the table, there are multiple protected bird species protected in the State of Florida. It would be difficult to familiarize an operator with each species. Additionally, it is difficult to determine the species of birds associated with a specific nest. Similarly, species identification is very difficult when visually observing eggs. If there are bird nests near the structure to be inspected, the operator shall fly at a relatively safe distance from the nests. If there are hatchlings or nestlings visible, it is best not to fly close to the nest to avoid harassing the nestlings.

3.8 CONCLUDING REMARKS

This document describes relevant FAA rules and regulations regarding operations of sUAS for structural inspections of bridges and HMLs. The information presented in this document applies mostly to public sUAS operations because of FDOT's status as a public entity. Information is also included regarding FAA regulations that apply to private entities such as private contractors. For both entity types, aircrafts must be registered with the FAA.

The FAA has been working hard to develop rules that can safely allow sUAS civil operations in NAS for a variety of applications (e.g., transportation infrastructure inspections). Recently, the FAA made public a formal proposal to update rules and processes for conducting civil sUAS operations. If approved, the new rules will significantly benefit these types of operations for both commercial and non-commercial purposes. Civil sUAS operations require that an aircraft be owned by civil entities such as private universities, private corporations, or private individual contractors.

The process to conduct public sUAS operations requires a registered aircraft and a public COA. On average, it takes a maximum of 60 days to obtain a public COA for a particular objective. This public COA approval duration could be feasibly incorporated into FDOT's inspection procedures by scheduling the submission of the respective public COA application at least 60 days prior to the inspection day. An example of a mission can be defined as using an sUAS for the visual inspection of various HMLs or bridges. A public COA to conduct an inspection of a bridge or HML can be immediately obtained if accidents or other unexpected situations result in critical damage. The process for private entities to conduct sUAS operations involve applying for exemptions to regulations under the provisions set forth by Section 333. The average time for the review process of exemptions is 120 days. Afterwards, civil entities may apply for civil COAs which take an average of 60 days, depending on operational complexity. This overall time period is larger, but it allows civil entities to operate sUAS for various applications.

Table 3-4 sUAS vs Micro UAS Provisions

Provision	sUAS	Micro UAS
Definition of sUAS	Up to 55 lbs (24 kg)	Up to 4.4 lbs (2 kg)
Maximum altitude	500 feet	400 feet
Airspace limitations	Class G and B, C, D, E with ATC permission	Only Class G
Distance from people and structures	No operations over any person not involved	Flying over any person is permitted
Ability to extend operational area	Yes, from a waterborne vehicle	No
Autonomous operations	Yes	No
Aeronautical knowledge required	Yes; knowledge test required	Yes; self-certification
FPV permitted	Yes; but still under VLOS rules	No
Operator training required	No	No
VO training required	No	No
Operator certificate required	Yes (must pass basic UAS aeronautical test)	Yes (no knowledge test required)
Preflight safety assessment	Yes	Yes
Operate within five miles of an airport	Yes	No
Operate in a congested area	Yes	Yes
Liability insurance	No	No
Daylight operations only	Yes	Yes
Aircraft must be made with frangible materials	No	Yes

Table 3-5 Protected Species Designations

Designation	Meaning
FE	Federally-designated Endangered
FT	Federally-designated Threatened
FT(S/A)	Federally-designated Threatened because of similarity of appearance
FXN	Federal Non-essential Experimental Population
ST	State-designated Threatened
SSC	State Species of Special Concern

Table 3-6 List of Protected Bird Species in Florida

Common Name	Scientific Name	Status
American oystercatcher	Haematopus palliates	SSC
Audubon's crested caracara	Polyborus plancus audubonii	FT
Bachman's wood warbler	Vermivora bachmanii	FE
Black skimmer	Rynchops niger	SSC
Brown pelican	Pelecanus occidentalis	SSC
Burrowing owl	Athene cunicularia	SSC
Cape Sable seaside sparrow	Ammodramus savannarum floridanus	FE
Eskimo curlew	Numenius borealis	FE
Everglade snail kite	Rostrhamus sociabilis plumbeus	FE
Florida grasshopper sparrow	Ammodramus maritimus mirabilis	FE
Florida sandhill crane	Grus Canadensis pratensis	ST
Florida scrub-jay	Aphelocoma coerulescens	FT
Ivory-billed woodpecker	Campephilus principalis	FE
Kirtland's wood warbler (Kirtland's warbler)	Dendroica kirtlandii (Setophaga kirtlandii)	FE
Least tern	Sterna antillarum	ST
Limpkin	Aramus guarauna	SSC
Little blue heron	Egretta caerulea	SSC
Marian's marsh wren	Cistothorus palustris marinae	SSC
Osprey	Pandion haliaetus	SSC
Piping plover	Charadrius melodus	FT
Red-cockaded woodpecker	Picoides borealis	FE
Reddish egret	Egretta rufescens	SSC
Roseate tern	Sterna dougallii dougallii	FT
Scott's seaside sparrow	Ammodramus maritium peninsulae	SSC
Snowy egret	Egretta thula	SSC
Snowy plover	Charadrius nivosus (Charadrius alexandrines)	ST
Southeastern American kestrel	Falco sparverius Paulus	ST
Tricolored heron	Egretta tricolor	SSC
Wakulla seaside sprarrow	Ammodramus maritimus juncicola	SSC
White-crowned pigeon	Patagioenas leucocephala	ST
Whopping crane	Grus americana	FXN
White ibis	Eudocimus albus	SSC
Worthington's marsh wren	Cistothorus palustris griseus	SSC
Wood stork	Mycteria americana	FE

CHAPTER 4

SELECT SYSTEM'S COMPONENTS

4.1 INTRODUCTION

An important task for the research team encompassed evaluation and selection of the main UAS components to be used throughout the research project. These main components are the UAV, the ground viewing station (GVS), and high-definition (HD) cameras. *Weighted factor analyses* were developed to provide a systematic decision-making analytical approach for the selection of each component. Weighted factor analysis allows the assignment of relative weights to evaluation criteria to ensure that the selections of the system's components are aligned with the research goals. The general process followed by the research team was the following:

- Identify operational parameters and other important criteria
- Determine relative importance of each criteria based on research goals
- Develop a list of alternatives
- Evaluate alternatives and make decision

This document describes the decision-making process for the selection of each equipment component.

4.2 OPERATIONAL PARAMETERS AND DESIGN CRITERIA

For each of the three main system components, the research team developed a list of criteria to be used in the decision-making process. The following sub-sections define the list of evaluation criteria for each component and the importance of each criterion in relation to the project goals.

4.2.1 WEIGHTED CRITERIA FOR UAV SELECTION

For the selection of the UAV component, a set of six criteria was developed according to the project needs. These criteria were selected based on a literature review effort, observation from experienced UAV flight operators, and field inspections conducted by a Senior Bridge Inspector from Florida's District 5. Please note that price was not included as a criterion for the UAV selection (as seen in the selection of the GVS and image capturing device) because the cost of purchasing each of the UAV alternatives was relatively similar. The following criteria were the basis for comparing the different UAV options:

- Maneuverability: The ability to navigate around corners, inside small spaces, to hover in a stable position, and recoverability from any loss of lift. These characteristics are desired in navigating under bridges and inspecting high mast poles.
- Adaptability: The ability to adjust desired physical characteristics such as platform type, battery size, propeller size, motor size, and GPS unit.
- Software Compatibility: The ability to modify the software-to-hardware interaction to accommodate future potential upgrades to the system.
- Payload: The maximum load capacity that the UAV can carry as payload once it is fully functional. The load includes the camera, sonars, and sensors.
- Size: The physical characteristics of the UAV such as overall size, weight, height, and the ability to be stored in a compact form when not in operation.

- User Controls: This parameter describes the human-interface controls, including the amount of user input needed for flight, the different sensors, and the total training time to master these abilities. The user-controls interface represents a very important component of the system. The need for a simplistic user interface with minimal controls is considered key for a successful inspection system transition.

After selecting the criteria, the next step was to assign relative weights to denote importance of each criterion for the selection process. Table 4-1 shows the weight distribution for each criterion used to evaluate UAV alternatives. Column (1) shows the criteria selected. Three separate researchers then graded the performance measures based on how each criterion related to the project, shown in column (2). Prior to assigning individual weights to the criteria, each of the three researchers gathered information from experienced FAA certified pilots, a review of the academic literature, and collaborative input from bridge inspectors from Florida's District 5. Column (3) shows the computed average of the individual grade. Column (4) shows the computed weights, which were calculated by dividing the average grade in column (3) for each criterion by the total sum in column (3).

Table 4-1 Weight Distribution for UAV Selection Criteria

(1) Criteria	(2) Individual Ranking 1 – 5: 1 (Little), 5 (Very)	(3) Group Avg.	(4) Weights (%) = (3)/20.00
User – Controls/Interface	5, 5, 5	5.00	25.0
Maneuverability	5, 4, 5	4.67	23.3
Software Compatibility	4, 3, 3	3.33	16.7
Adaptability	3, 3, 3	3.00	15.0
Size	2, 2, 2	2.00	10.0
Payload	2, 2, 2	2.00	10.0
	Total:	20.00	100.00

Table 4-1 shows that the largest weight was placed on the user interface and controls, since it was decided that the most important factor was to make the system easy to use for field inspectors with minimal training. Training time can be minimized to meet the current needs of FDOT by selecting advanced software capable of controlling normal user inputs. Maneuverability was assigned the second highest weight because of the importance of being able to properly fly the UAV around structures. Software compatibility was the third most important factor because it may be necessary to modify the software with future updates which could possibly increase the control of the UAV. Adaptability was given a relatively low weight because it was assumed that changing hardware components may not be critical if the higher weighted criteria are satisfactory. Load capacity and size were assigned the lowest weights of the list because the maximum expected payload weight is within the capacity of the entire alternative set of UAVs considered; therefore, these two parameters were treated as "soft" requirements.

4.2.2 Weighted Criteria for Selecting the Ground Viewing Station (GVS)

The criteria used for selecting the GVS are as follows:

- Software Compatibility: The ability to be fully integrated with the UAV and camera systems while all systems are in use.
- Portability: The ability to be moved to different locations with ease while maintaining functionality.
- Performance: The ability to display real-time video, store large quantities of photos and videos, and back-up files remotely in a seamless fashion.
- Battery Life: The total available operable time while maintaining full system utilization.
- Price: The actual cost of the viewing station.

Table 4-2 shows the weight distribution for the criteria used to evaluate GVS alternatives. Software compatibility was unanimously selected as the most important criteria for the GVS due to the importance of synchronization between the UAV, GVS, and image capturing components. Portability and performance were both rated equally important. These criteria are essential to allow proper, real-time control of all the equipment even in the most remote areas. Battery life was second to last in the criteria selection process because each of the equipment compared had life durations of over three hours between charges, which is more than adequate for at least two structural inspections. Price was last on the importance scale.

Table 4-2 Weight Distribution for GVS Selection Criteria

(1) Criteria	(2) Individual Ranking: 1 (Little), 5 (Very)	(3) Group Avg.	(4) Weights (%) = (3)/21.33
Software Compatibility	5, 5, 5	5.00	23.4
Portability	5, 4, 5	4.67	21.9
Performance	4, 5, 5	4.67	21.9
Battery Life	3, 4, 4	3.67	17.2
Price	3, 4, 3	3.33	15.6
	Total:	21.33	100.00

4.2.3 Weighted Criteria for Camera Selection

The following set of seven criteria was developed for the selection of the cameras:

- Performance: The ability to perform typical functions (e.g., powering up) capture real-time video, and store large quantities of photos and videos. Performance also considers the image and video resolution.
- Weight: The physical weight of the camera and any attached accessories.
- Dimension: The physical size of the camera
- Price: The cost of the camera
- Battery Life: The total available operable time while maintaining full system utilization

- Ease of Use: The level of difficulty to operate the camera's functions including controls, wireless technology, response time, and focusing. Ease of use also takes into account available accessories such as a waterproof case, Wi-Fi remote, rechargeable batteries, and mounts.
- Software Compatibility: The ability to be fully integrated with the UAV and ground systems while all system components are in use.

Table 4-3 shows the weight distribution for the criteria used to evaluate various cameras. Given the importance to be able to see structural defects in great detail during an inspection, performance was equally rated with software compatibility. Weight was separated from portability due to its direct impact on the UAV selection. Dimension and ease of use were next on the weighting scale based on the need to fit the image capturing device into the UAV and then be able to remotely control the image capturing device with minimum user input. Battery and price were given the least amount of weight.

Table 4-3 Weight Distribution for Camera Selection Criteria

(1) Criteria	(2) Individual Ranking: 1 (Little), 5 (Very)	(3) Group Avg.	(4) Weights (%) = (3)/28.00
Performance	5, 5, 5	5.00	17.9
Software Compatibility	5, 5, 5	5.00	17.9
Weight	5, 4, 4	4.33	15.5
Dimension	3, 5, 4	4.00	14.3
Ease of Use	4, 4, 4	4.00	14.3
Battery Life	4, 3, 4	3.67	13.1
Price	2, 2, 2	2.00	7.1
	Total:	28.00	100.0

4.3 List of Alternatives

A list of alternatives was compiled for the three major system designs: UAV, GVS, and image capturing device. Based on the alternatives and desired outcome, comparison tools were employed in the selection process. Each of the three major system components was selected from a list of current cutting edge technologies that fit the needs of this research project.

4.3.1 UAV Alternatives

This document considers different alternatives for the design of an airborne structural inspection system. During this study, three different system alternative designs were considered for the UAV. The current UAV industry has many different possibilities for an inspection system. The research team focused on aircrafts of type *vertical takeoff and landing* (VTAL). VTAL aircrafts are typically based on rotor technology (e.g., helicopter). The following three major types of VTAL systems have encompassed most of the unmanned copter-like vehicles:

1. Single rotors helicopter (typically gas powered)
2. Multi-rotor (battery powered)
3. 'Y' or coaxial configuration (redundant engines and rotors in the X and Y direction)

Table 4-4 provides a list of three selected general VTAL UAVs as alternatives to meet the research needs. Column (1) includes the general type of VTAL aircraft considered. Column (2) highlights the characteristics of each UAV type according to the criteria presented in Table 4-1, and column (3) provides a general photo of each type of UAV.

Table 4-4 UAV Alternatives

(1) Type of UAV	(2) Characteristics	(3) Picture
Single Rotor Helicopter	a. Requires constant user input b. Low maneuverability c. Moderate software compatibility d. Low adaptability e. Moderate size f. High payload capacity	
Multi-rotor Helicopter	a. Simplistic user interface b. High maneuverability c. High software compatibility d. Highly adaptable e. Moderate to large size f. Moderate Payload	
Coaxial Helicopter	a. Simplistic user interface b. Moderate maneuverability c. High software compatibility d. Moderate adaptability e. Moderate size f. Low/Moderate Payload	

4.3.2 Ground Viewing Station Alternatives

Table 4-5 shows the four types of GVS considered: Ultrabook, Laptop, Windows tablet, and Android tablet. Column (2) shows overall characteristics for each of the alternatives. The final selection was made based on narrowing down the type of technology to use, followed by selecting a specific device from that technology (i.e., if a windows-based tablet technology was selected, the Google Nexus 7 HD, Galaxy Note 10.1, Galaxy Tab 2, MeMO Pad 8, etc. would then be evaluated based on the criteria presented in Table 4-2). Due to the importance of system integration, software compatibility, and limited availability in MAC OS based components, Apple products were not considered as an option.

Table 4-5 GVS Alternatives

(1) Type of Viewing Station	(2) Characteristics	(3) Picture
Ultrabook	a. Good performance b. Good portability c. High price d. Medium weight e. High battery life f. Average compatibility	
Laptop	a. High performance b. Low portability c. Moderate to high price d. High weight e. Low to moderate battery life f. Average compatibility	
Windows-Based Tablet	a. High performance b. High portability c. Moderate price d. Medium weight e. Moderate battery life f. Average compatibility	
Android-Based Tablet	a. Good performance b. High portability c. Low to moderate price d. Low weight e. High battery life f. High compatibility	

4.3.3 Image Capturing Device Alternatives

Table 4-6 shows the three types of image capturing devices considered: GoPro HERO 3+ black edition, Sony AS15, and Flytron FM10x. The final selection was made based on a comparison of equipment that would fit the existing line of component selection while still satisfying all other criteria for the research needs. Column (2) shows overall characteristics for each of the alternatives. All of the choices presented fit the criteria of system integration; therefore, system integration was excluded as a parameter in the equipment selection process.

4.4 Evaluation of Alternatives

Based on the characteristics presented in Table 4-4 through Table 4-6, each system component was first chosen as a general item (i.e. multi-rotor copter, Windows-based tablet, portable camera). Afterwards, potential candidates were identified for each component (i.e., Galaxy tab 3, MeMO tablet, Vivobook, Transformer TF303). This process went through a series of collaborative group-think meetings, independent brainstorming, and decision models.

Table 4-6 Image Capturing Device Alternatives

(1) Type of Image Capturing Device	(2) Characteristics	(3) Picture
GoPro	a. Moderate to high performance b. Low weight c. Compact dimension d. Low to moderate price e. Moderate to high battery life f. Simplistic user interface	
Sony	a. Low to moderate performance b. Low weight c. Wide profile d. Low to moderate price e. Low to moderate battery life f. Highly interactive user interface	
Flytron	a. Low performance b. Low weight c. Compact dimension d. Low price e. Connects to UAV battery f. Simplistic user interface	

4.4.1 EVALUATION OF UAVS

From the list of UAV alternatives shown in Table 4-4, the multi-rotor helicopter system was selected based on its simplicity of user control, ease of maneuverability, degree of adaptability, and wide range of upgradability. Figure 4-1 shows a snapshot of the UAV selected for the research project. Table 4-7 shows the resulting weighted factor analysis for the selection process. A full list of components and accessories associated with this particular UAV is shown in Table 4-8. This UAV system includes a dual camera setup, remote control gimbal, and an autopilot configuration. It also includes open source programmable control software capable of automatic take-off, GPS waypoint Navigation, automatic landing, automatic flight adjustment, near real-time video with FPV camera, telemetry (i.e., real-time flight statistics), and operation boundary control.

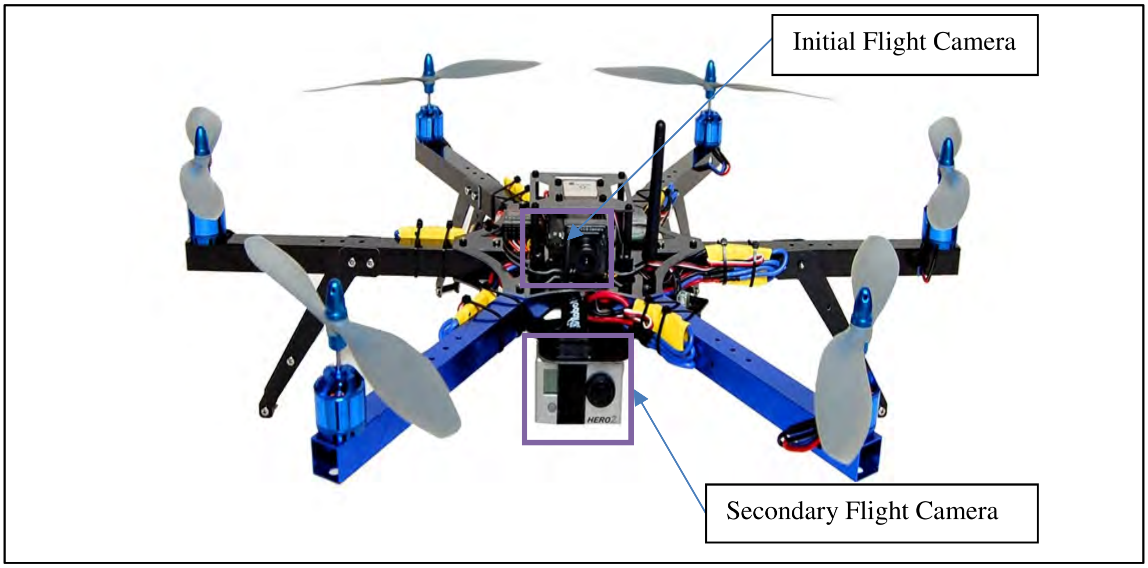

Figure 4-1 Ardu-Hexa-Copter

4.4.1.1 Dual Camera System

The initial flight camera (shown in Figure 4-1) was selected based on its integration into the Arduino software program and its ability to capture and transmit live stream video data from above the UAV's rotors. The Arduino program is an open source program easily manipulated through any windows-based device. The initial camera, upgradable through the manufacturer, is capable of in-flight video capture, and is remotely controlled through the same RC that controls the UAV system. The camera is capable of single axis tilt and displays real-time video through a variety of tablets, google glasses, and other similar devices.

The GoPro HERO 3 Black edition was chosen as the primary camera based on its performance of in-motion video capture, image quality, size, weight, and additional features such as low-light mode, the ability to be controlled by preloaded application software, and extended Wi-Fi range capabilities. The GoPro camera can be controlled by a Windows-based tablet PC during flight, viewed through a mobile cellular device, take still photos while in video capture mode, and take still photos at a rate of 20 photos per second to capture high-resolution images from multiple angles. There are also a variety of camera housings the can be fitted to the GoPro, making it weather and water resistant, as well as allowing the camera to float if dropped into water.

The GoPro Hero 3+ black edition camera is used as the primary video source on the Arducopter UAV. Mounted on a controllable gimbal arm on the underside of the copter, this camera is capable of capturing 4k resolution video. Capabilities beyond the ultra-high definition image quality include software support capable of near real-time video streaming, slow-motion play back, and the ability to capture still images from individual video frames after the video has been taken.

Table 4-7 Weighted Factor Analysis Results for UAV

Criteria		Rank: 1 (Low), 5 (High)	Group Avg.	Weight	Grade 1-10 poor = 1, Fair = 5, Good = 10			Final Weighted Score		
					Single Rotor	Multiple Rotors	Coaxial Rotor	Single Rotor	Multiple Rotors	Coaxial Rotor
1	Maneuverability	5, 4, 5	4.667	0.233	8.000	10.000	7.000	1.867	2.333	1.633
2	Adaptability	3, 3, 3	3.000	0.150	10.000	9.000	8.000	1.500	1.350	1.200
3	Software Compatibility	4, 3, 3	3.333	0.167	5.000	9.000	9.000	0.833	1.500	1.500
4	Load Capacity	2, 2, 2	2.000	0.100	10.000	8.000	9.000	1.000	0.800	0.900
5	Size	2, 2, 2	2.000	0.100	3.000	7.000	8.000	0.300	0.700	0.800
6	User Interface	5, 5, 5	5.000	0.250	4.000	9.000	9.000	1.000	2.250	2.250
Total			**20.000**	**1.000**	**Average Score**			**6.500**	**8.933**	**8.283**

Table 4-8 Ardu-copter System Components

Aircraft	Sensor
ArduPilot Mega 2.5 Micro Copter	MB1240 Sonar
APM Power Module with Deans	Advanced filter
Replacement Kit	**On Screen Display (OSD) and First Person View OSD**
Brushless motor 880Kv	3DR MinimOSD
3DR 20A ESC	Micro CCD Camera
Replacement arms	Video Transmitter
Replacement legs	Video Receiver
APC propeller set	Standard Batteries
Screws and spacers (different sizes)	Standard Cables
Camera Mount	**Battery Kit**
Pitch stabilized fiber glass camera mount	LiPo 3S 4200 mAh 11.1v
Metal gear servo motor	Lipo Balance Charger
170mm landing gear	LiPo Bag
Telemetry Electronics	**Radio Control**
3DR Radio Telemetry Kit	Dual RC setup
3DR Radio Air module	Spektrum RC with PWM Receiver
3DR Radio USB Ground module	FlySky RC
Telemetry Cable	FlySky D4R-II 2.4Ghz PPM receiver
USB Extension Type A Cable	FlySky DJT module
Antenna RP-SMA 2dBi	FS-TH9x (Er9x firmware)
XtreamBee Boards	
FTDI USB TTL Serial Cable	

4.4.1.2 PRE-LOADED SOFTWARE

The selected system has the ability to load pre-determined flight patterns with a beginning and ending destination thanks to the built-in Arduino software. This software also allows for automatic takeoff, automatic hovering, altitude detection, self-landing security protocols, and dual control capability (both radio and digital control) via point navigation through GPS signals. This process is depicted in Figure 4-2.

4.4.1.3 TELEMETRY ELECTRONICS

The equipped 3DR radio set was selected due to its interchangeable air and ground communication setup. Controllable through a user-friendly mobile application, this system allows for wireless communication from laptop or tablet with the copter. This radio set is capable of transmitting real-time in-flight data, and contains an open-source firmware for future upgradability.

Figure 4-2 Arduino Software Print Screen

4.4.1.4 DATA COLLECTION EQUIPMENT

Miscellaneous equipment for running and controlling experiments was also subject to the analysis process. Four WeatherHawk anemometers with tripod attachments and a tri-axis accelerometer were selected for the research. The anemometers are hand-held models capable of simultaneous data capture of maximum and average wind speed over three, five, or 10-second intervals. Accelerometers were also selected based on the need to measure tri-axial acceleration effects on the camera mount due to external wind effects and propeller down draft. Direct integration into existing software with a simple USB data link connectivity was the key factor in the selection process for the accelerometers.

4.4.2 EVALUATION OF GVS ALTERNATIVES

The Windows-based tablet was selected to best fit the needs of the research project based on its high performance, high portability, broad software compatibility, and low weight (see Figure 4.3). Its integration with both the Arducopter and camera software made it a prime candidate for the GVS. A complete evaluation can be seen in Table 4-9, where each alternative choice was graded based on the criteria selected in Table 4-2.

The Microsoft Surface Pro 3 tablet PC is used for various purposes. This tablet can control the GoPro camera during flight and show real time telemetry information to a ground base. It is a high-performance, high-portability, broad software compatibility, and low weight Tablet PC. Its integration with both the Arducopter UAV and camera software made it a prime candidate for field tests. The Microsoft Surface Pro 3 tablet boasts an ultra-high definition screen while maintaining its desktop-like performance levels capable of running UAV telemetry data with an expected battery life of eight hours.

Figure 4-3 Microsoft Surface Pro 3

4.5 SELECTED UAS COMPONENTS AND KEY RESEARCH EQUIPMENT USED

Table 4-10 lists some of the key equipment items that were used for research and their associated costs. Only items E_1 and E_2 were purchased with FDOT funds. Item E_1 is a GoPro Hero 3+ black edition camera, which can be seen in Figure 4-1 attached to the primary UAV (i.e., Arducopter) used for research tasks. Item E_2 is a Microsoft Surface Pro 3 tablet PC, shown in Figure 4-3.

Figure 4-4 shows the DJI Phantom 2 Vision+ copter, which is an off-the-shelf model quad-copter with built-in advanced stabilization software. The stabilization software is a rigid, non-editable, scripted code which shortens normal operator training time significantly. This copter comes with a two-axis brushless gimbal and a removable camera capable of remote control, near real-time streaming, and HD video capture. Although flight times and customization are limited, DJI branded hardware allows slight copter modifications such as color coded propellers, propeller guards, and nose extension to improve the visual in-flight copter orientation. Figure 4-5 shows DJI's latest small UAV model, the Inspire 1. This model provides the capability of dual remote control, which allows a second operator to operate the camera during flight while the UAV is being piloted by another person.

Figure 4-6 shows the Spider UAV, which is a customized quad-copter built in-house. This copter was designed for simplicity of operation and includes remote operating fail-safe features.

Table 4-11 gives a list of some of the items that were used in-kind during research tasks. Some of these items are shown in Figure 4-7 and Figure 4-8. The Data Physics shaker table (Figure 4-7, bottom right) was used to determine operating limits within which the main image capturing device can actively take videos and photos while maintaining a useable image as deemed fit for the project's needs. Power Breezer fans were instrumental in giving the research team the ability to control wind speeds and wind conditions in an indoor environment. These fans are capable of wind speeds in excess of 30 mph and give the ability to control wind speed with a linear variable control knob ranging from a speed of 1 to 10. The Flytron FM10X and FM36X cameras (Figure 4-8, middle left) were used as alternative FPV cameras. These cameras connect to a 1.2 GHz video transmitter for the ability to stream near real-time video with the capability of up to 10x zoom, controllable through Arduino software.

Table 4-9 Weighted Factor Analysis Results for Ground Viewing Station

Criteria		Rank: 1 (Low), 5 (High)	Group Avg.	Weight	Grade 1-5 poor = 1, Fair = 3, Good = 5				Final Weighted Score			
					Ultrabook	Laptop	Windows Tablet	Droid Tablet	Ultrabook	Laptop	Windows Tablet	Droid Tablet
1	Performance	4, 5, 5	4.667	0.219	4.000	5.000	4.333	3.333	0.875	1.094	0.948	0.729
2	Portability	5, 4, 5	4.667	0.219	3.333	4.000	5.000	4.667	0.729	0.875	1.094	1.021
3	Price	3, 4, 3	3.333	0.156	1.333	3.667	3.333	4.333	0.208	0.573	0.521	0.677
4	Battery life	3, 4, 4	3.667	0.172	4.333	2.667	4.667	5.000	0.745	0.458	0.802	0.859
5	Software compatibility	5, 5, 5	5.000	0.234	2.667	4.667	4.667	3.667	0.625	1.094	1.094	0.859
Total			**21.333**	**1.000**	**Average Score**				**3.182**	**4.094**	**4.458**	**4.146**

Table 4-10 Main Equipment Purchased with FDOT Research Funds

ID	Equipment	Cost ($)
E_1	GoPro HERO 3+ Black Camera w/ case	480
E_2	Microsoft Surface Pro 3	1,235
E_3	Arducopter (UAV)	1,925
E_4	DJI Phantom 2 Vision + (UAV)	1,389
E_5	Spider (UAV)	985
E_6	DJI Phantom 2 Vision (two training UAVs)	1,158
E_7	DJI Inspire 1 (UAV)	3,299
E_8	GoPro HERO 4	380
E_9	Nikon SLR 5300	1,100

Table 4-11 Equipment Used In-kind

Equipment	Description
Data Physics V20 Shaker Table	Vibration table used to test the maximum vibration allowable while maintaining acceptable image quality
Power Breezer fans	Wind flow generators for testing flight limitations
Flytron FM10X and FM36X (Cameras)	Alternative FPV in flight camera
Contour +2 (Camera)	Alternative primary image processing device
FPV To GO	1.2Ghz video transmiter/reciever
Low-Pass filter for FPV System	Improves video signal by removing signal inteferance
Cloverleaf antenna	Multi directional high-gain antenna
5,000 & 7,700 mAh Batteries	Alternative high-capacity batteries
Battery Cell Voltage Checker	Measures total and individual cell voltage with audible low voltage alarm
APC Composite 11 x 4.7 Propeller CW&CCW	Alternative propeller replacements
Dual Axis Carbon Fiber Camera Gimbal	Dual axis camera stabilization gimbal to improve video capture quality

Figure 4-4 DJI Vision 2 Plus with Remote Control

Figure 4-5 Inspire 1 UAV

Figure 4-6 Spider (Customized UAV with Advanced Fail Safe Features)

The Contour +2 (Figure 4-8, middle right) is also used in this research to evaluate its capability as an onboard image capturing device. The benefit of this device over its competition is the onboard GPS pinging and image coding, which allows users to locate where each video/photo was taken based on encoded information stored in each photo frame. The FPV to Go (Figure 4-8, bottom center) has been used with the low pass filter (Figure 4-8, bottom left) and cloverleaf antenna (Figure 4-8, bottom right) for video transmitter/receiver. This setup is capable of transmitting high quality analog video with a direct line of sight of up to 2,000 feet.

Battery options (Figure 4-8, center row) are used to test for weight, battery life, and payload capacity with the primary goal of copter stabilization and ease of maneuverability. Each battery is monitored by a battery cell voltage tester. This tester monitors each cell of the batteries in real-time and gives an audible warning when any cell hits a target threshold value. The carbon fiber propellers (Figure 4-8, top left) are tested for weight versus performance gain, measured by stability and maneuverability.

4.5.1 Evaluation of Image Capturing Device

The GoPro HERO 3+ black edition was selected to best fit the needs of the research project based on its high performance, low weight, compact dimensions, battery life, and user interface. This camera's additional FPV live video sharing was an integral factor in the decision process. A complete evaluation of the selection process can be seen in Table 4-12.

4.6 CONCLUSION

Weighted factor analyses were employed to select the UAS components based on the research objectives. Criteria for selecting each component were established by the research team based on information from various sources (i.e., input information from FAA certified pilots, FDOT's bridge inspectors, and a literature review effort). From the analyses, the final selection of UAS components included a multi-rotor aircraft (based on stability, high level of maneuverability, upgradability, and minimal training time), a GoPro HERO 3 Black edition camera, and a Windows-based tablet PC.

Figure 4-7 Equipment Used for Experiments In-Kind

Figure 4-8 Additional UAV Equipment Used In-Kind

Table 4-12 Weighted Factor Analysis Results for Image Capturing Device

	Criteria	Rank: 1 (Low), 5 (High)	Group Avg.	Weight	Grade 1-5 poor = 1, Fair = 3, Good = 5					Final Weighted Score				
					Hero3 White	Hero3+ Silver	Hero3+ Black	Sony AS15	Flytron FM10X	Hero3 White	Hero3+ Silver	Hero3+ Black	Sony AS15	Flytron FM10X
1	Performance	5, 5, 5	5.000	0.179	3.000	3.000	5.000	5.000	3.000	0.536	0.536	0.893	0.893	0.536
2	Weight	5, 4, 4	4.333	0.155	4.000	4.000	4.000	5.000	4.000	0.619	0.619	0.619	0.774	0.619
3	Dimension	3, 5, 4	4.000	0.143	3.000	3.000	5.000	3.000	4.000	0.429	0.429	0.714	0.429	0.571
4	Price	2, 2, 2	2.000	0.071	4.000	4.000	4.000	3.000	4.000	0.286	0.286	0.286	0.214	0.286
5	Battery life	4, 3, 4	3.667	0.131	5.000	5.000	4.000	4.000	3.000	0.655	0.655	0.524	0.524	0.393
6	Ease of use	4, 4, 4	4.000	0.143	5.000	5.000	5.000	4.000	1.500	0.714	0.714	0.714	0.571	0.214
7	Software compatibility	5, 5, 5	5.000	0.179	4.000	5.000	5.000	4.000	2.000	0.714	0.893	0.893	0.714	0.357
Total			**28.000**	**1.000**	**Average Score**					**3.952**	**4.131**	**4.643**	**4.119**	**2.976**

CHAPTER 5

INITIAL DEMONSTRATION

5.1 SESSION 1

Early in the life of the research project, the research team conducted an initial demonstration on Florida Tech's campus. The objective of this demo was to showcase research progress and to familiarize FDOT with some of the equipment to conduct research tasks. Representatives from FDOT (Research Center and District 5) participated in the demo. The demo was divided into three sessions. The first session included a presentation on UAV safety guidelines/features and capabilities, followed by an open floor for questions. During this session, UAV systems, cameras, gimbals, and varying pilot simulations were showcased. Figure 5-1 shows part of the set up and presentation for the first session of the demo.

Figure 5-1 Demo at Florida Tech - 1st Session

5.2 SESSION 2

The second session included brief indoor flight tests at Florida Tech's gymnasium. Different image capturing devices were demonstrated in their capabilities to stream near real-time images and video data from the aerial systems. UAV performance was also showcased through a controlled wind speed flight test. Figure 5-2 shows some snapshots taken from the second session of the demo.

Figure 5-2 Demo at Florida Tech - 2nd Session

5.3 Session 3

The third session included a mock inspection flight test on an onsite FIT pedestrian bridge, the Columbia Village (CV) Bridge. Pedestrian traffic control was provided by trained individuals from a local Florida UAV firm, whom also provided the experienced, licensed pilot for the flight tests. Figure 5-3 shows some snapshots taken from the third session of the demo.

Figure 5-3 Demo at Florida Tech - 3rd Session

CHAPTER 6

IMAGE QUALITY EVALUATION UNDER VARYING SCENARIOS

6.1 INTRODUCTION

This chapter describes the experimental approach taken –and results obtained—to evaluate UAV flight response in various controlled wind conditions, to measure image quality in different flight scenarios, and to determine image quality in low-light conditions. The main objective was to define parameters and identify limitations that will help to increase the chance that images captured will serve their intended purpose. Image purpose is understood to vary based on specific aspects such as bridge design, construction, and inspection type. As such, limitations based on flight conditions will be documented, but will be left up to the end user to interpret appropriate limitations based on the specific need to be fulfilled.

Comments and suggestions from an experienced PIC at the time of testing were used by the research team to make recommendations regarding initial UAV flight stability conditions and control limits. Further research will attempt to quantify varying levels of pilot experience and adjust levels of flight performance based on measured results. The goal of the quantified scaling factors would be to accurately adjust the allowable flight conditions acceptable to meet certain image quality levels.

In-flight image quality was evaluated in a two-step experimental approach. First, vibration data from camera gimbals (i.e., structure attached to a UAV to hold a camera in place) were captured during flight under different flight scenarios. These data were used to gain understanding about the levels of vibration that cameras are exposed to during flights. Second, cameras were attached to a commercial shaker table to simulate the in-flight vibration frequencies, and used to collect images of particular objects. The quality of the collected images was evaluated and conclusions by the research team were made.

Image quality testing in a low-lighting environment was conducted as an isolated event in order to accurately measure the effects of lighting. Direct light intensity and shadow effects were both tested as the evaluating measures. Further testing would be needed to define field performance with a combination of in-flight image quality with variable lighting.

This chapter is organized into six sections. Section 6.2 describes the UAV vibration testing setup and results. Similarly, Section 6.3 provides details about the camera vibration testing setup and results. These two sections combined were used to evaluate in-flight image quality. Section 6.4 describes testing setup and results from low-light image quality testing. Section 6.5 provides figures and explanation of developed wind profiles. Section 6.6 provides concluding remarks.

6.2 EVALUATING UAV FLIGHT RESPONSE IN CONTROLLED WIND CONDITIONS

The tests conducted to evaluate UAV flight response in controlled wind conditions were carried out using the Arducopter Mega V2.5 hexa-copter (see Figure 4-1). This UAV was chosen based on its capabilities to incorporate multiple sensors, as well as its high level of performance and ease of operation. The copter was flight tested under various controlled wind speeds with high gusts and high pressure gradients. These environmental conditions are expected to be experienced during bridge inspections in the transition of flying at deck level to either above or below the deck surface.

6.2.1 TESTING SETUP

The Florida Tech gymnasium was used as the indoor experimental facility for these tests. This facility provided adequate space and height to safely conduct indoor experiments that required UAV flights. Figure 6-1 shows part of the testing set up, which included two Power Breezer fans that were used in parallel to create high pressure wind profiles. These wind profiles were developed from measurements taken in a designated area measuring 4ft by 12ft in front of the fans (shown in Figure 6-1 as a rectangle area marked with blue tape). Wind speeds in this area were measured and recorded at 3ft intervals perpendicular to the fan's face, and at 1ft intervals parallel to the fan's face, measured 2ft in each direction of the fan's centerline. Wind speed measurements were taken using four Weatherhawk SM-18 anemometers in tandem.

Figure 6-1 UAV Flight Response Tests in Controlled Wind Conditions at FIT Gym

Wind profile data were collected at different fan performance levels by controlling a linear variable control knob integrated into the fans. At each instance of collected data, a wind profile was generated in AutoCAD Civil 3D.

6.2.2 RESULTS

Based on indoor controlled experiments, with constant wind speeds and an experienced UAV pilot, the research team made recommendations regarding minimum UAV-to-object flight clearances for safe operations. These recommended distances are shown in Table 6-1. In wind situations of less than 7 mph on average, and maximum wind gusts of 10 mph, it was acceptable for a UAV to be flown at a distance of 1ft from an object of interest. In scenarios that included average wind speeds of 15 mph, and maximum wind gusts of 20 mph, it is recommended to have a minimum UAV-to-object clearance of 3ft. These results are to be used as suggested flight limitations.

Table 6-1 Minimum Clearance (Object-to-UAV) in Gusty, High Pressure Wind Conditions

Average Wind Speed (mph)	Max Wind Gust (mph)	Clearance Required to Object (ft)
<7	10	1
10	15	2
15	20	3

In a flat, outdoor environment with little to no pressure difference and wind gusts of 15mph, a competent, less experienced operator was able to adequately control the UAV with an object-to-UAV clearance of 2ft. Further testing needs to be done using different UAV platforms in various environments to verify these results and more accurately determine UAV maneuverability in different levels of wind speed.

6.3 In-Flight Camera Vibration Testing

The process to conduct in-flight camera vibration testing was composed of two phases. The first phase involved using the UAV with either a brushless magnetic or servo motor driven camera gimbals (herein referred to as *brushless* and *servo* gimbals, respectively). These two types of gimbals are shown in Figure 6-2. An accelerometer was attached to the gimbals to capture continuous in-flight vibrations, herein referred to as *frequency* or *vibration frequency*, during flight. In the second phase, four image capturing devices were fixed to a shaker table to simulate the frequency responses obtained from the first phase to visually evaluate image quality for bridge or HML inspection purposes. The image capturing devices evaluated during this phase were the FM10X, FM36X, Contour +2, and the GoPro HERO 3 black edition cameras. The testing procedures for in-flight gimbal vibration frequencies and camera image evaluation are detailed in the following sections.

(a) (b)

Figure 6-2 (a) Brushless and (b) Servo Camera Gimbals

6.3.1 Phase 1: Testing Procedure for Gimbal Vibration Frequencies

This phase involved measuring the vibration frequencies at the exact location where the cameras were to be mounted on the gimbals during test flights. In place of the cameras, a tri-axis accelerometer was mounted on the gimbal to capture and store in-flight gimbal vibration frequencies. The accelerometer was coupled with small weights to match the weight of the camera to be tested in order to ensure proper frequency responses. Both the servo and brushless gimbals were tested to determine image quality results for each gimbal-camera pair. Image quality was rated based on a subsequent camera testing, performed at matching frequency levels found for each camera-gimbal combination.

The accelerometer was designed to measure g-force. Known as “true acceleration,” this term measures acceleration in each of the principal directions (X, Y, Z), factoring out any acceleration due to gravity and leaving only additional effects on the accelerometer that would indirectly cause additional weight to an object. Of particular interest from the accelerometer were the maximum displacements experience during flight (amplitude) and the rate at which the cameras would be subject to those displacements (frequency). The raw data were processed from the time to the frequency domain via means of a *Fourier Transform* in order to determine the frequency ranges experienced during any particular test flight. A description of data results from these tests is provided in Section 6.3.3 of this document.

The flight tests conducted to obtain vibration frequency data for this phase were performed in an outdoor environment and with a skilled operator flying the UAV. For each flight test conducted, Table 6-2 shows the type and weight of the camera used, as well as its associated flight speed. Some tests used the same configuration of camera and flight speeds (e.g., tests 1, 13, and 16 in the first row of Table 6-2), but with different gimbal or propeller types. During the time of testing, an average sustained wind speed of 8mph was recorded, with wind gusts of 13-15 mph. These wind gusts represent the maximum levels of wind gust operable with the UAV to maintain a safe operating distance of 2ft away from objects –as determined from the evaluation of UAV flight response in controlled wind conditions.

Flight tests consisted of a predetermined flight plan repeated with different UAV operating speeds. The testing speeds varied to allow flexibility of the operator to determine the optimal flight speed at the time of an inspection. The three operating speeds selected for this test were: slow (1mph), medium (5mph), and fast (10mph). The first flight path of the flight plan included straying left and right for 100ft in each direction, simulating capturing the length of a main girder on a bridge (see Figure 6-3). The second path in the flight plan included a climb and decent to a maximum height of 175ft, simulating inspecting an HML pole.

Tests 1 through 12 were performed using the UAV with a dual axis servo gimbal. This gimbal corrects camera position in the X and Y axis of motion for smoother video and image capture. The camera tilt can be controlled by the flight operator in the Y axis of motion and was used randomly throughout the experiments. Tests 13-15 were performed using the UAV with a dual axis brushless gimbal. The tests were performed in the same order and configuration as tests 1 through 3, with the exception of gimbal type. The brushless gimbal served the purpose of stabilizing the camera position in the X and Y axis of motion for smoother video and image capture. The camera tilt can be controlled by the flight operator in the Y axis of motion. The advantages of the brushless gimbal over the traditional servo gimbal are quicker response times, smoother transitions, and higher precision. However, the magnetic motors are much weaker than their servo counterpart and could only be tested to hold the equivalent weight of a GoPro camera. Tests 16 through 18 were performed as a replication of tests 13-15 with the exception of propeller type. Standard plastic propellers were replaced with carbon fiber propellers to test to effects of a more rigid propeller.

Table 6-2 Phase 1 Flight Test Configurations to Obtain Vibration Frequency Data (18 tests)

Test Number	Camera Model	Camera Weight (grams)	Flight Speed ±1 (mph)
1, 13, 16	GoPro HERO 3 black	70	1
2, 14, 17	GoPro HERO 3 black	70	5
3, 15, 18	GoPro HERO 3 black	70	10
4	FM10X and GoPro with protective case	130	1
5	FM10X and GoPro with protective case	130	5
6	FM10X and GoPro with protective case	130	10
7	FM36X and Contour +2	170	1
8	FM36X and Contour +2	170	5
9	FM36X and Contour +2	170	10
10	Contour +2 with protective case	340	1
11	Contour +2 with protective case	340	5
12	Contour +2 with protective case	340	10

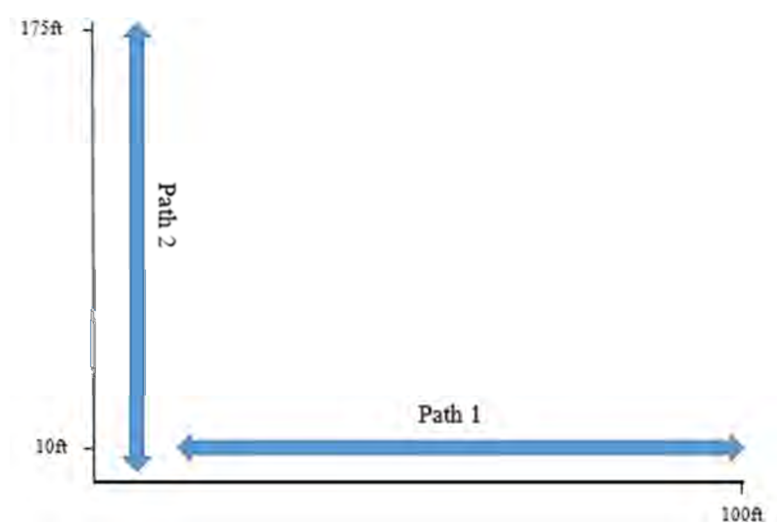

Figure 6-3 Vibration Flight Tests (Flight Plan Paths)

6.3.2 Phase 2: Testing to Evaluate Image Quality on Simulated Vibration Frequencies

Phase 2 image quality testing was conducted separate to the flight tests in an indoor environment. Camera image responses were measured by using a scaled image with multiple reference points representing the three different AASHTO reference concrete crack sizes. A Data Physics V20 shaker table attached to a RIGOL DG2041A waveform generator, shown in Figure 6-4, was used to match the frequency ranges found during the flight test portion of this experiment. The different cameras were mounted individually at fixed distances and angles intervals. For each setup, the cameras were shaken at 25Hz intervals over the entire expected range of 50-250Hz vibration during flight. Cameras were also tested at 10Hz, representing the lowest frequency realistically experienced during flight (excluding take-off, landing, and other extreme events not typical of normal UAV operation). The cameras were positioned towards the center of the reference image and set to record during testing. Upon video review, maximum camera resolution was determined based on the clarity of the reference image. Maximum camera resolution was recorded for each frequency interval.

Figure 6-4 Data Physics Shaker Table (left) and RIGOL Waveform Generator (right)

6.3.3 Results

Image quality was tested at the different frequency levels experienced during phase 1 of testing. The flight tests results were separated by gimbal type to determine if there were any measurable differences between effect results captured on the servo and brushless gimbals. The tests were also separated into camera weight test groupings to determine any adverse effects of camera weight on the structure and to match the phase 2 image quality results with the phase 1 experienced frequencies. The frequencies that yielded the best image quality in phase 2 were isolated and compared to the phase 1 flight tests to determine the optimum gimbal and flight speed for a specific camera. From this process, a comprehensive list can be made of optimal equipment combinations for specific end-user need (i.e., use a zoom capable camera with gimbal x flying at y speed with capabilities of seeing z resolution in omega levels of light).

6.3.3.1 Servo-controlled Gimbal

Figure 6-5 shows frequency responses for tests of all different camera weights performed on the servo gimbal. It was determined that the weight of the camera being tested controlled the frequency response more so than the speed at which the UAV flew. This phenomenon was expected when considering the varying levels of work that the mechanical servos have to perform on the different weighted cameras.

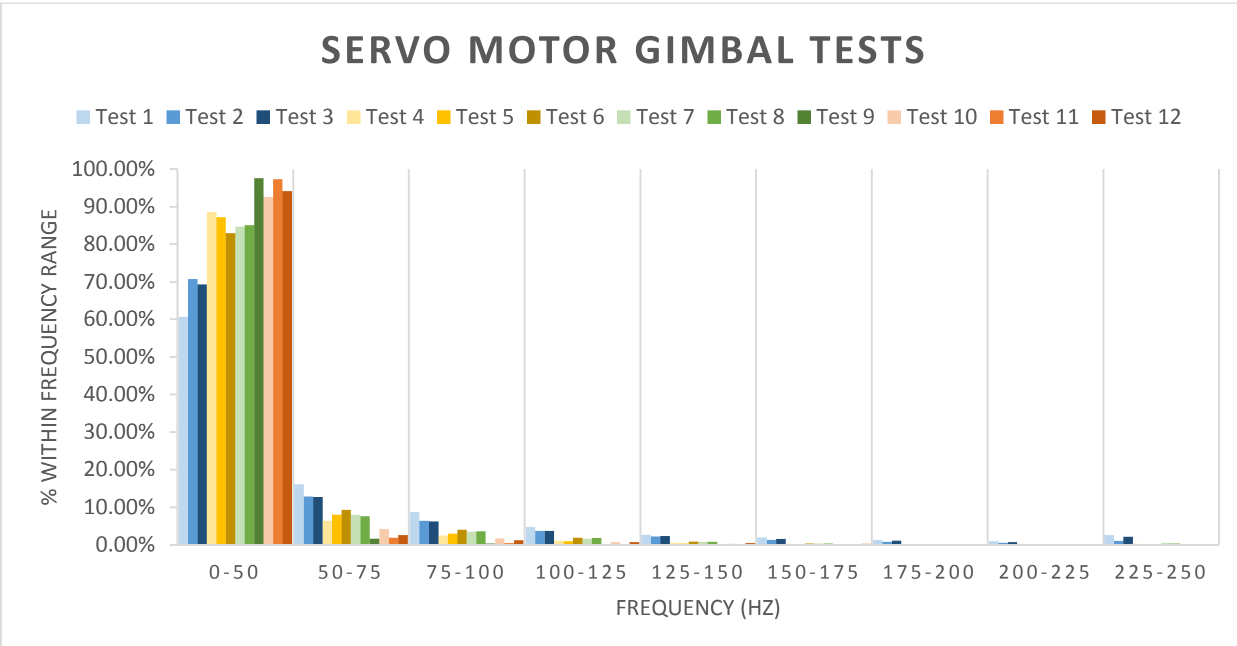

Figure 6-5 Percent of Frequencies Measured in Specific Ranges for the Servo Motor Gimbal

Table 6-3 lists the limitations on camera position to an object. This table also shows the portion of time that an acceptable frequency range was recorded in which the different cameras were able to maintain an image quality capable of detecting a moderate crack size in a given posture. Based on 2010 AASHTO bridge element inspection guidelines, moderate crack sizes range between 0.02 and 0.08 inch wide. Each of the cameras tested had the ability to capture a moderate crack size with an acceptable distance and attack angle towards an object of interest over 90% of the time during all test flights.

Table 6-3 Percentage of Acceptable Camera Frequency at Specific Camera Positioning

Camera	Camera Tilt (degrees)	Maximum Distance to Target (ft)	Percent Within Optimal Range
GoPro HERO 3 black	0, 30, 60	4, 4, 4	>93%
FM10X	0, 30, 60	4, 4, 3	>94%
FM36X	0, 30, 60	4, 4, 2	>91%
Contour +2	0, 30, 60	4, 2, 2	>97%

6.3.3.2 BRUSHLESS GIMBAL

Due to motor capacity limitations, the brushless gimbal was only able to carry the weight of the GoPro. The six tests performed with this weight configuration, shown in Figure 6-6, only varied by flight speed and propeller type. Overall, the brushless gimbal experienced higher amounts of the lower frequency than its servo driven counterpart. Counter-intuitive to what brushless gimbals are known for, these data could be indicative of the low weight limit of the motors being reached. Newer iterations of this gimbal have since admitted this fault, which leaves this experiment open for further testing. The carbon fiber propeller data fit the advertised offerings of a smoother ride with quicker response at lower throttle levels, as backed by the pilot at the time of testing. Although the cameras can work within the ranges of frequencies measured, frequency responses above the 0-50Hz level are desirable as it is shown to drastically reduce video shuttering and improve frame by frame image quality.

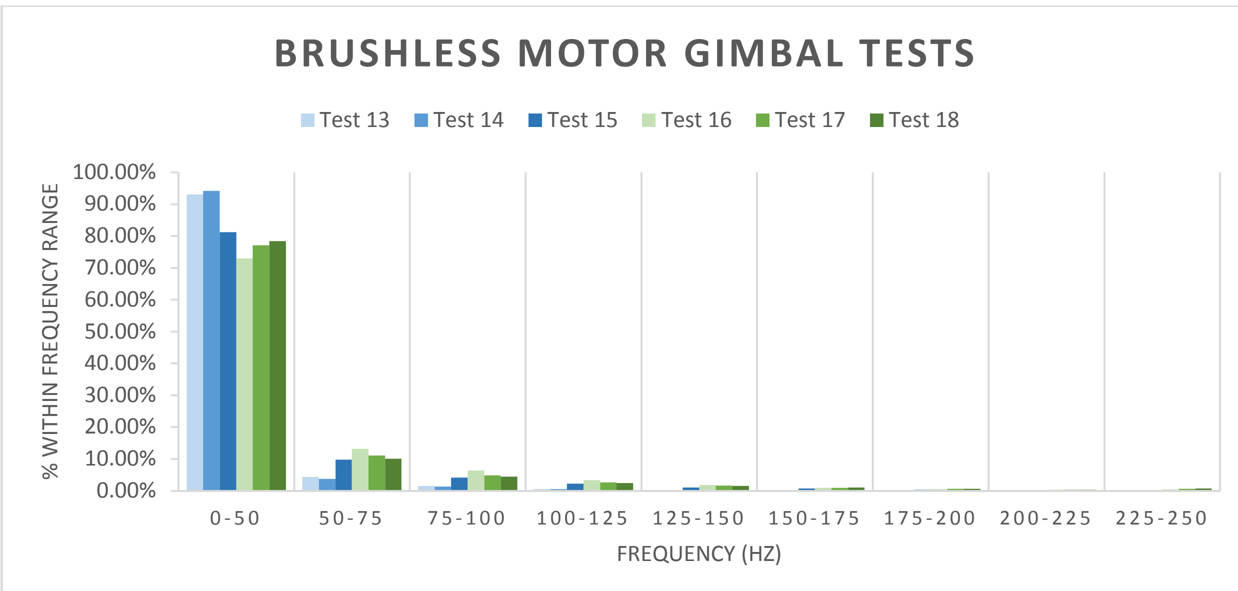

Figure 6-6 Percent of Frequencies Measured in Specific Ranges for the Brushless Motor Gimbal

The addition of carbon fiber propellers resulted in at least 90% of the frequencies to be less than 100Hz, but the 0-50Hz bin decreased in size again. While more testing is needed to draw firm conclusions, upon first glance the carbon fiber propellers with a brushless gimbal seem to give the steadiest ride for all tested flight speeds.

6.3.3.3 GOPRO HERO 3 BLACK

Figure 6-7 shows the results obtained by testing with the GoPro camera. The image quality testing showed that this camera would be able to detect a moderate crack at a distance of 4ft or less from the target. This resolution can be achieved at any preset resolutions tested at 1080p or above and at angles of up to 60 degrees while being subjected to frequencies below 125Hz. All configurations of gimbals and propellers met this performance requirement at or above the 90% mark. The resolution can be achieved with or without the protective case.

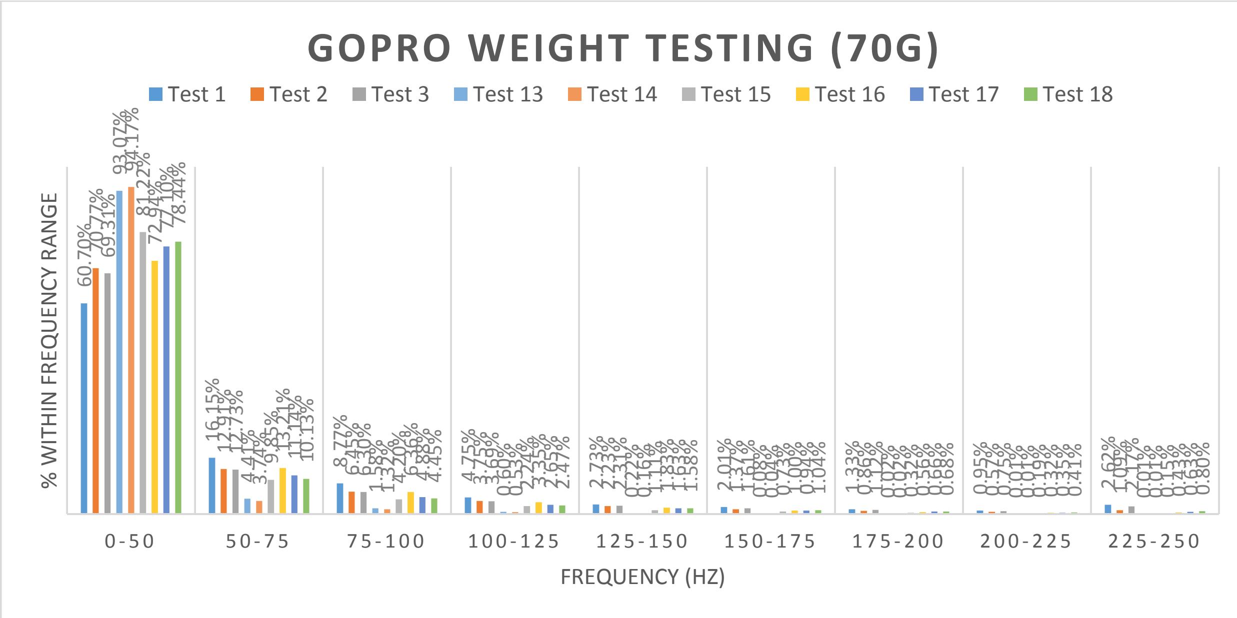

Figure 6-7 Frequency Ranges Experienced by Testing All Gimbals with GoPro Weight

6.3.3.4 FM10X

Figure 6-8 shows the results obtained by testing with the FM10X camera. This camera was found to work best under a frequency of 150Hz, at or under and angle of attack of 30 degrees, and at a distance of up to 4ft from the target. Although this camera has a resolution of only 700tvl, its zoom capabilities allow it to see a resolution down to the moderate crack size, given the aforementioned conditions. The current version of the brushless gimbal could not support the weight of this model camera; nonetheless, the servo driven gimbal provided an appropriate frequency for this camera.

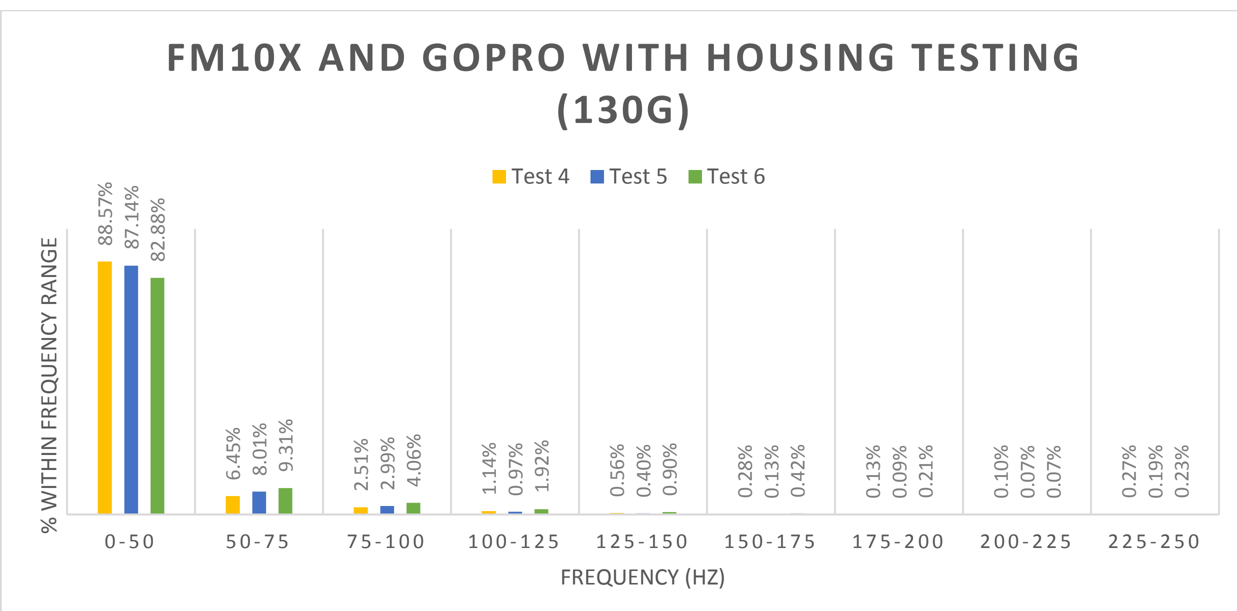

Figure 6-8 Frequency Ranges - Testing Servo Gimbal for FM10X and GoPro with Housing Weight

A drawback of this type of camera is the need for an external battery source and transmitter that would have to be mounted to the UAV. This extra weight lowers the overall UAV flight time. Constant user input would also be required to maintain proper zoom levels on the camera. This camera can benefit the system by adding an additional live-stream that could be monitored by an outside party member to the operator. This additional party member would also be able to control the optical zoom to alleviate the pilot's tasks.

6.3.3.5 FM36X

Figure 6-9 shows the results obtained by testing with the FM36X camera. At or under a viewing angle of 30 degrees, the FM36X worked best at all frequencies except those in the 75-125Hz range, where it could otherwise detect a moderate crack width. This frequency range accounted for less than 10% of the frequencies generated during the flight tests (i.e., under 10% frequency in the range of 62.5-137.5Hz). This camera can be a great option for inspecting HMLs, in particular, those poles and structures that extend over the highway and require an optical zoom.

As with the younger version of this camera, the FM10X, there is a need for an external battery source and transmitter which would have to be mounted to the UAV. This extra weight lowers the overall UAV flight time and would require constant user input to control the zoom level of the camera. Similar to the FM10X, this camera can benefit the system by adding an additional live-stream that could be monitored by an outside party member to review and operator. This additional party member would be able to control the optical zoom of the camera.

6.3.3.6 CONTOUR +2

Figure 6-10 shows the results obtained by testing with the Contour +2 camera. This camera was capable of capturing moderate crack size widths while taking angled video at 30 or 60 degrees, but only up to 2ft from the target. At 0 degrees, this camera can achieve a maximum resolution able to detect a moderate crack from up to 4ft away. A drawback of this camera is its shear bulk, weighing over two times the weight of GoPro camera. The benefit of this camera comes when the requirement of geo-locating is at task. This camera compresses its images with GPS encoding built into each frame. This technology allows the user to review images and be able to determine the exact location of the image and other reference objects in the frame. This technology could greatly benefit an initial inspection where this information is needed for verification or position. Further testing would be needed to verify to precision and accuracy of this feature.

6.4 LOW-LIGHT IMAGE QUALITY TESTING

A set of indoor experiments were performed to evaluate the ability of the cameras to perform in low-light conditions. The cameras were tested individually while being held fixed at the maximum distance in which that particular camera could see a desired resolution. A "desired resolution" was defined as the crack size range of a moderate severity rated crack.

The lighting conditions were controlled with a combination of an industrial grade light dimmer, controlling two 75 watt LED dimmable light bulbs, and by casting a shadow over the test area. Upon initial review, shadow impairment had a visible effect on image quality during testing –although not all cameras were affected equally by this visual impairment. The lighting levels were measured continuously with a Digital Illuminance/Light Meter. The light output at the point of testing was measured at 30 lux, equivalent to the lighting at dusk. The lowest output of light tested was 1 lux, which is equivalent to twilight.

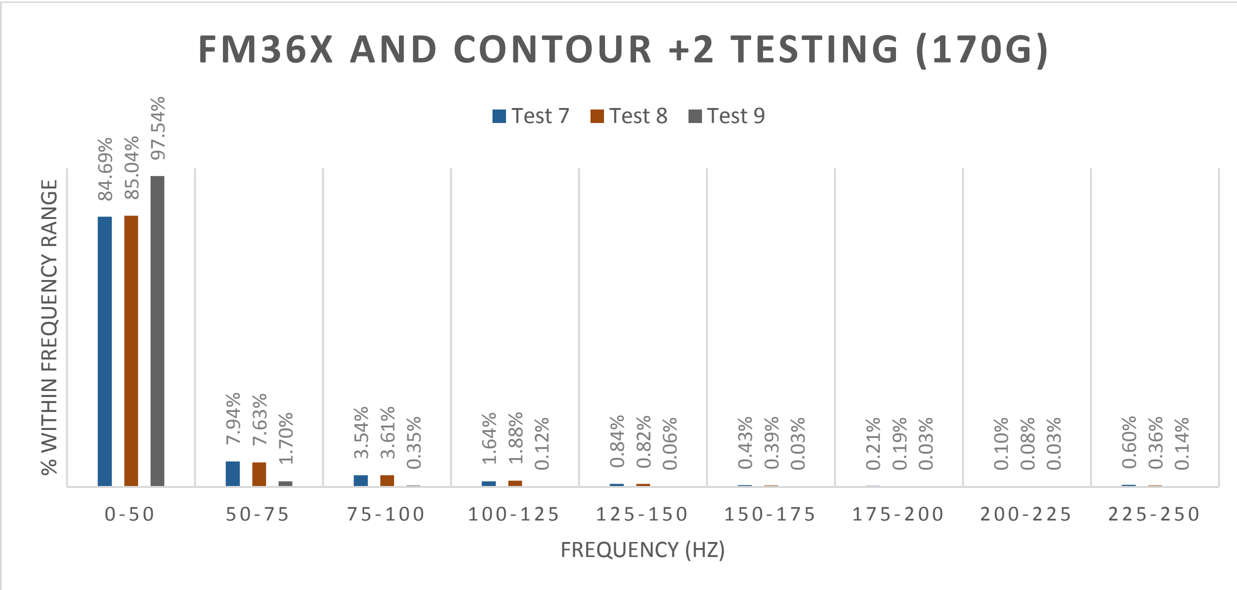

Figure 6-9 Frequency Ranges - Testing Servo Gimbal for FM36X and Contour +2 Weight

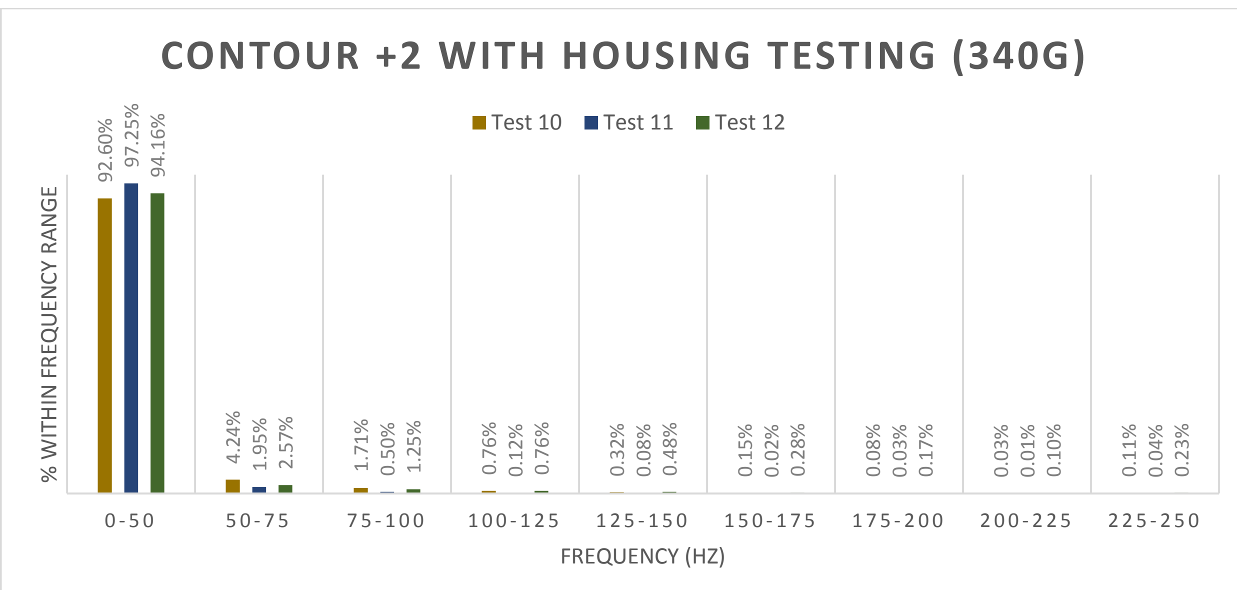

Figure 6-10 Frequency Ranges - Testing Servo Gimbal for Contour +2 with Housing Weight

For comparison purposes, light levels were measured under a bridge with a solid concrete deck to ensure no light penetration. Here, light levels were measured at 250 lux during midday hours. Between the hours of 7:30 and 7:35 AM (Eastern Time) on September 6, 2014, the light levels dropped from two to one lux. Readings were taken at the farthest eastward girder above the abutment where the lowest levels of light were recorded. Figure 6-11 shows the test site and conditions at the time of testing.

Figure 6-11 Low-Light Reference Measurement Benchmark Site

6.4.1 GoPro HERO 3 Black

The GoPro camera was tested at the same resolutions as the previous image quality tests: 4k, 2.7k, 1440p, and 1080p. The test was conducted in the aforementioned lighting conditions at an elevated height of 3ft from the same reference image used in the image quality testing, as shown in Figure 6-12. The GoPro struggled to achieve a 0.08" resolution under 24 lux when testing at 2.7k, 1440p, and 1080p; however, when tested at 4k, the image quality held at under 0.08" down to the 14 lux lighting levels. While night-time flying would be out of the question with this camera in this current configuration, alternate proposals can be made to increase camera capabilities in low-light scenarios. Such alternate proposal could be artificial enhancement of the images/video through specialized software, adding additional luminary devices to the UAV, or a combination of the proposed ideas. Future GoPro editions have rumored to dramatically increase low-light video and image quality.

6.4.2 FM10X

The FM10X with zoom capabilities was a top performer in the low-light testing. At a distance of 4ft from the reference image, zoomed in with 4x magnification, the FM10X maintained a constant level of resolution able to see down to a moderate crack size at a lux level down to one and including a shadow effect. Further testing would be required to test this capability during a real flight scenario under various conditions, but initial low-light testing results have shown to be very promising, as advertised by the manufacturing company.

Figure 6-12 Low-Light Testing (Lux Meter (left), Reference Image (center), and Scale (right))

6.4.3 FM36X

The FM36X with zoom capabilities was also a top performer in this test. At a distance of 4ft from the reference image, zoomed in with 4x magnification, the FM36X maintained a constant level of resolution able to see down to a moderate crack size at a lux level down to one, shadow effect included. More impressive was the ability for this camera to detect colors at lux levels as low as five, demonstrating a new technology not implemented in its younger counterpart, the FM10X. The FM36X also out-performed its counterpart in the image quality testing, making it a prime candidate for future testing.

As mentioned in the image quality testing, the major downfall of this system is the added weight of the additional transmitting equipment necessary to operate, and the necessity of a second user to monitor and control camera zoom. Its performance benefits and operability disadvantages are both significant based on the performance benchmark initially proposed for the criteria evaluation of a successful UAV platform. This camera provides a unique benefit to the system that could not otherwise be achieved; however, the cost associated with this setup would vary based on the situational need of its use.

6.4.4 Contour +2

The Contour +2 camera maintained color contrast down to 7 lux, but lost resolution quality under 24 lux when tested at 3ft from the reference image. Practical application of this camera can be realized when inspecting and mapping the bridge deck surface. The advanced geo-locating, coupled with the color contrast present in low-light environments, present a unique toolset required to inspect a bridge deck for defects such as efflorescence, discoloration, deflection, and spalling. These unique camera characteristics present an opportunity to conduct further research on its usability to detect the aforementioned defects.

6.5 Generated Wind Profiles

Figure 6-13 and 6-14 show wind contour maps based on data collected from the Power Breezer industrial fan testing. These maps were created using AutoCAD Civil 3D. Each data point can be read, from top to bottom, as the reading number, the wind speed recorded in mph, and the wind speed setting on the fan being tested. The points are situated such that the bottom most center point represents the center of the fan's face. Each point parallel to the fan's face was taken at 2ft intervals, and each point taken perpendicular to the fan's face was taken at 3ft intervals. Another way to read the figures is to view them as a typical contour map, where each line represents a single wind speed. For example:

- Reading number 34 in Figure 6-13(a) shows that at a fan speed setting of five, with a distance of 3ft perpendicular to the fan, and a distance of +2ft parallel to the centerline of the fan, the average wind speed recorded over 10 seconds was 3.70 mph.
- Reading number 63 in Figure 6-13(b) shows that at a fan speed setting of seven, with a distance of 6ft perpendicular to the fan, and at the centerline of the fan face, the average wind speed recorded over 10 seconds was 17.0 mph.
- Reading number 91 in Figure 6-14(a) shows that at a fan speed setting of 9, with a distance of 9ft perpendicular to the fan, and a distance of -4ft parallel to the centerline of the fan, the average wind speed recorded over 10 seconds was 0.60 mph.
- Reading number 124 in Figure 6-14(b) shows that at a fan speed setting of 10, with a distance of 12ft perpendicular to the fan, and a distance of +2ft parallel to the centerline of the fan, the average wind speed recorded over 10 seconds was 15.80 mph.

6.6 CONCLUSION

The research results presented in this document provide evidence that an sUAS can be adequately operated in high pressure zones, maintain safe flying proximity of 2-3 feet to a target, and can detect crack sizes down to 0.02 inches. These findings, coupled with the ability to maintain adequate resolutions under relatively low-light conditions, highlight the high potential practical value from using UAV systems to assist bridge and HML inspectors during field inspections.

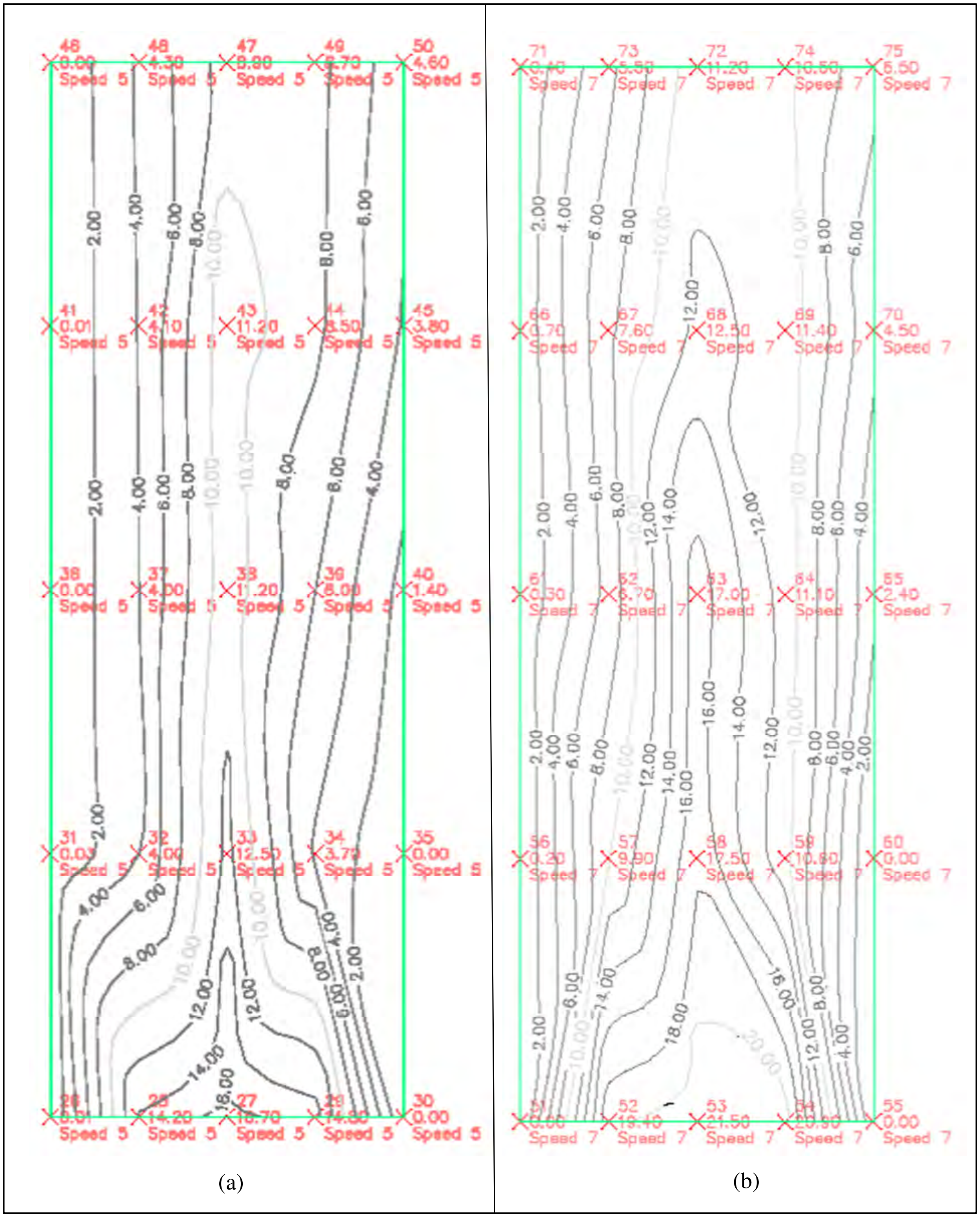

Figure 6-13 Power Breezer Wind Profiles Generated from (a) Speed Setting 5 and (b) 7

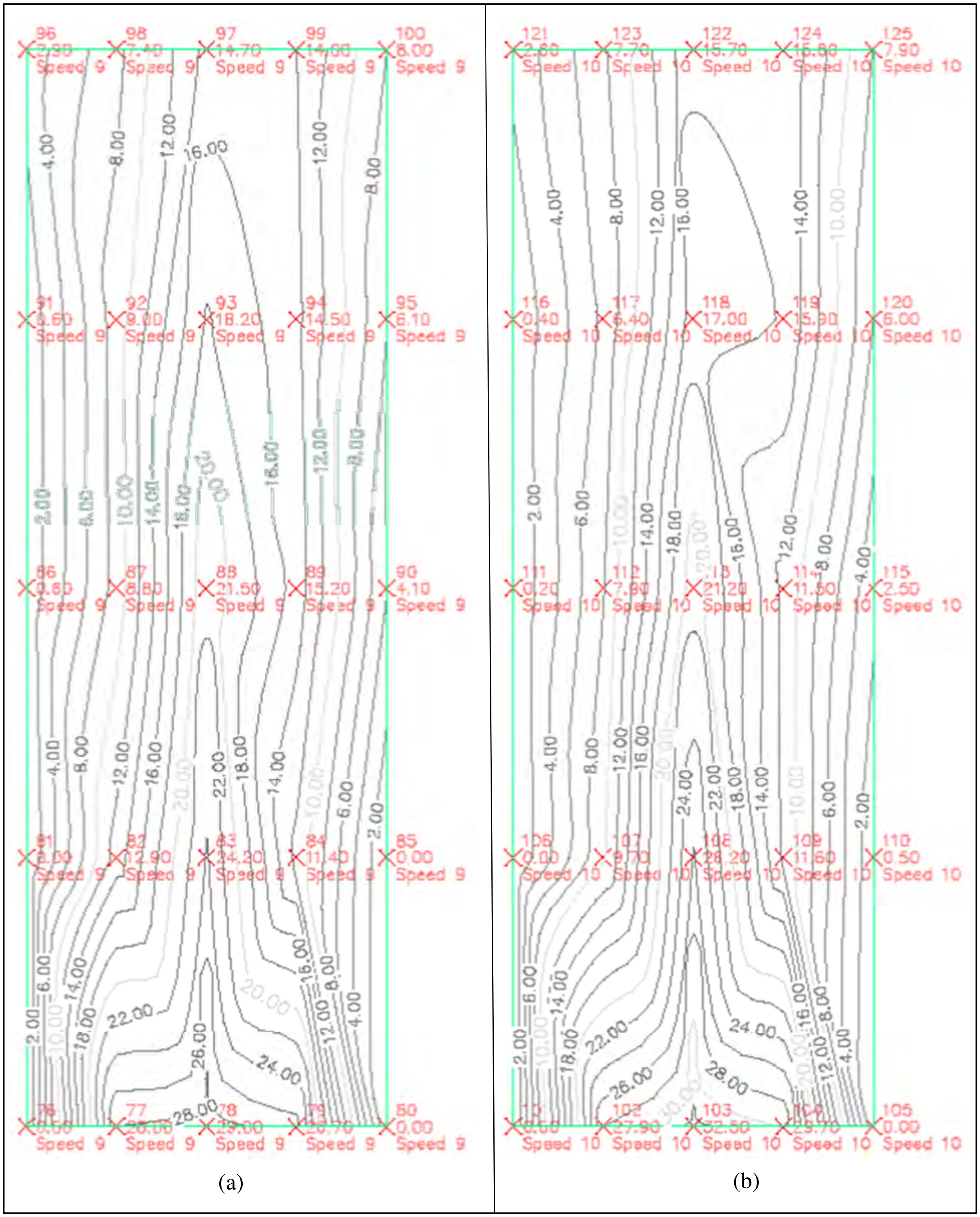

Figure 6-14 Power Breezer Wind Profiles Generated from (a) Speed Setting 9 and (b) 10

CHAPTER 7

Conduct UAV Component Evaluation

7.1 Introduction

This chapter describes the approach –and results obtained—to evaluate the main sUAV system selected for this research project for various environmental conditions and mission objectives (see Figure 4-1). Various propeller types, battery types, and configurations were used in the evaluation of this sUAV to estimate its maximum working altitude, motor power capabilities, battery life expectancy under different loads, and maneuverability constraints. The popular DJI Phantom Vision +2 quad-copter, shown in Figure 4-4, was also tested and compared to the hexa-copter where possible.

This chapter is organized into five sections. Section 7.2 describes the UAV altitude tests conducted by the research team. Sections 7.3 and 7.4 describe the executed payload and maneuverability tests, respectively. Each of these sections describes testing setup and results. Section 7.5 provides concluding remarks.

7.2 Altitude Testing

Altitude tests were carried out using both the hexa and quad-copters. These two copters represent choice copters of two different size and complexity categories. Both UAVs were tested on the same day, operated by the same pilot, and evaluated on maneuverability and visibility criteria at various altitudes. The UAVs were flown below 400ft during all test flights to satisfy current flight guidelines. Figure 7-1 shows a snapshot of the hexa-copter during some of the altitude experiments.

Figure 7-1 Hexa-Copter in Test Field Area (viewed by quad-copter's camera)

7.2.1 Testing Setup

Altitude experiments were held on a partly cloudy day with wind gusts of up to 15mph. The hexa-copter was set to monitor the following telemetry information:

- Battery performance
- UAV orientation
- GPS position
- Altitude

Telemetry data were read through a ground station (i.e., Microsoft Surface 3 Pro tablet PC) and monitored by a non-piloting person. The same telemetry data were monitored for the quad-copter during flights using a smartphone and DJI's package software application. It should be noted that the pilot wore glare resistant sun-glasses during all altitude testing.

Altitude tests involved the following:

- Flying the UAVs straight up at 50ft intervals
- Flying in random patterns to change aircraft orientation
- Determining if the operator was able to discern aircraft orientation

The pilot was required to repeatedly tell a telemetry monitoring person the copter's orientation during flight. This person would then compare the pilot's understanding of the copter's orientation with the true orientation data read from the ground station. In cases where the pilot was unable to successfully determine copter orientation, the pilot lowered the copter to attempt to discern the orientation, which was again verified against data from the ground station. This same procedure was performed for the range test on a horizontal scale.

7.2.2 RESULTS

The pilot relied on two approaches to determine copter orientation. One approach was to focus on the colored light-emitting diode (LED) lights that copters typically have. Figures Figure 7-2 and Figure 7-3 show the LED lights that are installed on the hexa and quad-copters, respectively. The second approach was to use the assistance of a smartphone as first-person-view (FPV). That is, a video transmitter on the copter would feed live stream data that would be shown by the smartphone in near real-time. Figure 7-3 shows the radio controller set up with a smartphone used as FPV for the quad-copter.

With the LED lights turned on, the hexa-copter was able to fly at an altitude of 250ft before the pilot – after a series of random, disorienting flight patterns –needed the assistance of ground station read-outs or flight checks to know the copter's orientation. A flight check involved flying the UAV left for a short distance, followed by flying right another short distance. This procedure allowed the pilot to regain a sense of aircraft orientation without the help of the ground station read-outs. Below 200ft, the pilot was able to determine the orientation of the hexa-copter solely with the copter's LED lights. These results were true for the hexa-copter when flying against a clear or cloudy sky; however, the quad-copter being tested blended against a cloudy sky above 100ft.

The effect of flying UAVs with the assistance of FPV systems was also evaluated during altitude testing experiments. When experimenting with the quad-copter in FPV mode, the pilot was able to keep copter orientation at the maximum allotted altitude of 400ft. Accurate sense of flight orientation was influenced by the pilot's familiarity with the surroundings shown real-time with the packaged software read-out on the FPV screen. The same was true for testing on a horizontal scale up to 1,500ft, which is the horizontal range factory limit for this particular quad-copter. Identical results were obtained when testing with the hexa-copter in FPV mode.

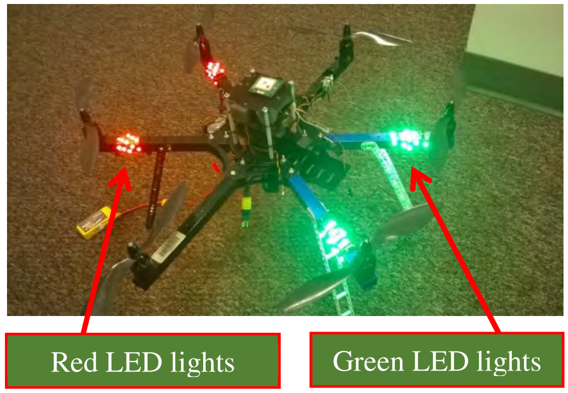

Figure 7-2 LED Lights (hexa-copter)

Figure 7-3 LED Lights and FPV (quad-copter)

7.3 Payload Testing

Payload tests were conducted with the hexa-copter. An open-source ground control software application called *Mission Planner* was used to plan, save, and load autonomous missions with simple point-and-click way-point entry on Google maps (see Figure 7-4). Utilizing this GPS-guided software application to establish the same mission area for each flight test helped to reduce any experimental noise that may have resulted from varying flight patterns.

In an open field, the flight plan was coordinated and saved into Mission Planner to be recalled for each battery-weight setup. To block out external weather conditions, battery testing was carried out in a random manner in terms of battery tested and weight applied. The following subsections describe the setup procedures and results for these tests.

Figure 7-4 Snapshot of the Mission Planner Software

7.3.1 TESTING SETUP

The hexa-copter was tested in its bare configuration with only GPS and telemetry hardware. To this bare weight configuration, additional payload was added in 0.5lbs increments to simulate different equipment configurations. Figure 7-5 shows the hardware setup for incremental weight payload testing.

Telemetry link was established to the copter via a ground station link with the necessary software to read flight characteristics such as battery voltage, amperage draw, and used capacity measured in milliampere-hours (mAh). The telemetry link also set and saved the flight plan for each battery test. The flight plan consisted of taking off from a GPS-linked location, climbing to an altitude of 25ft, flying forward 350ft to a second GPS linked location, climbing an additional 15ft, and then returning to its initial GPS-linked location for one completed loop. The time to complete one loop, the number of completed loops, and the amount of battery capacity to complete any and all completed loops were recorded for post analysis.

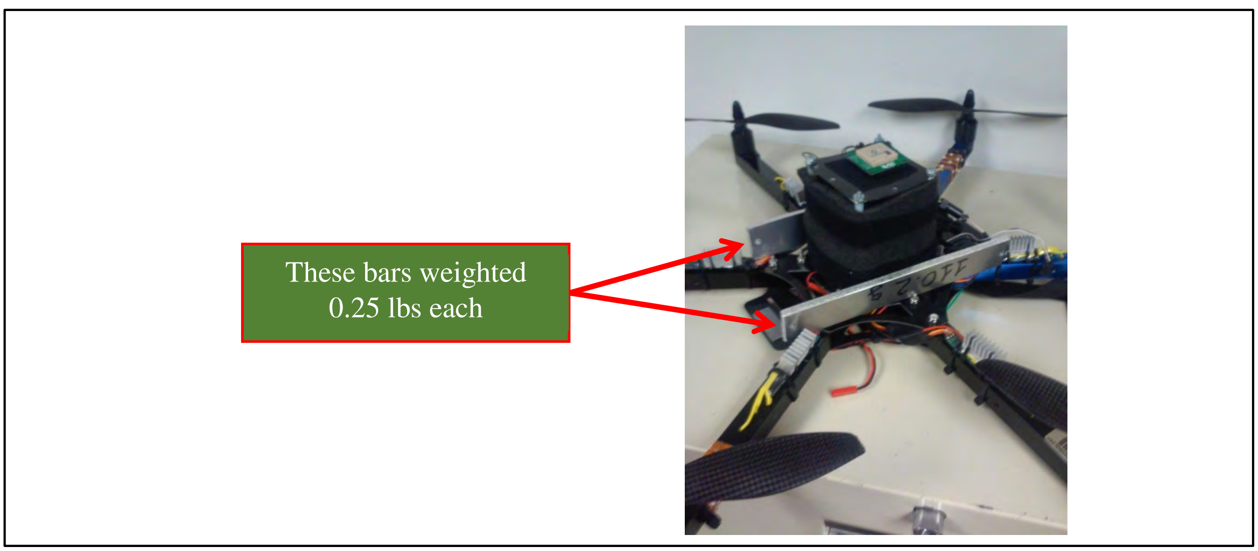

Figure 7-5 Hardware Setup for Payload Testing (incremental weight)

7.3.2 RESULTS

Various types of batteries were evaluated during this testing phase. The input parameters considered were capacity and total payload weight (i.e., battery plus added experimental weight). The output parameter considered was maximum flight time. Figure 7-6 depicts the performance of the tested small-to-midsized batteries based on their total capacity and flight duration. The legend in the figure shows battery capacity, added payload, and battery type: Zippy (ZY), Thunder Power (TP), Max Amp (MA), or Poly Quest (PQ). The steeper the line in the graph, the quicker and less efficient the battery discharge rate was. The last data point in each line represents an estimation of flight time based on unused battery capacity projected from the highest recorded discharge rate measured during the given flight test. Safe practice dictates that flights should be terminated when reaching a threshold of 20 percent remaining battery life; therefore, flight time was collected when there was 20 percent remaining battery life for each flight.

Table 7-1shows maximum flight times for each small-to-midsized battery configuration. The "Added Weight" column represents any payload weight excluding the battery weights (e.g., cameras or other imaging sensors). Without any camera weight, the results showed a maximum hexa-copter flying time of 14.36 minutes. With 0.5 lbs payload weight (which is the weight of the GoPro Hero 3 camera plus a weather proof case), the results showed a maximum hexa-copter flying time of 10 minutes. The maximum flying times with 1.5 and 2 lbs were 8.23 and 7.52 minutes, respectively.

Propeller type was also tested among the battery tests. The first test conducted involved the 7700 mAh batteries. Figure 7-6 shows experiments with the 7700 mAh TP battery using plastic propellers (TP) and with carbon fiber propellers (TP2). The data collected showed approximately a minute and thirty seconds of additional flight time, which represented a significant 10 percent gain. This gain prompted all consecutive tests to be conducted using only carbon fiber propellers.

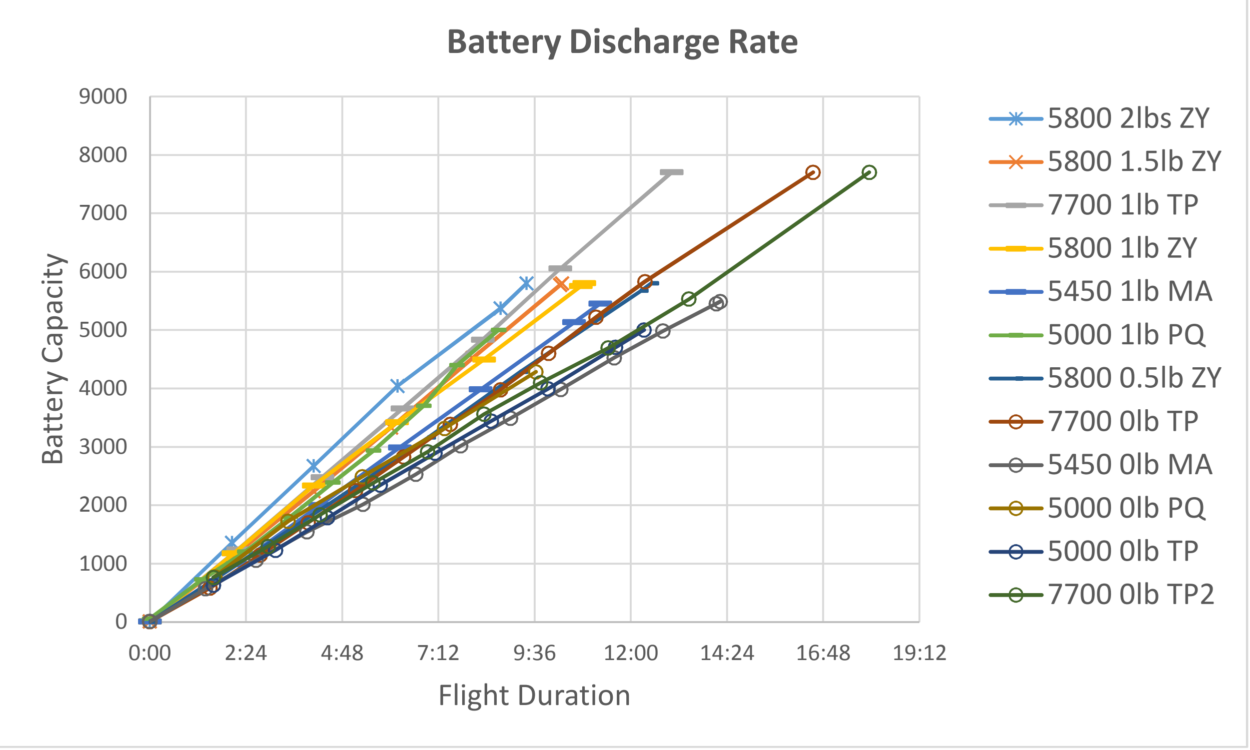

Figure 7-6 Midsize Battery Performance

Table 7-1 Midsize Battery Performance

Battery	Capacity (mAh)	Battery Weight (lbs)	Added Weight (lbs)	Total Payload (lbs)	Maximum Flight Time After Draining Battery (minutes)	Maximum Flight Time with 20% Battery Life (minutes)
Thunder Power	5000	1.02	0	1.02	12.33	9.87
Polyquest	5000	1.26	0	1.26	11.02	8.81
Polyquest	5000	1.26	1	2.26	8.70	6.96
Max Amp	5450	1.10	0	1.10	14.13	11.31
Max Amp	5450	1.10	1	2.10	11.23	8.99
Zippy	5800	1.25	0.5	1.75	12.52	10.01
Zippy	5800	1.25	1	2.25	10.83	8.67
Zippy	5800	1.25	1.5	2.75	10.28	8.23
Zippy	5800	1.25	2	3.25	9.40	7.52
Thunder Power	7700	1.72	0	1.72	17.95	14.36
Thunder Power*	7700	1.72	0	1.72	16.55	13.24
Thunder Power	7700	1.72	1	2.72	13.00	10.40

* Plastic Propellers

Additional tests were performed with larger batteries and comparable smaller batteries wired in parallel. Wiring two batteries in parallel lessens the load on any single battery by allowing a slower draw of power from each of the batteries' four cells. This slower draw of power allows a more uniform discharge rate across each of the batteries cells, prolonging the life of the batteries. In the cases of low capacity batteries, pairing the same batteries in parallel increases the maximum amount of draw for the copter by splitting the required power equally among the batteries.

Figure 7-7 shows the performance of the large batteries and midsize batteries that were tested in parallel. The legend in the figure gives the battery capacity (followed by a P for parallel tests), added payload, and battery type: Zippy (ZY), Thunder Power (TP), or Max Amp (MA).

Table 7-2 shows maximum flight times for each large-sized battery configuration. Without any camera weight (i.e., zero added weight), the results showed a maximum hexa-copter flying time of 24.47 minutes. With a payload weight of 1.0 lbs, which is more than enough to easily carry a GoPro Hero 3 camera plus a weather proof case on a stabilizing gimbal, the results showed a maximum hexa-copter flying time of 20.17 minutes.

7.4 Maneuverability Testing

Maneuverability tests for this testing phase were an extension of the initial wind tests described in Chapter 6. While the wind testing benchmarked the copters ability to fly at different wind speeds, the second part of the maneuverability tests focused on different levels of operator experience and its influence on flight in confined spaces. The testing setup and results for the quad and hexa-copters are presented in the following subsections.

7.4.1 Testing Setup

Initial wind testing was conducted indoors in a controlled environment. A highly turbulent wind flow was introduced to the testing area via two industrial Power Breezer fans configured in parallel to produce a testing area measuring approximately 6ft wide by 5ft high by 12ft long. Controlled wind speeds were measured with four Weatherhawk anemometers in parallel to the fans' face at fixed intervals. The designated testing area was marked with a high visibility tape to allow the operator a frame of reference in which to fly while giving the observing party a marker with which to associate different wind speeds.

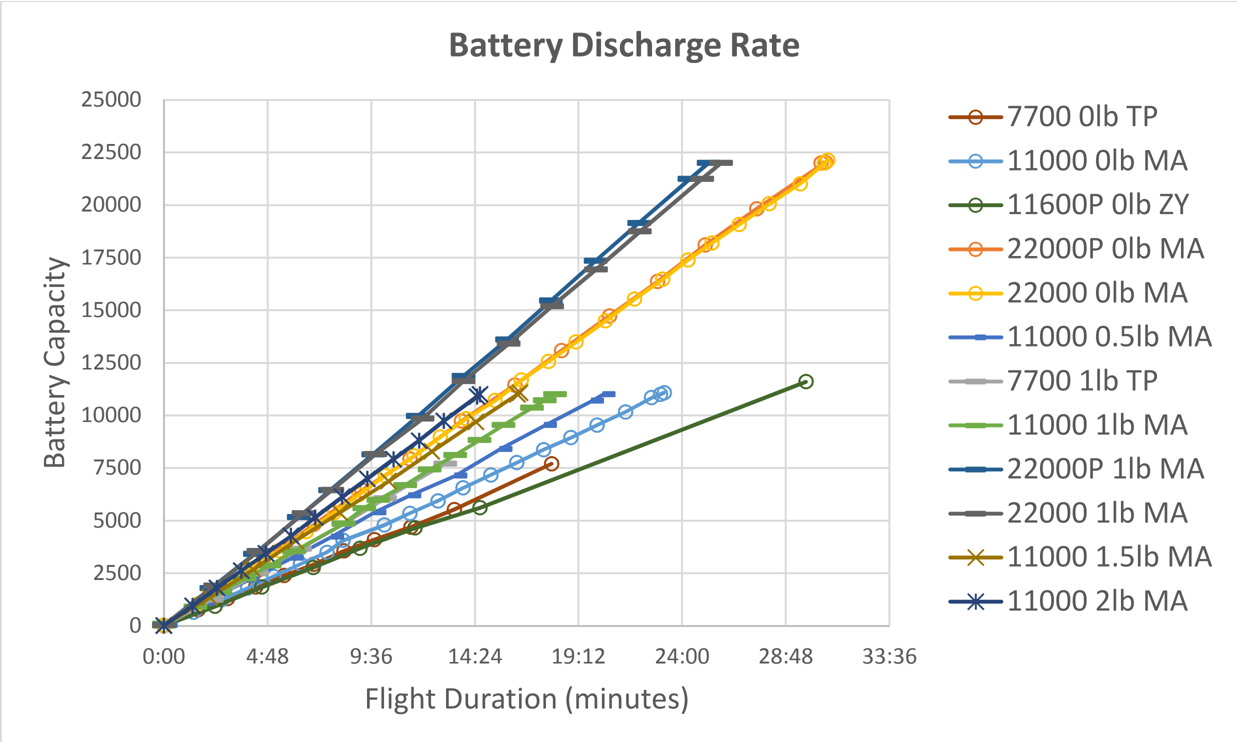

Figure 7-7 Large Battery Performance

Table 7-2 Large Battery Performance

Battery	Capacity (mAh)	Battery Weight (lbs)	Added Weight (lbs)	Total Payload (lbs)	Maximum Flight Time After Draining Battery (minutes)	Maximum Flight Time with 20% Battery Life (minutes)
Thunder Power	7700	1.72	0	1.72	17.95	14.36
Thunder Power	7700	1.72	1	2.72	13.00	10.40
Max Amp	11000	1.90	0	1.90	23.00	18.40
Max Amp	11000	1.90	0.5	2.40	20.35	16.28
Max Amp	11000	1.90	1	2.90	18.10	14.48
Max Amp	11000	1.90	1.5	3.40	16.37	13.09
Max Amp	11000	1.90	2	3.90	14.63	11.71
Zipppy x2	5800 x2	2.50	0	2.50	29.73	23.79
Max Amp	11000 x2	3.80	0	3.80	30.43	24.35
Max Amp	11000 x2	3.80	1	4.80	25.22	20.17
Max Amp	22000	3.80	0	3.80	30.58	24.47
Max Amp	22000	3.80	1	4.80	25.80	20.64

The two fans were controlled by a linear control knob. Three basic flight maneuvers were performed and characterized at varying wind speeds. The first flight maneuver consisted of flying into the highly turbulent wind flow from above, and then below the test area. The second flight maneuver was to maintain flight within the designated testing area while demonstrating copter control. The final maneuver involved flying the copters perpendicular to the fan in the direction of increasing wind speed such that copter operations were inhibited due to the wind.

Further maneuverability testing involved determining the required clearance around the UAVs needed to perform a range of maneuvers and to determine if operator experience had a significant impact on the clearance required. Maneuvers included flying in a straight line within the bounded area in both forward and sideways copter orientations, and turning the copter 180 degrees within the bounded area to simulate capturing video within a confined area. Furthermore, a level of risk was associated with maneuvers performed based on the subjectivity of the copter operator and third party observer. Risk was assessed based on the ease of operation with which the copter was able to perform within the area, measured against the ability of the operator to recover the craft during flight within the bounded area shown in Figure 7-8.

Figure 7-8 Maneuverability Testing

7.4.2 Results

Based on indoor maneuverability tests under constant wind speeds of 15mph, it was concluded that the hexa-copter could be properly operated by a skilled operator at a minimum clearance of 3ft from a target. Under constant wind speeds of 18mph and wind gusts of 21mph, it was concluded that the hexa-copter could be properly operated by a skilled operator at a minimum clearance of 5ft from a target.

Based on outdoor maneuverability tests using a highly skilled operator, it was concluded that the hexa-copter could be properly operated through a 6ft opening (i.e., between girders), with a 1.5ft distance of clearance in any direction. The quad-copter also required a clearance of 1.5ft in any direction from an object (i.e., 5ft opening) to fly with the same level of comfort. Due to the small form factor, the quad-copter could also be properly operated through a 4ft opening in the hands of a highly skilled operator. In the hands of a moderately skilled pilot, the hexa and quad-copters required 2.5ft clearance in any direction, resulting in an opening of over 7ft and 6ft, respectively.

7.5 Conclusions

The research results presented in this document support the use of UAVs to assist in bridge and HML inspections. Altitude, payload, and maneuverability tests were conducted using quad and hexa-copters to understand performance and limitation parameters that would directly relate to the use of UAVs for transportation infrastructure inspections. Altitude testing results showed that FPV systems provide a pilot the capability to easily detect copter orientation up to at least 400ft vertically and 1,500ft horizontally. These tests also showed that the maximum vertical distance to reliably detect copter orientation is significantly limited (250ft for the hexa-copter) if relying only on the copters' LED lights. Payload testing results showed that in one case, carbon fiber propellers resulted in a 10 percent increase in flight time. These tests also resulted in a table that shows maximum flight times as a function of battery type, battery configuration, and payload weight. Maneuverability testing results showed that the hexa-copter could be properly operated by a skilled operator at a minimum clearance of 3ft from a target and with constant wind speeds of 15mph. These tests also showed the minimum dimensions required to properly fly the hexa and quad-copters through tight areas (e.g., in-between girders from a bridge's superstructure that supports the bridge's deck).

CHAPTER 8

CONDUCT HML POLE FIELD TESTING AND DEFECT EVALUATION

8.1 INTRODUCTION

The research team conducted field tests to collect HML image data using sUAV systems equipped with high-definition cameras. The main objective of this task was to provide proof-of-concept evidence on the use of sUAVs to assist inspectors during the inspection process of HML structures. These HML proof-of-concept tests were first performed on the main campus of Florida Institute of Technology (FIT or Florida Tech). HMLs at FIT's baseball field were used as targets for evaluation in order to establish a testing process. Once the testing process was in place, FDOT District 5 personnel and the FIT research team conducted various field tests on HMLs owned by FDOT. Data collected from these HML field tests were evaluated to determine the usability of UAVs to show various defect types.

This chapter is organized into four sections. Section 8.2 describes the experimental procedures and results from conducting field tests with HMLs at the Florida Tech campus. Similarly, Section 8.3 describes the experimental procedures and results from conducting field tests with FDOT-owned HMLs. Section 8.4 provides concluding remarks. Appendices A and B show snapshots of HML sections from the field tests conducted with HMLs owned by FDOT.

8.2 HML FIELD TESTS CONDUCTED AT FLORIDA TECH

Two preliminary field tests were carried out on Florida Tech grounds under controlled conditions. The objectives of these tests were to evaluate the operation of in-house customized gimbals, understand the level of maneuverability required to capture live data of HML elements in an open field with varying winds speeds, and establish a general testing process for subsequent field tests with FDOT inspectors.

8.2.1 FIELD TEST #1 – BRIEF DESCRIPTION AND OBJECTIVES

The HML inspected during the first field test was 90ft high with a 15-light structure clamped onto a galvanized steel pole (shown in Figure 8-1a). An objective of this test was to determine operating conditions at high altitudes in order to validate previously conducted indoor tests regarding safe operating distances to maintain from the structure. Another objective was to gain understanding on operator vantage locations to conduct flights around HML structures. Prior to initializing the remote sensing aerial platform, the research team held a meeting to go over safety rules and plan of operations. Immediately following the briefings, the research team proceeded to the setup location, shown in Figure 8-1b.

The remote sensing aerial system from Figure 4-1 was tested in two different configurations. The first configuration included flexible propellers to steady copter movements through ascents and descents. The second configuration included rigid propellers to provide additional compensation to gusty scenarios. Each configuration included a high-definition camera to take images of slip-joints, light fixtures, and light supports.

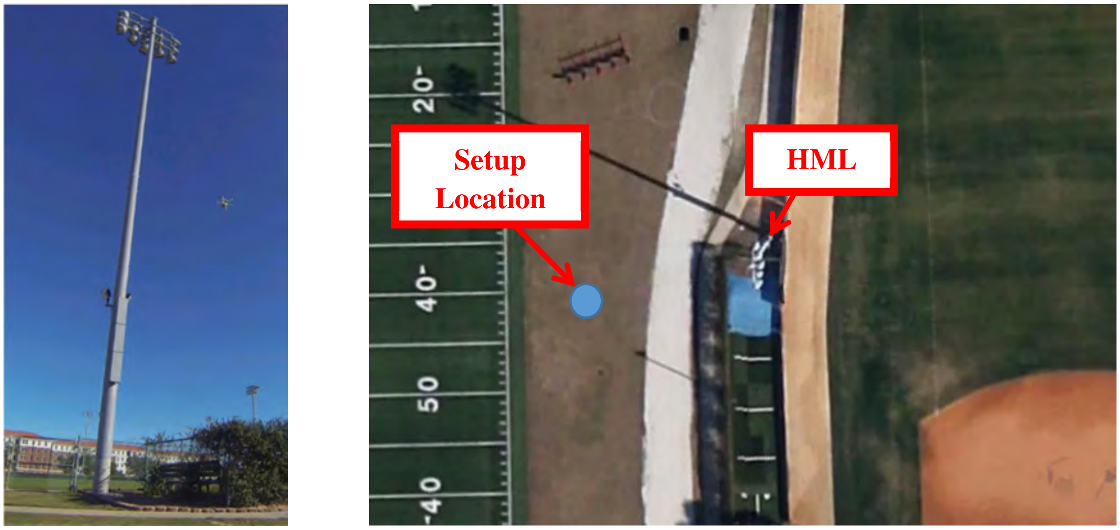

(a) (b)

Figure 8-1 (a) 90ft Galvanized Steel HML with 15-Light Structure (b) Top View of Setup Location

8.2.2 Field Test #1 – Summary of Results

Figure 8-2 shows an example of an image captured during flight. Images were processed through free software provided by the high-definition sensor used for data capture. Post-processing included zoom and removal of image distortion, otherwise known as fish-eye.

Figure 8-2 Sample HD Image Extracted from Sensor Data

Figure 8-3 shows an example of a close-up image focusing on a single light fixture of the HML. This figure illustrates the capability of capturing high-definition images from vantage points not otherwise accessible from a ground-based visual inspection. Figure 8-4 shows the light support structure in its entirety. Post-flight analyses determined that a pre-defined flight-path should be determined to optimize the data capturing process to include 100% coverage of the HML structure in an optimized manner.

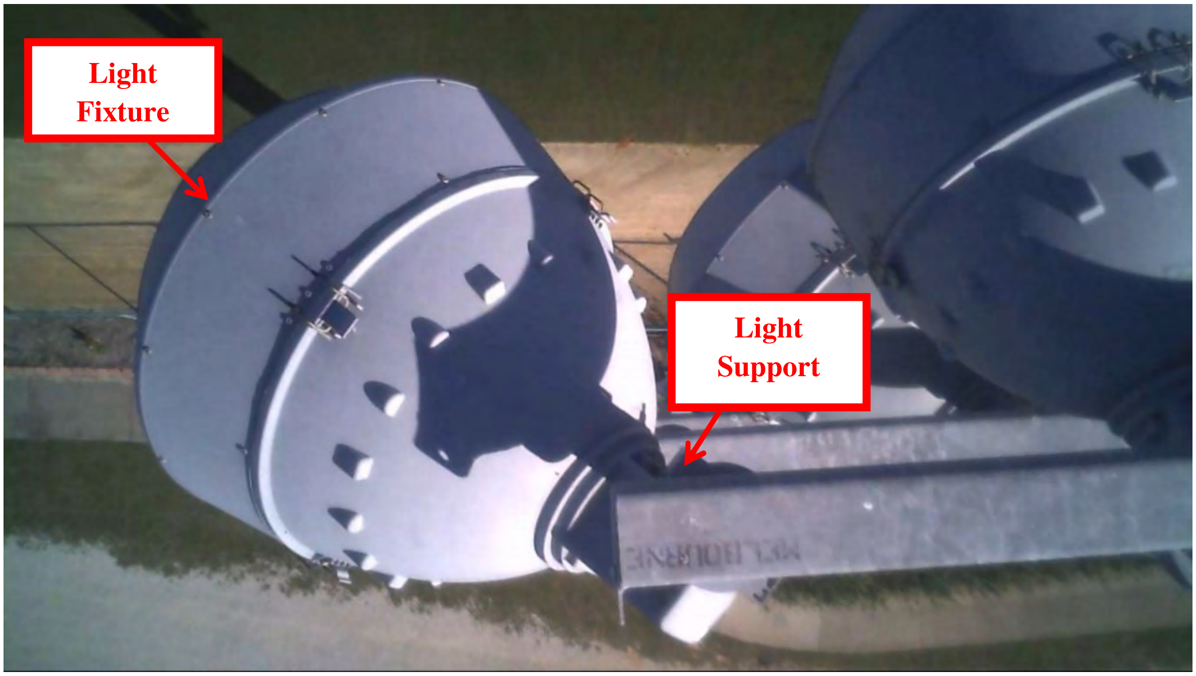

Figure 8-3 Close-up Bird's Eye HD Image of Light Fixture

Figure 8-4 Light Fixture Support and Mounting Structure

The average wind speed during this field test was 10mph, with maximum wind gusts of 20mph. A clearance of around 4ft between UAV and HML was easily maintained during flight. The closest clearance that was attempted by the team was around 2ft, which was successfully maintained for a period of 30 seconds. This particular test was performed to show successful maneuverability of the sUAV in such close proximity to the HML structure. Using a GoPro Hero 3+ Black Edition camera, a clearance of 5ft was more than adequate to obtain high-quality images that could be fully used for HML inspection purposes.

8.2.3 Field Test #2 – Brief Description and Objectives

The HML inspected during the second field test was 90ft high with an 8-light structure clamped onto a galvanized steel pole. The primary objective of this field test was to determine an optimal flight pattern to capture HML components from the base of the HML to the top of the light fixtures. The following three flight patterns were evaluated:

- Pattern 1: *Circle Around*
  This pattern involved flying around HML sections in 5ft height increments.
- Pattern 2: *Constant Spiral*
  This pattern involved spiraling upward around an HML.
- Pattern 3: *Up, Down, and Around*
  This pattern involved flying straight up and down the pole in the North, South, East, and West facing directions, followed by circling the light fixtures.

Prior to initializing the remote sensing aerial platform, the research team held a meeting to go over safety rules and plan of operations. Immediately following the briefings, the research team proceeded to the setup location.

Two different remote sensing aerial systems were used during this field test. The first system was a smaller UAV with a standard high-definition sensor (see Figure 8-5a). The second system was a medium-sized, fully built in-house UAV with an advanced high-definition imaging sensor capable of capturing video at four times the standard high-definition rate (see Figure 8-5b).

Figure 8-5 Small and Medium-Sized Quad-Copters

8.2.4 Field Test #2 – Summary of Results

Figure 8-6 shows an example of an image captured during flight with the medium-sized sUAV, which was equipped with the 4k resolution high-quality camera. Figure 8-7 shows images that were captured with the smaller of the platforms tested, which included a high-definition camera with a resolution of up to 1080p. While this platform was able to get close enough to the HML such that the images did not have to be modified in any post-processing program, a highly experienced operator was required to operate the platform under such wind conditions and at such close proximity (i.e., 2ft) to the HML to capture these images. Figure 8-8 shows a top view of the HML light structure, which was easily captured with the aerial system.

Figure 8-6 Sample Light Fixture Image Captured from HML Inspection

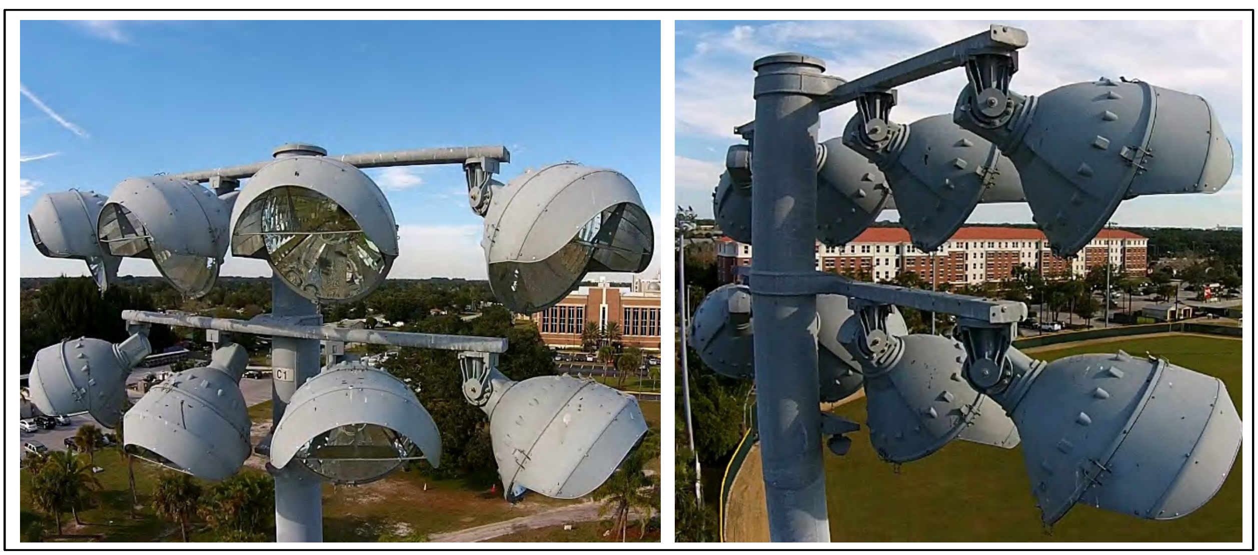

Figure 8-7 Front and Back Views of the HML Light Support Structure

Various flights were conducted to collect data and determine an optimal flight pattern to capture HML components from the base of the HML to the top of the light fixtures. Pattern 1 yielded excellent results in terms of area coverage and defect location referencing. However, Pattern 1 tests resulted in the longest total flight duration with an average of almost 13 minutes. Pattern 2 tests yielded weak results, requiring various flight tests to be coordinated to cover the entire HML structure. Identifying defect location during post-processing was difficult because of the spiral upward movements around the HML. Pattern 3 tests yielded excellent results in terms of full constant coverage of the HML structure, and defect location referencing. Pattern 3 tests also resulted in the shortest average total flight duration of 8.5 minutes. Based on these results and after discussions with FDOT inspectors regarding their current practice of describing defect location by a compass direction and approximate elevation, Pattern 3 was selected for subsequent field tests with HMLs owned by FDOT.

Figure 8-8 Top View of Light Structure

8.3 HML FIELD TESTS CONDUCTED AT FDOT SITES

The Florida Tech research team joined FDOT inspectors during routine inspections of two HML structures owned by FDOT. The first structure was a weathering steel HML, and the second one was a galvanized pivot mount HML (see Figure 8-9). The following subsections provide a description of the objectives of each field test and the results obtained.

8.3.1 WEATHERING STEEL HML – BRIEF DESCRIPTION AND OBJECTIVES

The Florida Tech research team participated in a field test with FDOT inspectors to collect image data of an HML located on the south bound exit ramp of SR528 onto SR417. The HML was approximately 120ft high with a 4-light structure bolted atop a weathering steel pole. Before the remote sensing platform was initialized, a preliminary safety briefing and plan of operations meeting was held by the team. Based on the recommendations of the FDOT inspectors, the primary focus of this field test was on the three slip joints (SJ) and wires in the light structure.

8.3.2 WEATHERING STEEL HML – SUMMARY OF RESULTS

Figure 8-10 highlights the electrical box with its four sheathed wires. Figure 8-11 highlights foreign debris fixed on the top of the light structure and its slip critical bolts/nuts. Figure 8-12 provides an overall picture of the light structure including wires, lights, and structural components. These figures offer varying perspectives of the expressed areas of concern by the FDOT inspection crew.

(a) (b)

Figure 8-9 FDOT-Owned HMLs

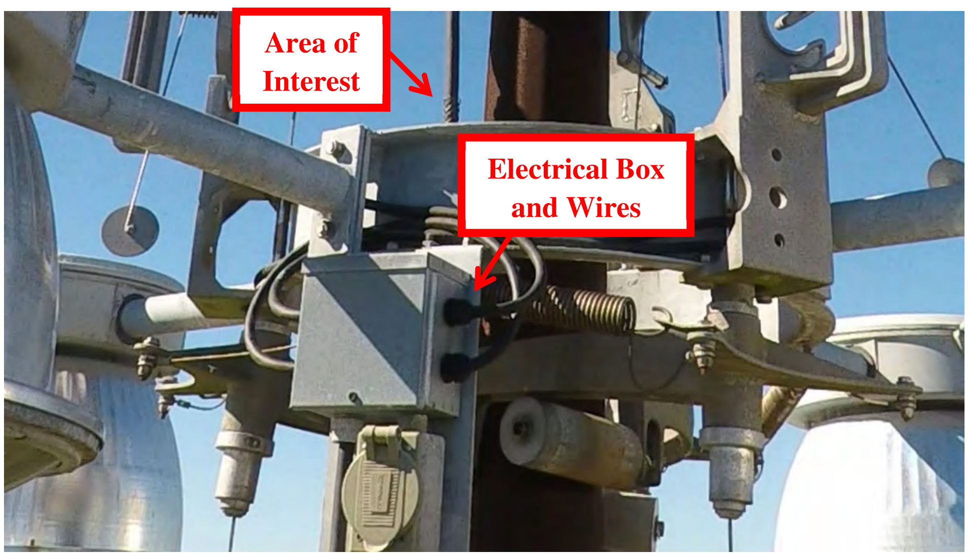

Figure 8-10 East Face Light Structure (bottom)

The expressed concern of exposed wires was investigated with the remote sensing platform. The yellow arrow in Figure 8-12 shows a wire mesh-like covering over the main wire extending from the top of the light structure to the junction box on the light structure; however, no exposed wires were found, except the unsheathed steel cables (shown with a red arrow).

Figure 8-11 East Face Light Structure (top)

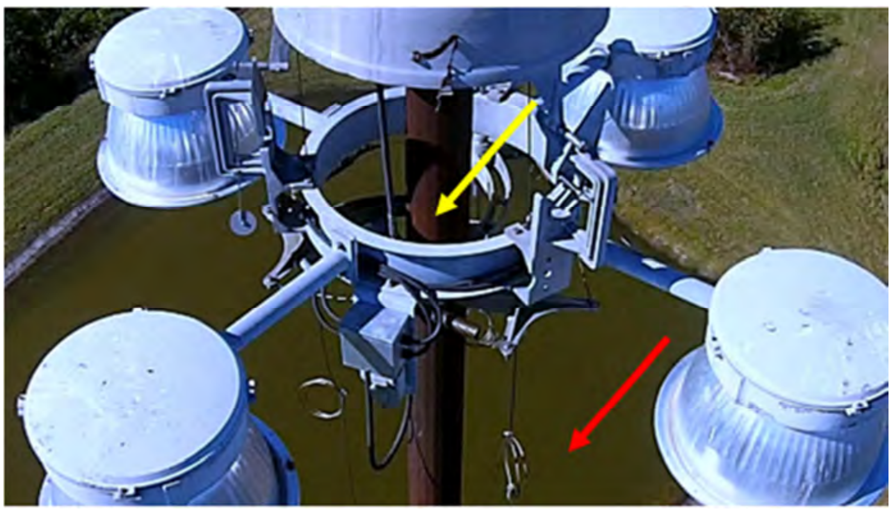

Figure 8-12 East Face Light Structure (complete)

Figure 8-13 show areas where the patina had been scratched off of the pole. The location on the pole of these defects are noted by the direction the pole is facing and the location relative to the SJ, where SJ 1 represents the first slip joint from the base of the structure and SJ 3 represents the top-most SJ in the structure. Figure 8-13b shows a pair of smaller scratches through the patina above SJ 2. While much smaller than the scratch found below SJ 1, these scratches still represent an eventual loss of section as the steel weathers to protect the exposed area with another layer of patina. Figure 8-13c shows cracks above SJ1 (circled in red), which represent areas of concern that should be investigated as to their depth and severity. For a more complete list of images offering varying perspectives on the aforementioned defects and critical areas, please refer to Appendix A.

(a) (b) (c)

Figure 8-13 Scratch Through Patina (a) Below SJ1 (b) Above SJ1 (c) Possible Steel Crack Above SJ1

8.3.3 GALVANIZED PIVOT MOUNT HML – BRIEF DESCRIPTION AND OBJECTIVES

The Florida Tech research team participated in a field test with FDOT inspectors to collect image data of an HML located on the SR528 east bound exit ramp onto SR520. The HML was approximately 120ft high with a 4-light structure bolted atop a galvanized steel pole. Before the remote sensing platform was initialized, a preliminary safety briefing and plan of operations meeting was held by the team.

Two main objectives were identified based on the recommendations of an experienced FDOT inspector. The first objective was to collect image data of difficult-to-inspect locations. Of particular interest was to capture images of the top of the HML. Emphasis on this location also resulted from prior meetings with FDOT bridge inspectors and engineers. Currently, the inspection process to reach locations documented in the proposed methodology requires special equipment to lower the entire HML or to hoist an inspector over 120ft into the air. The second objective was to obtain close-up high-definition images of the slip joints.

8.3.4 GALVANIZED PIVOT MOUNT HML – SUMMARY OF RESULTS

Two small aerial platforms, each equipped with different high-definition cameras, were used to focus on key points of the HML. The different sensors took images of these difficult-to-inspect locations around each of the four luminaries. Total duration flight times averaged 12 minutes per flight. Figure 8-14 shows a still frame that was extracted from a video, with post-processing zoom being the only correction done to the image.

Figure 8-15 shows an example of a light fixture with impact damage to the enclosure. No other damage was detected on the light fixture at the time of inspection. Figure 8-16 shows an example of a missing cover plate screw in the west facing light fixture. This instance may pose potential issues to the light fixture as water may enter through the void and potentially corrode and/or cause the other contained equipment to spark and ignite.

Figure 8-14 Top of Light Fixtures

Figure 8-15 Cosmetic Impact Damage to Light Fixture

8.4 CONCLUSION

This document presents information regarding field tests conducted by the Florida Tech research team to collect image data of HML structures using small aerial systems equipped with high-definition imaging sensors. Two field tests were conducted at the Florida Tech main campus, and two were performed on FDOT selected sites. FDOT inspectors participated in the field tests and provided critical information based on their experience that lead to establishing clear objectives for each mission. The main objective of this task, which was to provide proof-of-concept evidence for using sUAV systems to assist inspectors during the inspection of HML structures, has been achieved. The research team recommends conducting further field tests to analyze data regarding the duration of complete HML inspections.

Figure 8-16 Missing Cover Plate Screw on West Light

CHAPTER 9

CONDUCT UNDERSIDE BRIDGE FIELD TESTING AND DEFECT EVALUATIONS

9.1 INTRODUCTION

The research team conducted field tests to collect image data of bridges using small sUAV systems equipped with high-definition cameras. The main objective of this task was to provide proof-of-concept evidence on the use of sUAVs to assist inspectors during the inspection process of highway structures. These proof-of-concept tests were first performed on the main campus of Florida Tech. Bridges at Florida Tech's main campus were used as targets for evaluation in order to establish a testing process. Once the testing process was in place, FDOT District 5 personnel and the Florida Tech's research team conducted various field tests on bridges owned by FDOT. Data collected from these field tests were evaluated to determine the usability of UAVs to show various defect types.

This chapter is organized into four sections. Section 9.2 describes the experimental procedures and results from conducting field tests on bridges at the Florida Tech campus. Similarly, Section 9.3 describes the experimental procedures and results from conducting field tests on FDOT-owned bridges. Section 9.4 provides concluding remarks.

9.2 BRIDGE FIELD TESTS CONDUCTED AT FLORIDA TECH

Two preliminary field tests were carried out on Florida Tech grounds under controlled conditions. Throughout these tests, the sUAVs utilized were modified, adjusted, and tested in an iterative process. The objectives of these tests were to:

- Conduct rigorous testing of equipment, proper positioning of the sensors, and proper sUAV maneuverability to capture live data of bridge defects
- Evaluate the capability of sUAV systems to assist in the inspection of main joists, underside bracings, light mast supports, and hard-to-reach bridge areas
- Evaluate the capability of sUAV systems to serve as an inspection tool in low-rise structures with dense overgrowth and weed
- Demonstrate reasonably safe flight conditions

Figure 9-1 shows snapshots of the two bridges where the field tests took place. The following subsections provide a description of each field test and a summary of results.

9.2.1 FIELD TEST #1 – BRIEF DESCRIPTION AND OBJECTIVES

The CV Bridge was the target for the first field test conducted at Florida Tech's campus. This small pedestrian bridge was built over a narrow stretch of Crane Creek. The bridge contains an underside steel support structure with notable rust where paint had peeled off. Therefore, the main focus of this field test was to evaluate the current sUAV equipment configuration and determine the level of detail capable of being captured –on the steel structure below bridge deck level –with various onboard sensors. Particular structural areas of interest were the floor beams, the underside bracing, and the light mast support of the bridge, since these are considered hard-to-reach areas for inspectors.

(a) (b)

Figure 9-1 Bridges at FIT: (a) Underside CV Bridge (b) Wooden Pedestrian Bridge

The research team held operational and safety meetings –including flight plans –prior to initializing the remote sensing aerial platform. The safety briefing included fail-safe plans, responsibilities of each team member, minimum clearance tolerances, and crowd control over the bridge. Figure 9-2 shows an aerial photo of the setup and bridge location.

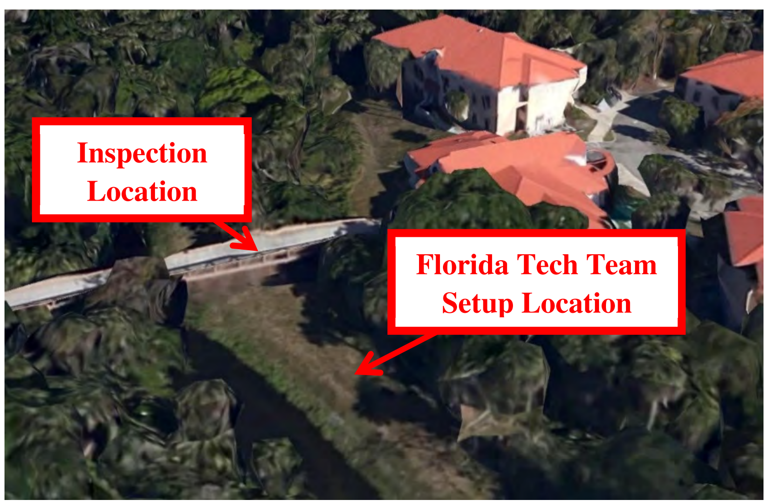

Figure 9-2 Equipment Setup and Field Test Location

The remote sensing platform used for this field test was equipped with a high-definition camera mounted to the bottom of the platform, interfaced to a two-axis stabilizing gimbal. The sensor was inclined to its maximum range in order to capture data of the underside of the bridge.

9.2.2 FIELD TEST #1 – SUMMARY OF RESULTS

Figure 9-3 shows some of the common defects found during this field test. Images were all captured within three separate flight clips taken, totaling less than 15 minutes of video needed to be edited. Defects captured during flight were merely extracted from the video frames. Post-processing of the videos was done to remove image distortions (i.e., "fish-eye" distortion) caused by the ultra-wide lens used on the camera.

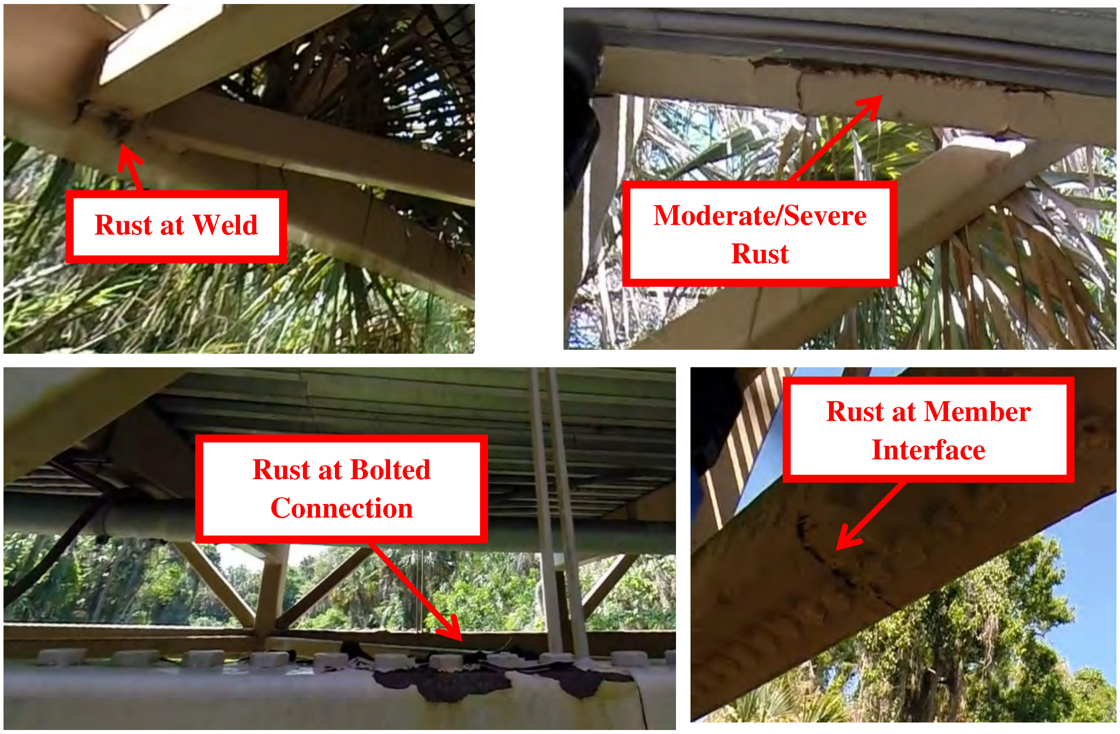

Figure 9-3 Defects Detected with Remote Sensing Aerial Platform

The top left of Figure 9-3 shows an example of rust detected at a welded interface. On the top right, the figure shows an example of moderate-to-severe rust where the steel showed visible loss of section. The bottom left of the figure shows an example of rust at a bolted connection, and the bottom right shows an example of rust at a member splice. All photos of rust and further video of visible paint peeling point to a recommendation of paint maintenance to prevent further loss of section. Due to safety restrictions, the Florida Tech team did not fly above deck height to inspect the luminary structure affixed to the bridge. Figure 9-4 shows a close-up photo of the support structure holding the luminary to the bridge.

9.2.3 Field Test #2 – Brief Description and Objectives

A wooden low-height pedestrian bridge was the target for the second field test conducted at Florida Tech's campus. Figure 9-5 shows a side view of the bridge and setup location. The main objectives of this field test were to demonstrate reasonably safe flight conditions through overgrowth and weeds, and to collect image data of hard-to-reach components. Of particular interest were the bridge seats and beams on the underside of the bridge. Images of these hard-to-reach beams and seats were taken of a single bridge segment. Emphasis on these components resulted from prior meetings with FDOT inspectors and engineers.

Limited access in nature preserve locations present additional safety concerns for inspectors due to wildlife activity and natural hazards. The ability to be able to inspect such environments with a remote sensing platform would not only present a benefit in the inspection process, but also protect inspectors during inspections.

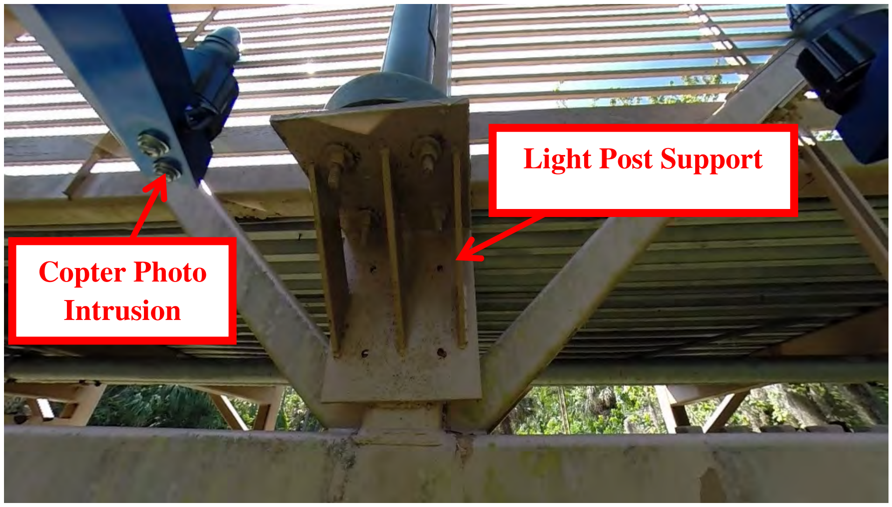

Figure 9-4 Luminary Support Structure

Figure 9-5 Low-Height Wooden Bridge and Setup Location

9.2.4 Field Test #2 – Summary of Results

Figure 9-6 shows an example of a captured stress crack through a center beam. Images of the hard-to-reach bridge underside were extracted from videos totaling less than 10 minutes. These images were extracted through post-processing using open source free video editing software. Images were only corrected for distortion (i.e., fish-eye) due to the ultra-wide lens used on the high-definition camera.

Figure 9-7 shows examples of other defects captured within the flight duration. The image on the left of the figure shows a stress crack that extends all the way to the bearing area. The image to the right of the figure shows a longitudinal crack extending the length of a guard rail support. Due to the nature of this guard rail support structure crack running through the anchor bolt holes, further investigation should be prompted.

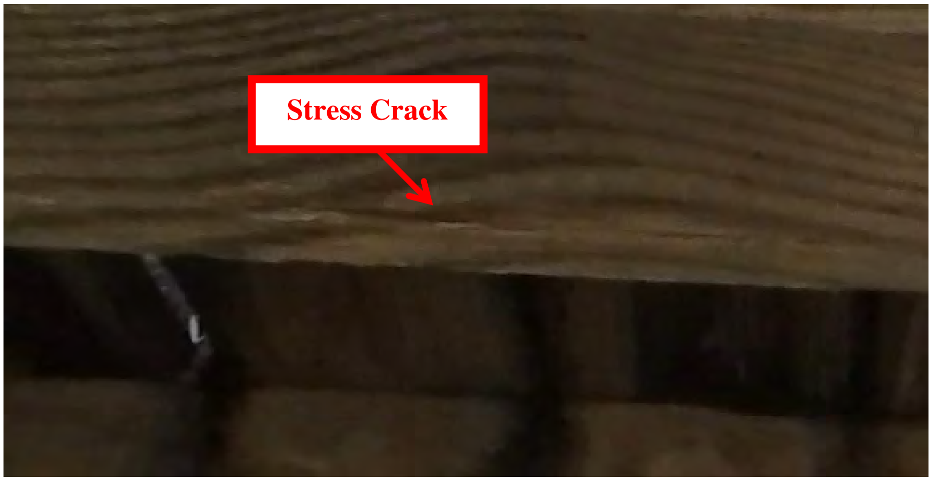

Figure 9-6 Longitudinal Stress Crack in Center Bearing Beam

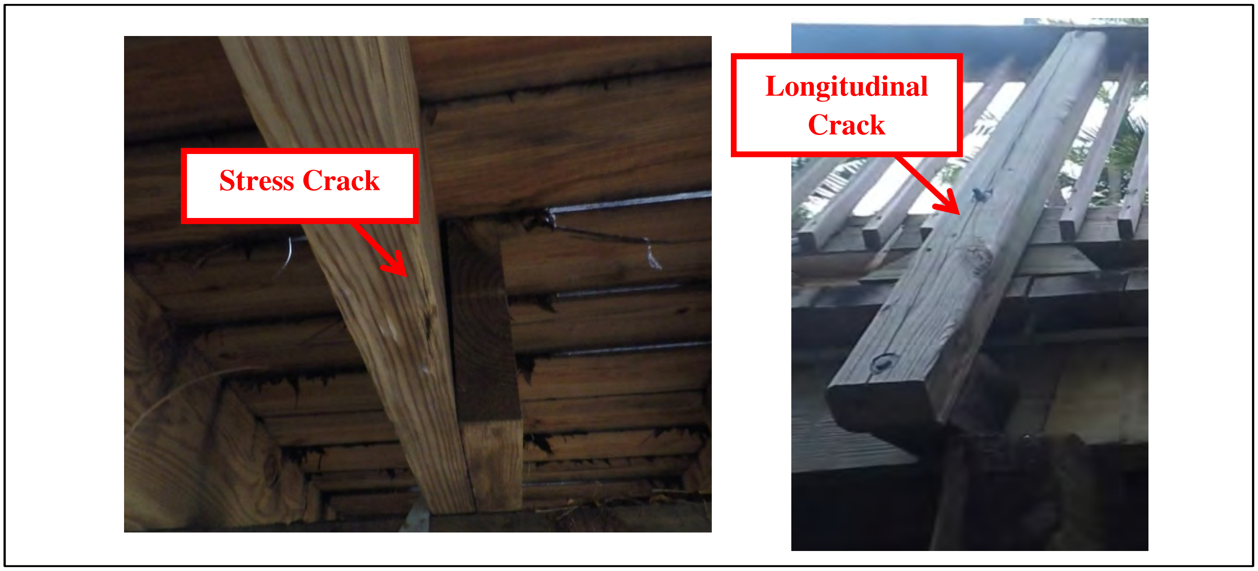

Figure 9-7 Defects Captured with High-Definition Sensors

9.3 BRIDGE FIELD TESTS CONDUCTED AT FDOT SITES

The Florida Tech research team joined FDOT inspectors during routine inspections of three bridges to obtain video data of underside bridge components using the remote sensing aerial platforms. Each bridge represented a field test. It took several weeks of preparation time prior to each field test to develop a flight plan, conduct preliminary dry run tests on open fields, monitor weather conditions, and conduct any UAV modification necessary based on collective input from FDOT inspectors and research team.

Each of the field tests targeted a different type of bridge. For the first field test, the target was a concrete girder highway bridge. For the second field test, the target was a steel superstructure railway bridge. For the third field test, the target was a highway concrete bridge with a steel girder mid-span. The following subsections provide a description of the objectives of each field test and the results obtained.

9.3.1 Concrete Girder Highway Bridge – Brief Description and Objectives

The Florida Tech research team participated in a field test with FDOT inspectors to collect image data of an underside section of a concrete girder highway bridge. Figure 9-8 shows the area of interest and setup location for the research team. The main objective of this field test was to capture high-quality images between concrete girders, store the collected video data for post analyses, and stream near real-time video data to a ground station held by an FDOT inspector. The idea was to get feedback from FDOT inspectors regarding the usability of the video images during real inspections. Visual inspection of areas between girders is of utmost importance to transportation managers because the current process requires the use of bucket trucks, resulting in lane closures and public traffic delays.

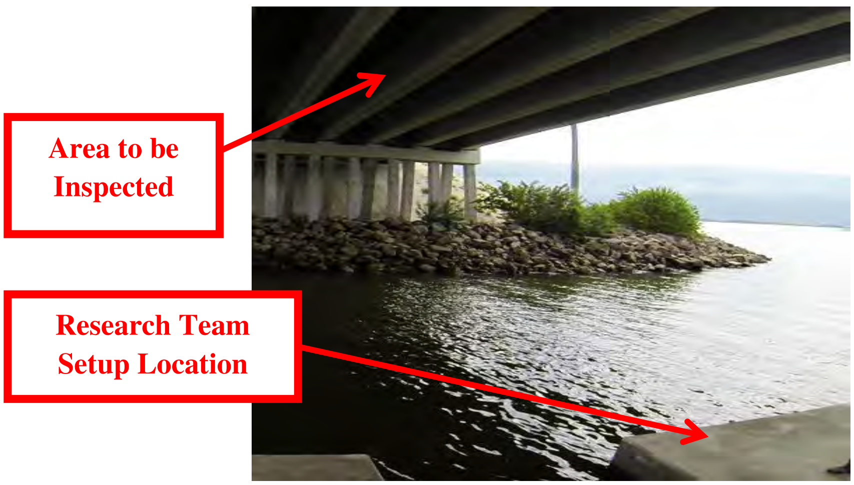

Figure 9-8 View of Area of Interest and the Setup Location for the Research Team

9.3.2 Concrete Girder Highway Bridge – Summary of Results

During this field test, the average wind speed under the bridge was measured at 12mph, with estimated wind gusts of 18mph. The hexa-copter shown in Figure 9-9a was initially used for data collection. This copter was operated by an experienced sUAV pilot who holds a Private Pilot's license. Getting the copter between girders was a straight forward task. However, keeping the copter stable in such confined space for a prolonged period of time was an issue because its strong motors would create a "turbulence effect". Therefore, the research team decided to use the quad-copter shown in Figure 9-9b. The pilot was able to keep the quad-copter stable for the most part, successfully collecting high definition video images. The turbulence effect was present at times, indicating that it would be beneficial to think about copter alternatives that would not create turbulence effects, or even different copter configurations (e.g., different propellers and/or motors) to serve specific purposes.

FDOT inspectors guided the pilot to focus on specific areas of interests based on the video streamed to the ground station in near real-time. Figure 9-10 shows an example of the real-time video feed to the ground station. The inspectors were impressed by the quality of the images coming from the sUAV system. The inspectors stated that the quality of the images showing defective areas were the same as pictures taken the day before by an inspection team consisting of seven members (see Figure 9-11). Figure 9-12a shows inspectors being lifted by a bucket truck to see between girders. This snapshot was taken a day before the research team's field test. Figure 9-12b shows the sUAV collecting and streaming video data within the same concrete girders during the field test.

(a) (b)

Figure 9-9 sUAV Systems

Figure 9-10 Ground Station Showing Near Real-Time Video Feed

Figure 9-11 Inspection Team Consisting of Seven Members

(a) (b)

Figure 9-12 (a) FDOT Inspection Team in Bucket Truck (b) sUAV In-Between Girders

Figure 9-13 shows some of the common defects found during the inspection process with the remote sensing platform. Images of such defects were captured during four flight clips totaling less than 10 minutes of video needed to be edited. Defects captured during the inspection were only post-processed with zoom and removal of image distortion (i.e., fish-eye).

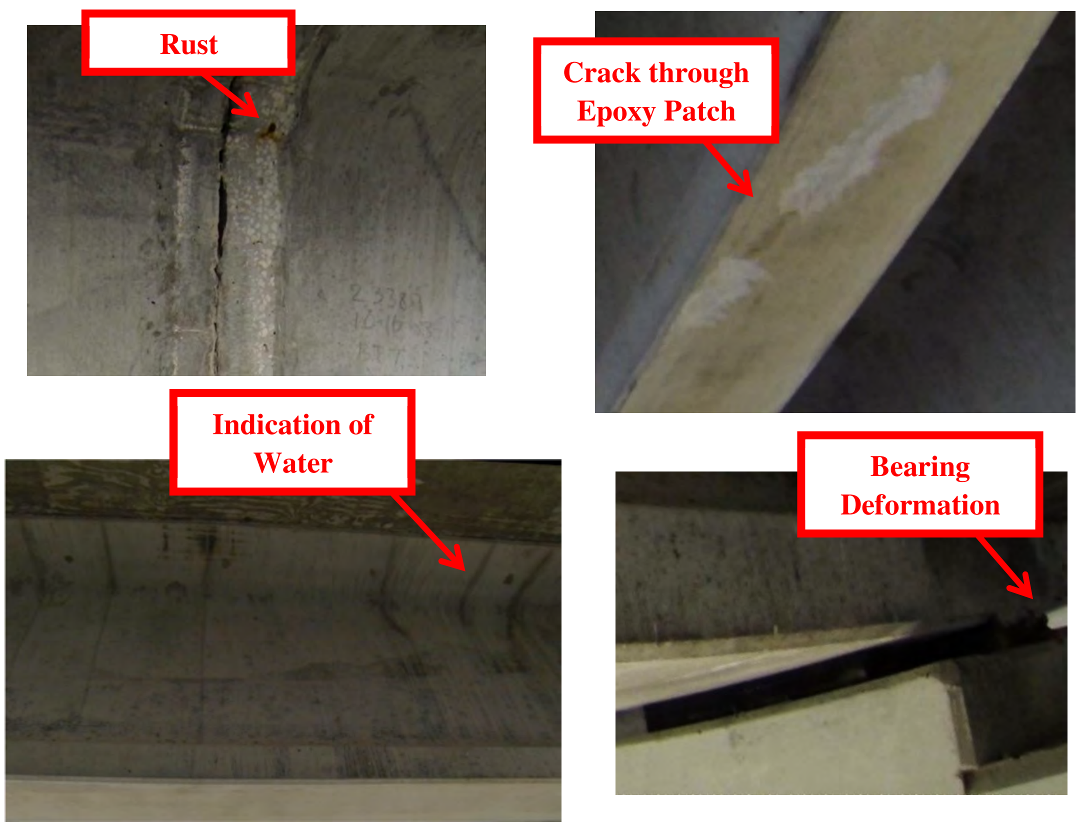

Figure 9-13 Defects Detected with Remote Sensing Platform

The top left image of Figure 9-13 shows an example of a rust spot. The top right image shows an example of a crack that has spread through what appears to be an epoxy patch. The bottom left image shows dark lines possibly resulting from water drainage between the separated partially composite girder and bridge deck. The bottom right image shows what appears to be excessive deformation in a neoprene bearing. The dark lines typically appeared at locations coinciding with markings indicating the location of the shear studs. Further investigation would be needed to identify true cause of the markings. Other epoxy patches observed showed little to no signs of wear, and besides a lateral translation of a bearing shown in Figure 9-14, no other reoccurring defects were observed. Figure 9-15 shows an instance of a separation of interface between the girder and the deck surface. Without knowledge of the designed interface between the two segments, the research team would only speculate its importance.

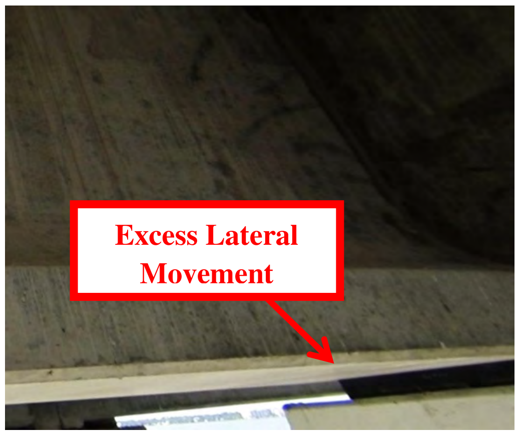

Figure 9-14 Indication of Excess Lateral Movement in Bridge Bearing

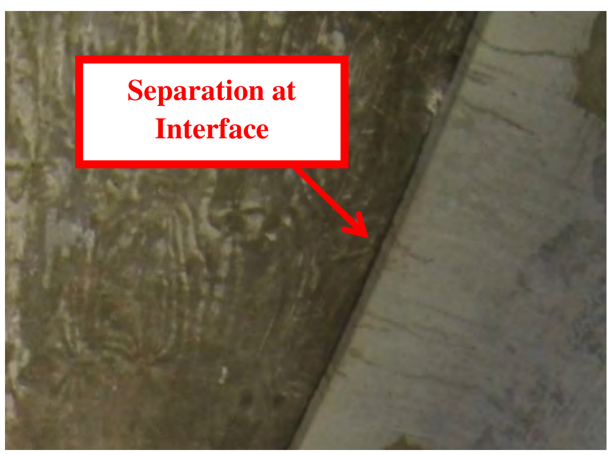

Figure 9-15 Separation between Girder and Deck

9.3.3 STEEL RAILWAY DRAWBRIDGE – BRIEF DESCRIPTION AND OBJECTIVES

The Florida Tech research team participated in a field test to collect image data of a steel railway drawbridge owned by FDOT. During the day of the field test, this bridge was undergoing a special inspection, led by AECOM and URS, to conduct balance testing. The Florida Tech research team, joined by two FDOT bridge inspectors, was given permission to observe the inspection from a safe distance.

The research team was also allowed to utilize remote sensing platforms to collect high-definition images of bridge components.

The main objective of the field test was to collect image data of hard-to-reach components. Of particular interest was to capture images of gusset plates. Emphasis on gusset plates resulted from prior meetings with CSX and FDOT bridge inspectors and engineers. Furthermore, gusset plate failures have been identified as key players in major bridge collapses [52], and highly-inaccessible during inspections [53].

Prior to the inspection, operational and safety briefings –including bridge protocols and signaling—were given to the Florida Tech team. Immediately following the briefings, the FDOT crew assisted Florida Tech onto a bridge pile cap adjacent to the drawbridge for equipment setup (see Figure 9-16).

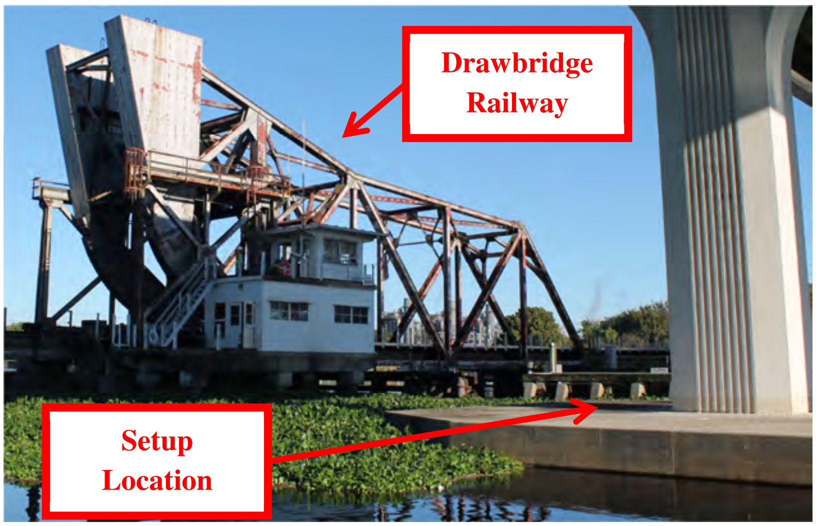

Figure 9-16 Railway Drawbridge and Setup Location

Two separate remote sensing platforms (see Figure 9-9), each equipped with different high-definition cameras, were used to focus on key points of the railroad bridge. The different sensors took images of these hard-to-reach critical gusset plates on the east side of the railroad bridge.

9.3.4 Steel Railway Drawbridge – Summary of Results

During this field test, the average wind speed around the bridge was measured at 7mph, with estimated wind gusts of 17mph. Figure 9-17 shows an example of a critical gusset plate. Images of the hard-to-reach gusset plates were captured within a single eight-minute video. Appendix C shows various still frames that were directly extracted from this single video, with post-processing zoom and rotation being the only correction done to the images.

Figure 9-18 shows an example of a gusset plate with partially and completely missing nuts. This particular defect was found to be common among the top gusset plates along the main members, moment resisting connection splice, and top X-braces. In some instances, as much as 80% of the bolt fasteners were missing on a single member connection, holding together with little more than rust and a frozen state easily broken by the vibrations associated with operating the bridge. The bolts appear to be in critical condition consistently throughout the images. Figure 9-19 shows closer images of gusset plates showing missing nuts.

Figure 9-17 Critical Gusset Plates on Railroad Bridge

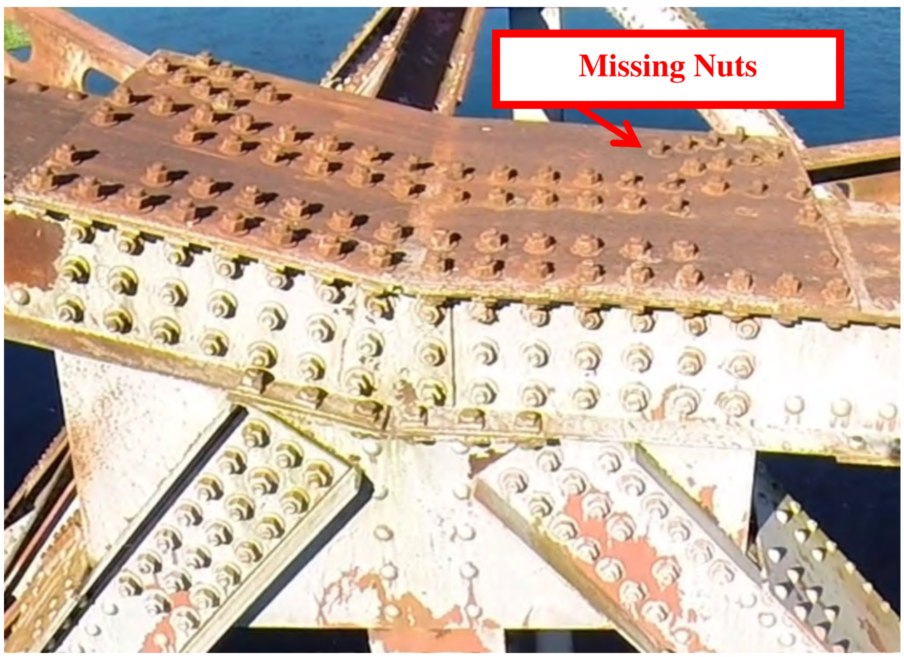

Figure 9-18 Top East-Side Gusset Plate (3rd from the South-most part of the bridge)

FDOT inspectors guided the pilot to focus on specific areas of interests based on the video streamed to the ground station in near real-time. Figure 9-20 shows a snapshot of the sUAV during data collection, as well as snapshots of the ground equipment (being held by FDOT inspectors) that showed the streamed video images. The inspectors were very impressed by the quality of the images coming from the sUAV system.

Members from the Florida Tech research team presented the results from this field test at the FDOT District 5 office in Deland, FL. The results prompted the District 5 office to send out a team a day after the presentation to correct the defective gusset plates.

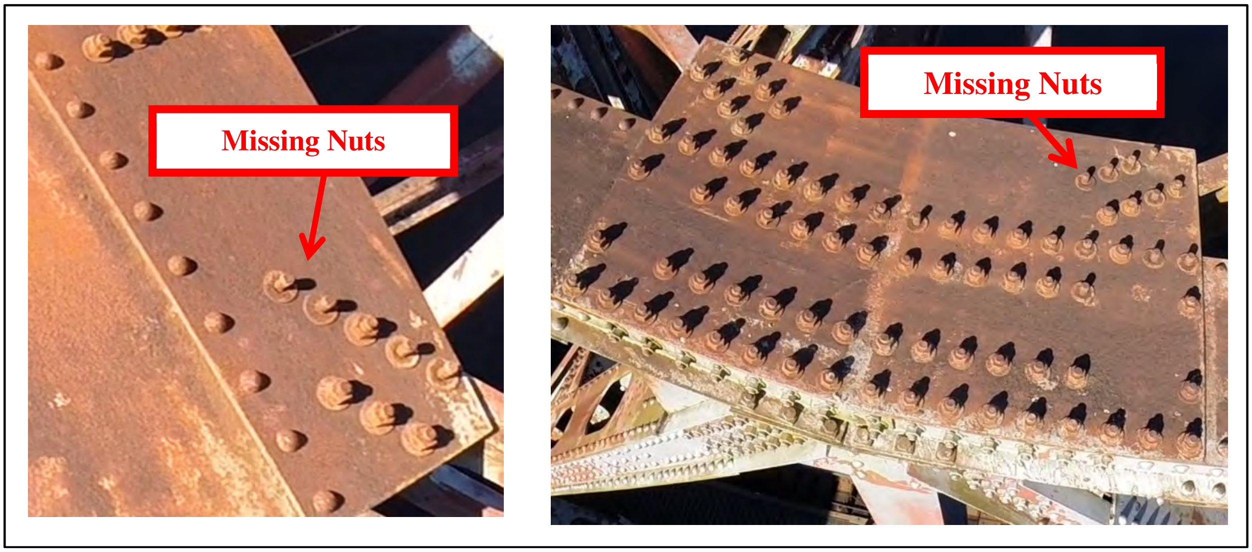

Figure 9-19 Gusset Plates Located on the Top-Side of the Bridge Showing Defects

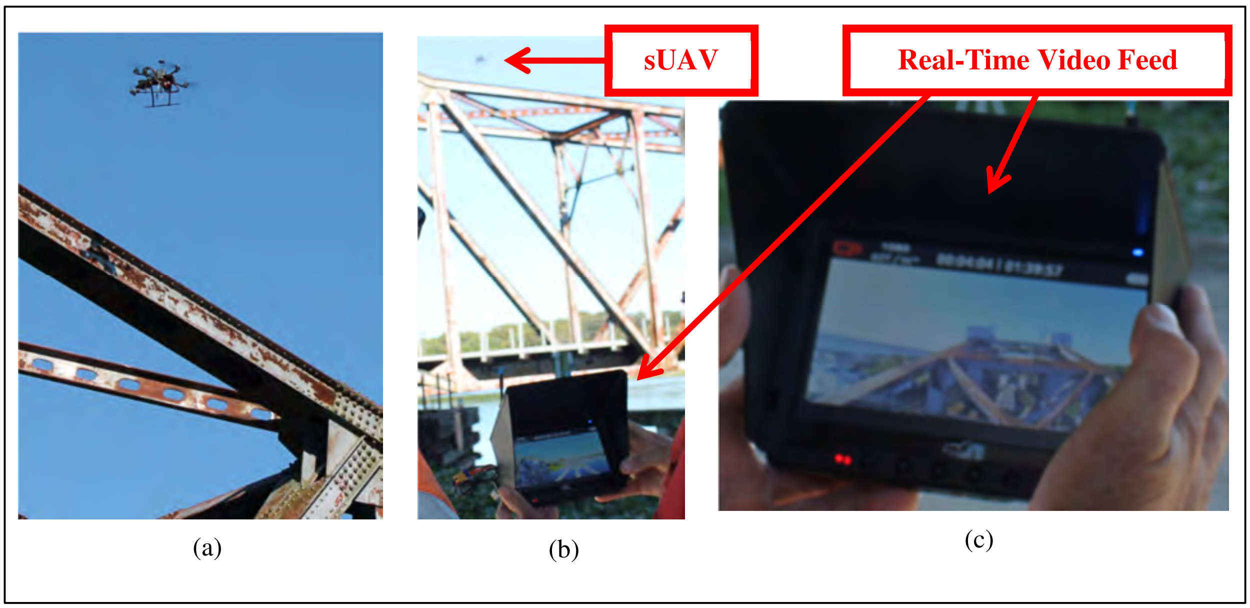

Figure 9-20 (a) sUAV Streaming Data (b, c) Ground Station Showing Real-Time Video Feed

A requirement derived from this field test was that a UAV platform should be designed to house multiple sensors in order to offer multiple vantage points. This way, overall vision flexibility can be maximized on a single flight, resulting in less overall flights.

9.3.5 Concrete with Steel Mid-span Bridge – Brief Description and Objectives

The Florida Tech research team participated in a field test to collect image data of the underside mid-section of a bridge. This bridge, which for the most part is made out of concrete members, has a steel-girder mid-section (see Figure 9-21). The main objective of this field test was to capture high-quality images between steel girders (always below deck level), store the collected video data for post analyses, and stream near real-time video data to a ground station held by FDOT inspectors. The idea was to get feedback from the inspectors regarding the usability of the video images during real inspections. Visual inspection of areas between girders is of utmost importance because the current process requires the use of bucket trucks, resulting in lane closures, public traffic delays, and higher safety concerns for inspectors. Five FDOT officials were present during the field test.

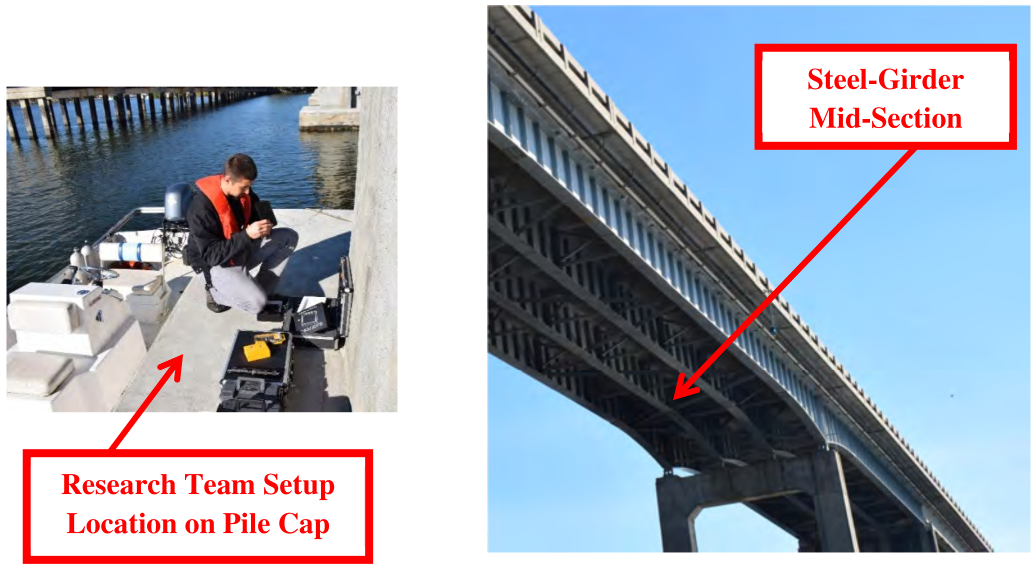

(a) (b)

Figure 9-21 Concrete Bridge with Steel-Girder Mid-Section

Two separate remote sensing platforms, each equipped with different high-definition cameras, were used to focus on key points on the steel sections. For this field test, and based on limitations encountered during previous field tests, the quad-copter from Figure 9-9b was significantly updated. Figure 9-22 shows a snapshot of the updated quad-copter, which included more efficient motors and propellers, and improved control system, among various other updates.

9.3.6 Concrete with Steel Mid-span Bridge – Summary of Results

Images of defects were captured during two separate five minutes flights. Figure 9-23 shows some of the common defects found during the field test using the remote sensing platform. Defects captured during flights were only post-processed with zoom and removal of image distortion. Figure 9-24 shows an example of a transverse brace with moderate-to-severe corrosion. This particular defect was found to be common not only among the transverse bracing, but also among the bottom chords of the main four steel girders. In some instances, concrete sections showed signs of wear at the interfaced locations between the two materials (see Figure 9-23). Figure 9-25 shows an instance of a separation of interface between the girder and the deck surface.

FDOT inspectors guided the pilot to focus on specific areas of interests based on the video streamed to the ground station in near real-time. The inspectors were very impressed by the quality of the images coming from the sUAV system.

Figure 9-22 Significantly Updated Quad-Copter

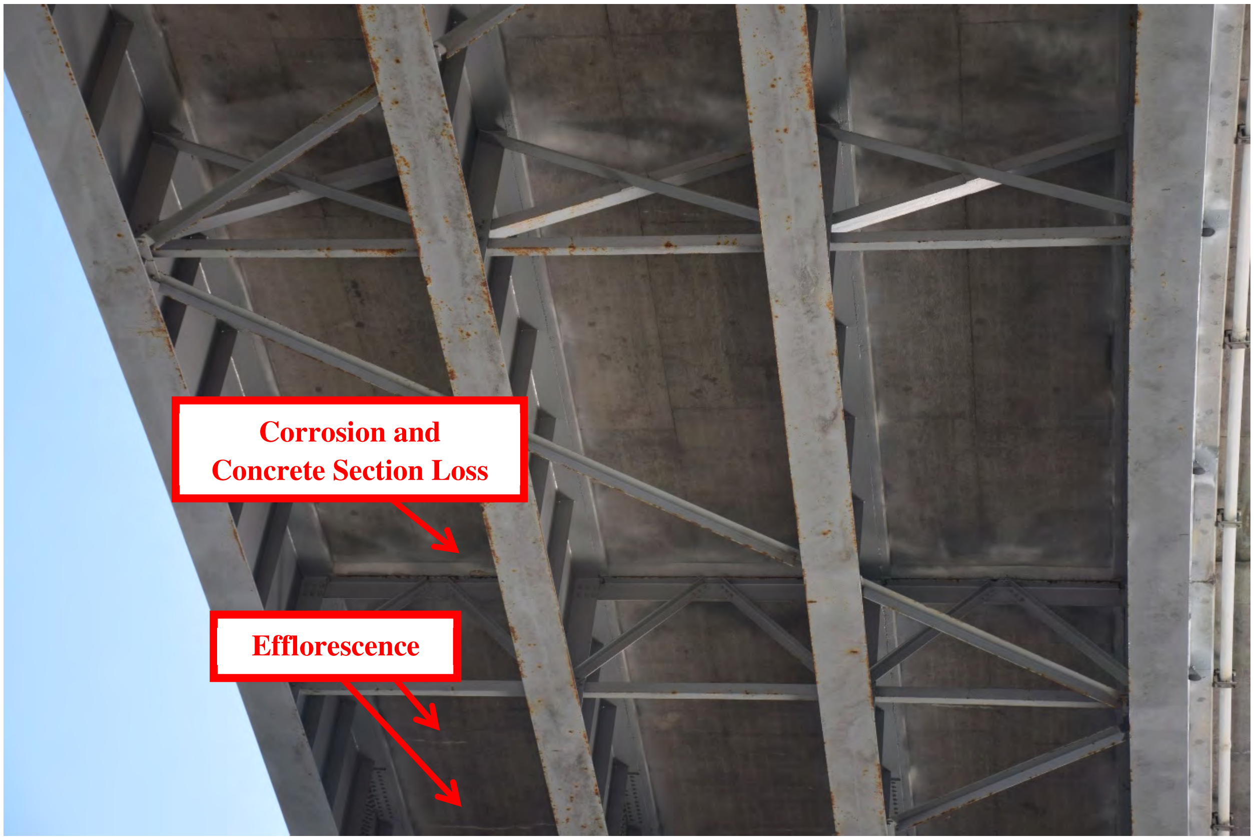

Figure 9-23 Defects Detected with Remote Sensing Platform

During this field test, the average wind speed underside the bridge was measured at 17mph, with estimated wind gusts of 25mph. In some instances, wind gust were estimated to be 30 mph below the bridge deck. Due to the volatile nature of the wind during these conditions at the time of testing, the field tests were cut short to only five minute flights. This final field test led to an additional requirement to include environmental equipment capable of measuring and transmitting wind speeds from the sUAV to a ground station.

Figure 9-24 Advanced Corrosion on Transverse Girder Bracing

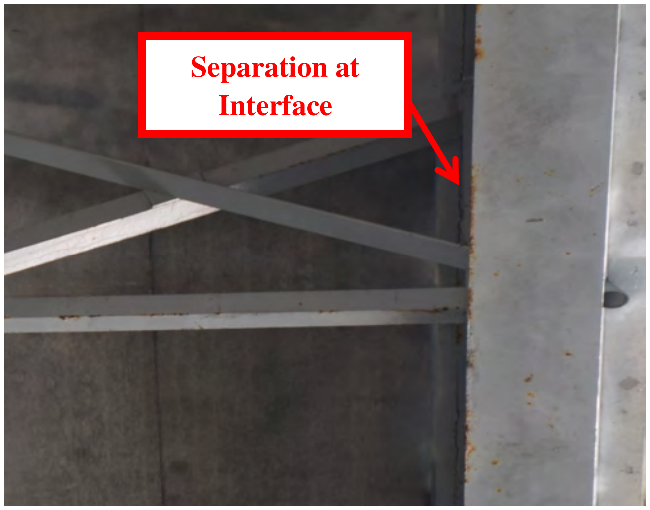

Figure 9-25 Separation Between Girder and Deck

9.4 Conclusion

This document presents information regarding field tests conducted by the Florida Tech research team to collect image data of underside sections of bridge structures using small aerial systems equipped with high-definition imaging sensors. Two field tests were conducted at the Florida Tech main campus, and three were performed on FDOT selected sites. FDOT inspectors participated in the field tests and provided critical information based on their experience that lead to establishing clear objectives for each mission. The main objective of this task, which was to provide proof-of-concept evidence for using sUAV systems to assist inspectors during the inspection of bridge structures, has been achieved. The research team recommends conducting further field tests to analyze data regarding the duration of complete bridge inspections.

CHAPTER 10

DEVELOP MAINTENANCE PROCEDURES

10.1 INTRODUCTION

Small multi-copters are often very robust and simple aerial platforms. These sUAV systems require pre-flight and post-flight visual inspections to minimize the risk of component failures and improve the chances of completing operations safely.

Visual and physical inspections of major structural and propulsion components significantly increase safety operational levels. An sUAV propulsion system is a subsystem that produces thrust to keep the aircraft aloft, and uses thrust differential to maneuver the sUAV in any direction. The main components that work to keep an sUAV in the air are motors, electronic speed controllers (ESC), propellers, and batteries; therefore, it is important to ensure that these components are of high-quality. Depending on the type of sUAV, failure of any of these components is unacceptable for safe operations.

This chapter describes maintenance procedures and service schedules (based on number of flight-hours) for key individual sUAV components. Maintenance procedures include pre-flight and post-flight inspections –both visual and physical –of the following components:

- Motors
- ESCs
- Propellers
- Airframe
- Batteries

Figure 10-1 shows a small-size hexa-copter with arrows and text that indicate the key individual sUAV components. An example of a visual inspection activity is to inspect the propellers for structural cracks and alignment of blades with respect to each other and the hub. An example of a physical inspection activity is to inspect the rotation of the motors by hand to ensure that each motor spins smoothly and freely. While conducting these and other inspection activities, it is of utmost importance to make sure that batteries are disconnected from the airframe.

This chapter is organized into three sections. Section 10.2 describes maintenance procedures for the identified key sUAV components. Section 10.3 provides concluding remarks.

10.2 MAINTENANCE PROCEDURES

Adequate maintenance and inspection activities are necessary to promote safe and efficient sUAV missions. The following sections describe recommended maintenance activities for motors, ESC components, propellers, airframe, and batteries.

10.2.1 MOTOR INSPECTION AND REPLACEMENT

Currently, most multi-rotor sUAV systems use a type of motor called "*brushless outrunner dc*" (BLDC). The term "*outrunner"* defines a "*brushless*" motor that spins its outer shell around its windings. The term "*brushless*" defines motors that must be electronically commutated and are powered by a DC electric source. "*Commutation*" is defined as changing motor phase currents at appropriate times to produce rotational torque. With BLDC motors, electrical current powers a permanent magnet that causes the motors to move. These motors are very efficient at producing torque. Other advantages of these types of motors are that they are relatively light, simple, and have very few failure points. Figure 10-2 shows snapshots of high-quality versus low-quality BLCD motors.

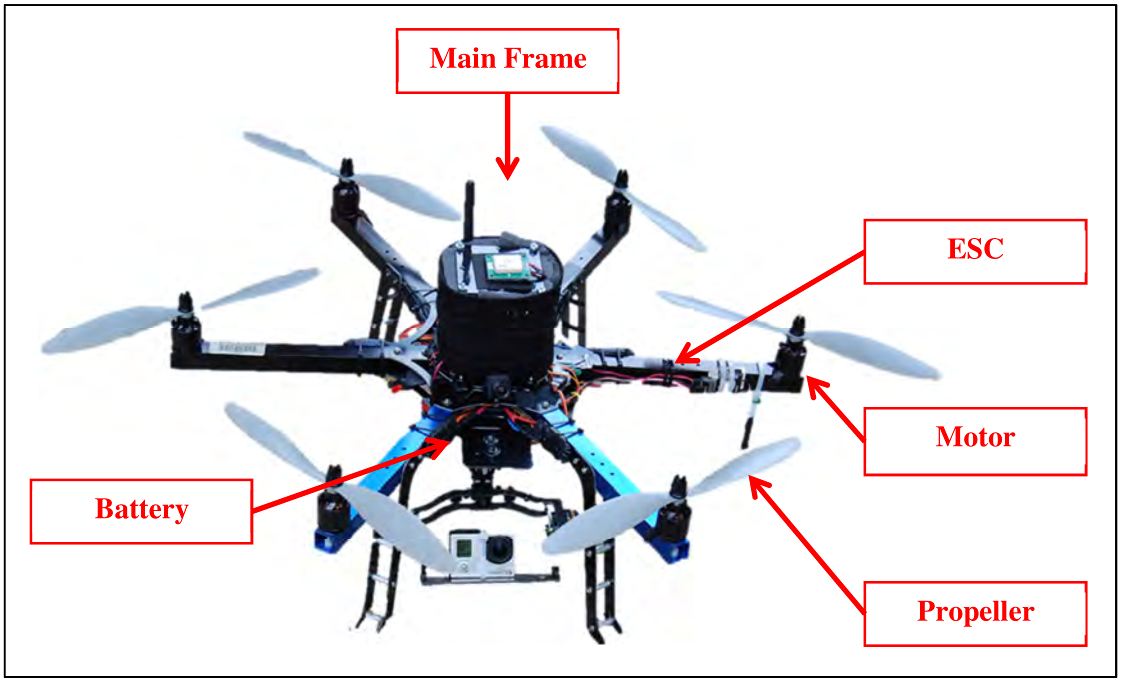

Figure 10-1 Key Individual sUAV Components

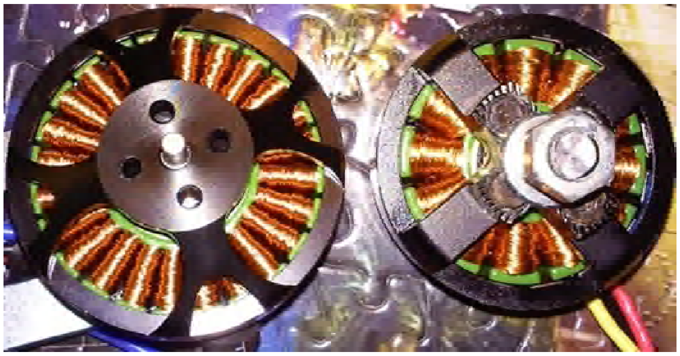

Figure 10-2 Examples of High-Quality (left) and Lower-Quality BLDC Motors

The lifespan of BLDC motors depends on the quality of the ball bearing used, as well as the quality of windings of the motor coils and wires. The average lifespan of a BLDC ball bearing is 10,000 hours. However, a motor may burnout prior to the 10,000 operational hours if it continuously operates at maximum amperage (amps). The overall lifespan of BLDC motors depends on factors such as:

- Environmental condition in which the motor is operated
- Weight per motor required
- Excessive vibrations

- Magnet misalignment/dislocation
- Mechanical damages to the propeller shaft
- Temperature and high winds
- Manufacturing quality

Bearings are an important component of BLDC motors. It is critical to never oil the motors by pouring oil on top of the bearings, as doing so creates a risk of getting dirt into the bearings. Figure 10-3 provides examples of motors showing inner/outer bearings. Bearings are shielded/sealed to prevent dirt from getting inside the coils, given that dirt as small as 0.005mm (0.000196 in) will cause damage to the bearing. Applying oil to the bearings will slowly washout their grease and replace it with oil. As a result, the bearing will not operate optimally. Moreover, the oil accumulated on the coils will attract dirt and other small debris, eventually resulting in complete motor seizure.

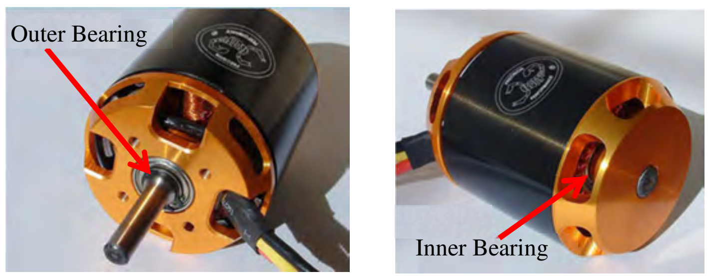

Figure 10-3 Examples of Outer and Inner Motor Bearings

To maintain BLDC motors in optimal conditions, it is recommended to use compressed air to remove any foreign particles, dust, and grains accumulated on the outside and inside of the motors. It is also recommended to keep a log of the operation times for each motor. Motor ball bearings should be replaced at around 150 to 300 hours of operational time based on visual inspection. A motor must be completely replaced after its manufacturer's estimated time to failure (typically around 300 hours). Finally, BLDC motors must be kept away from strong magnets, as they can demagnetize the motors' magnets.

Figure 10-4 provides snapshots of various motor parts such as motor coils, motor case, and propeller adaptor. The figure also provides snapshots of defects such as a bent shaft, rust, motor case damage, and deep scratches on the motor case.

BLDC technology is evolving at a very fast pace, becoming more reliable and efficient. It is very important to keep a log of every sUAV mission and note any unexpected noises or behaviors during flight. Such log could help to track down sUAV operational issues and keep the system in safe operating conditions. Table 10-1 shows a recommended list of inspection activities to be conducted on BLDC motors on a pre/post-flight basis. Table 10-2 shows various inspection activities that are recommended to be performed at least every 25 hours of sUAV operation. These activities are of equal importance as pre/post flight inspection activities.

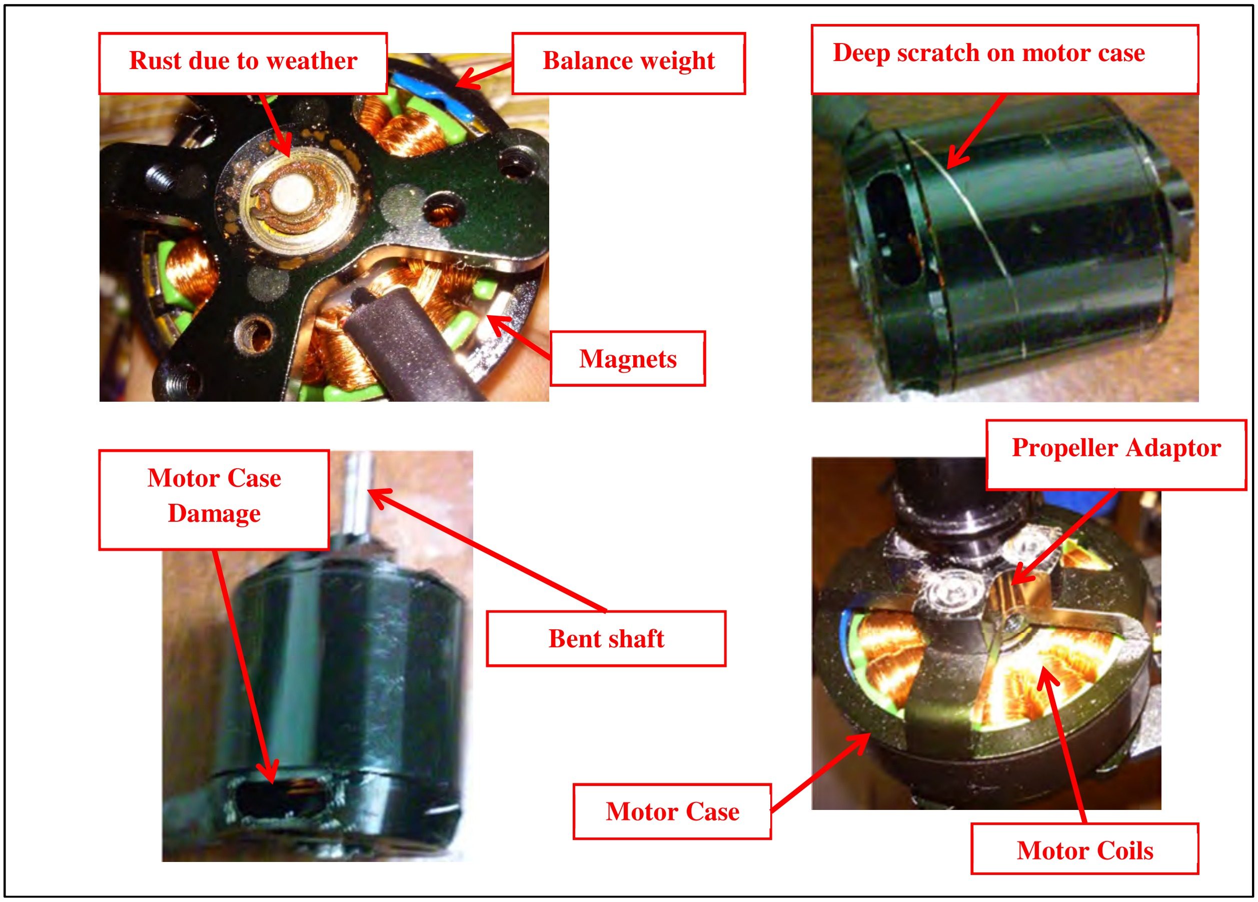

Figure 10-4 Various Motor Parts and Defects

Table 10-1 Recommended List of Inspection Activities on BLDC Motors Pre/Post Flight

No.	Description
1	Verify that there are neither dents nor scratches in the motor casing, as they could offset the dynamic balance of the case and could lead to excessive vibrations.
2	Verify that there is not debris between coils and motor casing.
3	With batteries disconnected, spin a motor by hand. The motor must spin freely, smoothly and without any friction. Repeat this step for each motor.
4	When spinning a motor by hand, verify that there is no ball bearing high-pitch/grinding noise.
5	When spinning a motor by hand, check for shaft vertical misalignment.
6	Looking through the openings in the top section of the motor case, verify that all of the motor magnets are attached to the motor case.
7	Prior to sUAV take-off, use the remote control to apply very small bursts of throttle to verify that all motors are responding simultaneously. If any motor seems to be out of sync, the sUAV must not be made operational until the issue is solved.

Table 10-2 Recommended List of Detailed Inspection Activities for Every 25 Hours of Operation

No.	Description
1	Verify that there are no excessive clearances in the shaft by slightly applying very little rolling force from left to right. If there is a movement, the ball bearing must be replaced.
2	Verify that there are no discolorations on the coils, which may be indicative of motor burnout. In case of a motor burn out, replace the motor.
3	Apply very light taps with a small screw driver (with non-magnetic tip) to the case. Magnets are epoxied to the case, so the light taps should not damage or misalign them.

10.2.2 ESC Inspection and Replacement

An ESC is an electronic unit whose main purpose is to control the speed and torque –based on instructions from a flight controller board –of a connected electric motor. It is a generally accepted rule-of-thumb to replace an ESC unit if its associated motor needs replacing. If properly used (i.e., operating under specified amps) and maintained, ESC components are relatively long-lasting. Table 10-3 shows a recommended list of ESC inspection activities to be conducted pre and post-flights. Table 10-4 shows an inspection activity that is recommended to be performed at least every 25 hours of sUAV operation.

Table 10-3 Recommended List of ESC Inspection Activities Pre/Post Flight

No.	Description
1	Verify that each ESC unit is securely attached to the airframe.
2	Verify that soldering joints are intact.
3	Verify that ESC and motor power plugs, if equipped, are properly plugged-in and tightly seated.
4	Verify that all wires are free from any damage (e.g., bends, insulation damage, and bad soldering).
5	Verify that ESC units are not operating any motors with missing magnets. Missing magnets will constraint an ESC to properly set the timing on a motor, which may result in increased ESC operation temperatures.
6	Use the remote control to apply small and gradual bursts of throttle to verify proper propulsion-throttling response. Verify that each motor-propeller units are working simultaneously (i.e., motor sync issues).

Table 10-4 Recommended ESC Inspection Activity Every 25 Hours of Operation

No.	Description
1	Verify that the temperature of each ESC unit is similar to the rest. An ESC unit that is significantly warmer than the rest may be indicative of issues with one or more propulsion system components.

Figure 10-5 shows a snapshot of a damaged ESC due to overheating. This figure also shows an ESC heat sink component that can be used for overheating prevention.

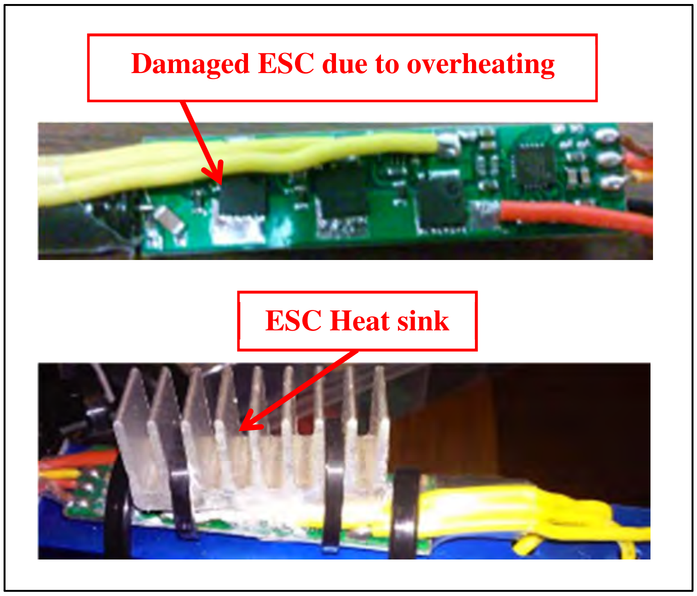

Figure 10-5 Snapshot of Damaged ESC Due to Overheating and a Heat Sink as Prevention Method

10.2.3 Propeller Inspection Activities

Propellers are critical components of an sUAV propulsion system that convert motor motion into thrust to keep an sUAV aloft. There are two main areas related to propeller inspection that must be addressed on a pre/post-flight basis, as they directly affect the overall reliability of an sUAV system. One of these areas is propeller balancing, and the other one is structural propeller health.

Inadequately balanced propellers will induce extra vibrations to an airframe and its motors, which may result in overall damage to the sUAV system. BLCD motors are vulnerable to vibrations, and extra vibration transmitted through the frame might loosen up some of the critical fasteners. Furthermore, extra vibrations will reduce clarity of video data obtained during a mission and reduce operational efficiency.

The structural health of propellers may also negatively affect an sUAV overall system. Damaged propellers (e.g., cracks or missing propeller tips) will make an sUAV propulsion less efficient by reducing thrust, increasing power requirements, and increasing extra vibrations throughout an airframe and its motors. Figure 10-6 shows examples of various types of propeller defects that must be inspected on a pre/post-flight basis.

10.2.4 Inspection Activities of Structural Integrity of Airframe

Structural components of the airframe must be inspected regularly. The frame must be visually inspected for any missing, loose and/or damaged hardware. The joints of the frame must be inspected for any tears, cracks, buckling, and/or deformations. Furthermore, the clearance between each pair of propellers must be inspected. Inconsistencies between these clearances are an indication that at least one of the arms is bent, deformed and/or missing a fastener. Table 10-5 shows the airframe areas that should be inspected, and Figure 10-7 shows a snapshot of a hexa-copter with arrows and text that indicate some of these areas.

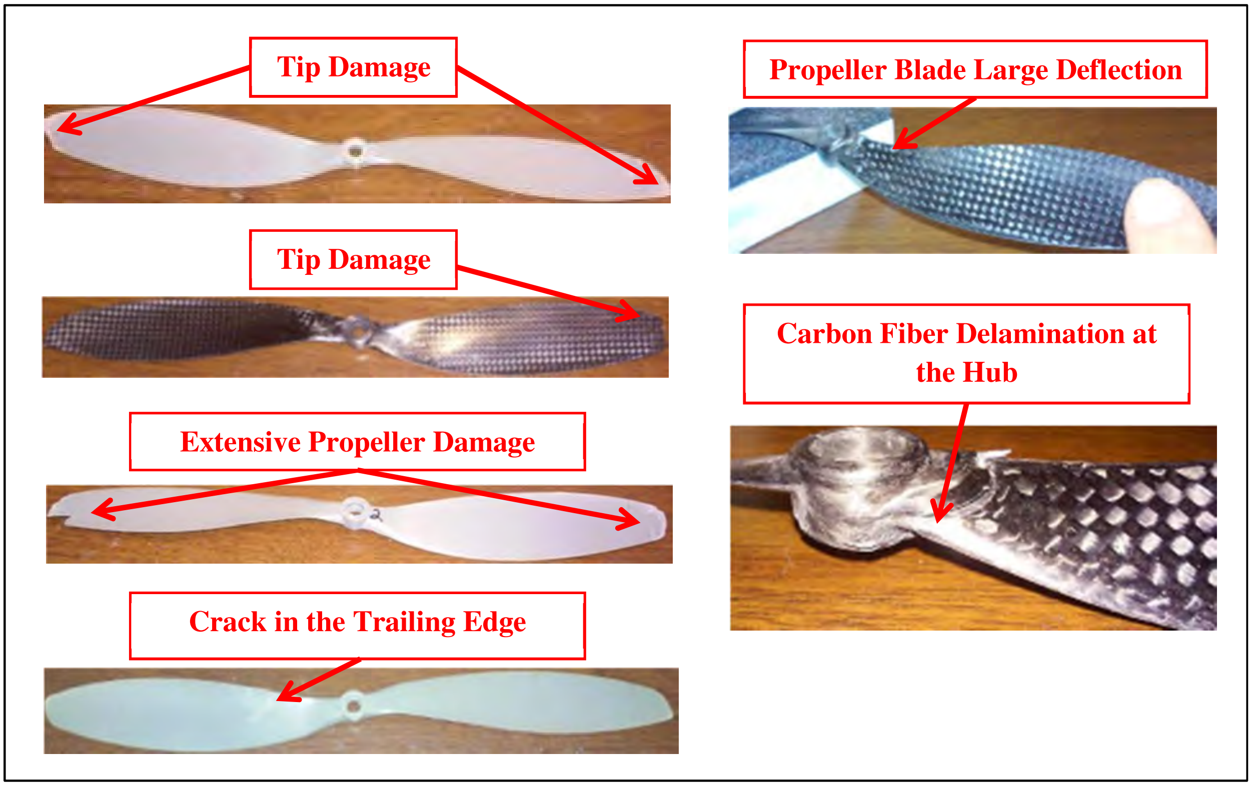

Figure 10-6 Various Propeller Defects

Table 10-5 Areas of Airframe Inspections Pre/Post Flight

No.	Airframe Area
1	Motor to Motor Plate
2	Motor Plate to Motor Arm
3	Motor Arm to Center Plate
4	Landing Gear to Center Plate / Motor Arm (depending on setup)
5	Center Plate Hardware

10.2.5 Batteries

The types of rechargeable batteries used to power sUAV systems are lithium polymer (LiPo) batteries. The life span of these types of batteries typically ranges between 200 and 500 charging cycles. Used with most sUAV systems, single LiPo batteries typically yield a flying time of around 15 minutes. If using a LiPo battery rated at 300 charging cycles, for example, this represents a maximum flying time of 75 hours (i.e., 15min x 300 = 4,500 min = 75 hours).

Due to their chemical composition, LiPo batteries can be fire hazardous; therefore, they must be handled with care. If a LiPo battery shows any indication of being damaged or defective in any way, they must not be used and instead must be properly disposed. The use of proper storage for LiPo batteries (e.g., metal containers or LiPo safe bags) greatly reduces fire risks during storage or charging of the batteries.

Figure 10-7 Areas of Airframe Inspections

There are many factors that influence the life time of LiPo batteries. One of these factors is the type of material and manufacturing process used to develop batteries. Other factors, which may reduce the lifespan of a LiPo battery and/or cause permanent damage, are listed in Table 10-6. Figure 10-8 shows various types of common defects associated with batteries, which should be inspected on a pre/post-flight basis.

Table 10-6 Factors that May Influence LiPo Battery Life

Factor	Comments
Over-discharging	It is recommended to not use a LiPo battery below 20% of its capacity (e.g., flying an sUAV when the battery's individual cell voltage drops below 3.0 volts).
Overcharging	Charging a battery after its individual cell voltage has been reached will reduce the battery's lifespan.
Over-heating	External overheating occurs, for example, if leaving a battery on a car on a hot sunny day.
Physical Damage	Examples of these types of damage are dents and dips.
Improper Storage	An example of improper storage is to store a fully charged battery for over 10 days.

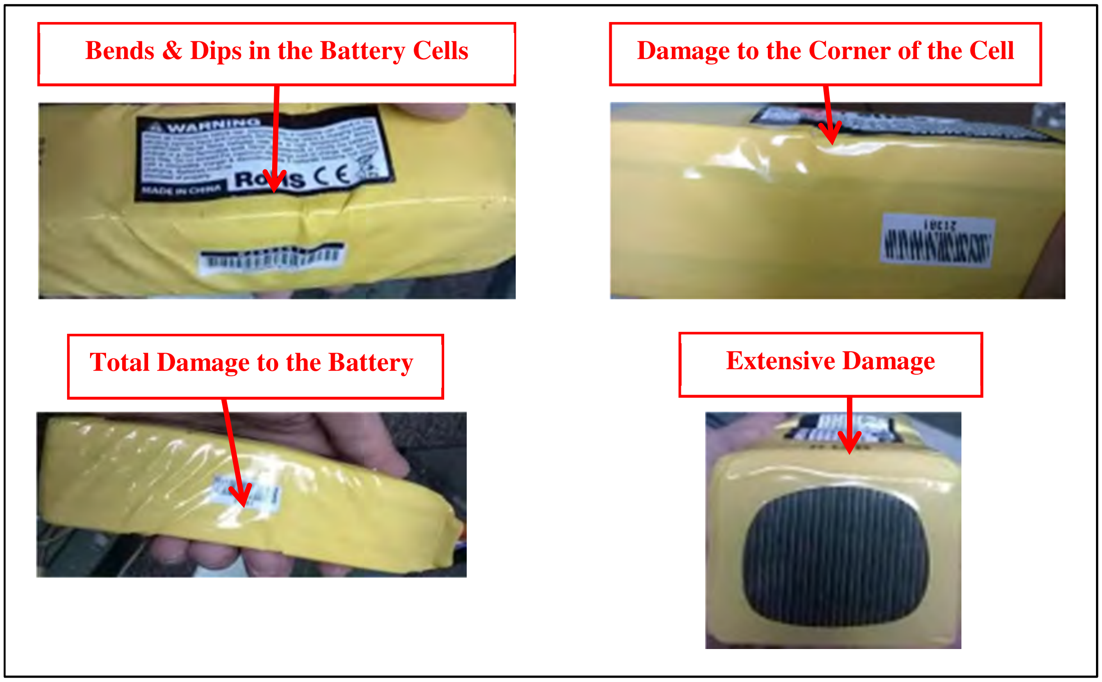

Figure 10-8 Common Types of Battery Defects

10.3 CONCLUSION

This chapter described maintenance procedures and service schedules for key individual sUAV components. These components are motors, ESCs, propellers, airframe structure, and batteries. Maintenance procedures include pre/post-flight inspection activities, and in some cases, inspection activities that are recommended for every 25 hours of sUAV operation.

CHAPTER 11

ESTIMATE OPERATOR TRAINING TIMES

11.1 INTRODUCTION

One of the objectives of this proof-of-concept research study was to gain an understanding of expected training times for inspectors to acquire necessary skills to safely operate an sUAV during the inspection process of bridges and HML. With this in mind, the Florida Tech research team developed a basic sUAV flight training program. FDOT inspectors and other individuals with different technical backgrounds participated in this task by going through the basic training program. The idea was to collect data on a preliminary set of parameters (e.g., trainee prior experience operating any type of sUAV or similar remote controlled systems) and determine if any correlation existed between the input parameters and the total time that it took to successfully complete the basic training program.

At the start of the proof-of-concept study, the research team thought that it was necessary to conduct experiments to answer the question of whether or not stabilizing and control equipment fitted to an sUAV had a significant effect on training time. After conducting many sUAV flights in indoor/outdoor tests, and consulting with experienced sUAV operators, it was clear that the answer to this question was 'yes'. Therefore, it was deemed unnecessary to conduct further experiments on this subject. Moreover, for safety purposes, it was established as a rule-of-thumb that basic sUAV foundation and maneuverability training requires the use of aerial platforms with stabilizing software capabilities.

The main purpose of this chapter is to describe a basic sUAV flight program developed by the Florida Tech research team to train inspectors in basic theory, operations, and maneuverability of sUAV systems. The results from this 1st stage training program –conducted in a wide-open field, miles away from airports and residential units –are used to estimate the time that it would take inspectors to safely operate sUAV systems in open space. Open space environments are typically encountered during HML inspections; therefore, it could be assumed that this training task equips inspectors with necessary basic skills to conduct HML inspections. Due to the small sample size of participating testers during experiments, only general conclusions can be made regarding training time estimates. This program lays the ground work to develop more detailed programs that will further equip inspectors to safely operate sUAV systems during underside bridge inspections.

This chapter is organized into five sections. Section 11.2 provides a general description of the basic sUAV flight training program. Section 11.3 describes the data obtained from the training activities, leading to estimates of expected total training times. Section 11.4 provides information regarding sUAV modifications for operations over water and/or in tight spaces. Section 11.5 provides concluding remarks. Appendix D shows the training flight guides used.

11.2 DESCRIPTION OF BASIC sUAV FLIGHT TRAINING PROGRAM

Various purpose-built sUAV systems have up to this point been constructed and investigated to better understand their strengths and weaknesses during flight. Indoor and outdoor training locations were also investigated as to their effect on UAV operator control. From these investigations, it was determined that a basic-level sUAV with software capable stabilizing code flown in an outdoor environment, open to external conditions, was ideal for initial training. Figure 11-1 shows a side view of the open-field training area.

Figure 11-1 Side View of Training Area

Figure 11-2 shows the sUAV that was used for training purposes. This sUAV is a bare-bones aerial system equipped with only a GPS capable of code-oriented software assisted stability during flight. The fitted GPS is capable of autonomously and continuously correcting for altitude and coordinate positions, and it is accurate to a 2ft radius. This sUAV, while extremely limited as a tool to conduct bridge and HML inspections, proved to be very effective to train individuals on flight maneuvers expected to be required to successfully perform tasks in line with this research. Individuals with varying skill levels, spreading from novice to experienced levels, benefitted from using this simple sUAV during training.

Figure 11-2 Bare Bones DJI Phantom 2 sUAV

A total of 10 people participated in the training task, which included four FDOT bridge inspectors. The trainees were individually briefed on the training regimen on a one-on-one basis. The regimen consisted of four introductory phases, each with internal modules designed to incrementally introduce complexity through different levels of sUAV maneuvers. Each module ended with *performance-based tests* that the trainee was required to perform. Furthermore, each phase required a trainee to conduct a final *objective-based flight test*, which was designed to mimic either a portion of a bridge or HML inspection. The modules were accompanied by a *visual module supplement* such as the one shown in Figure 11-3. Visual module supplements were designed to further reinforce flight plans and procedures, and were reviewed before each flight. A complete list of training flight guides and visual module supplements can be found in Appendix D.

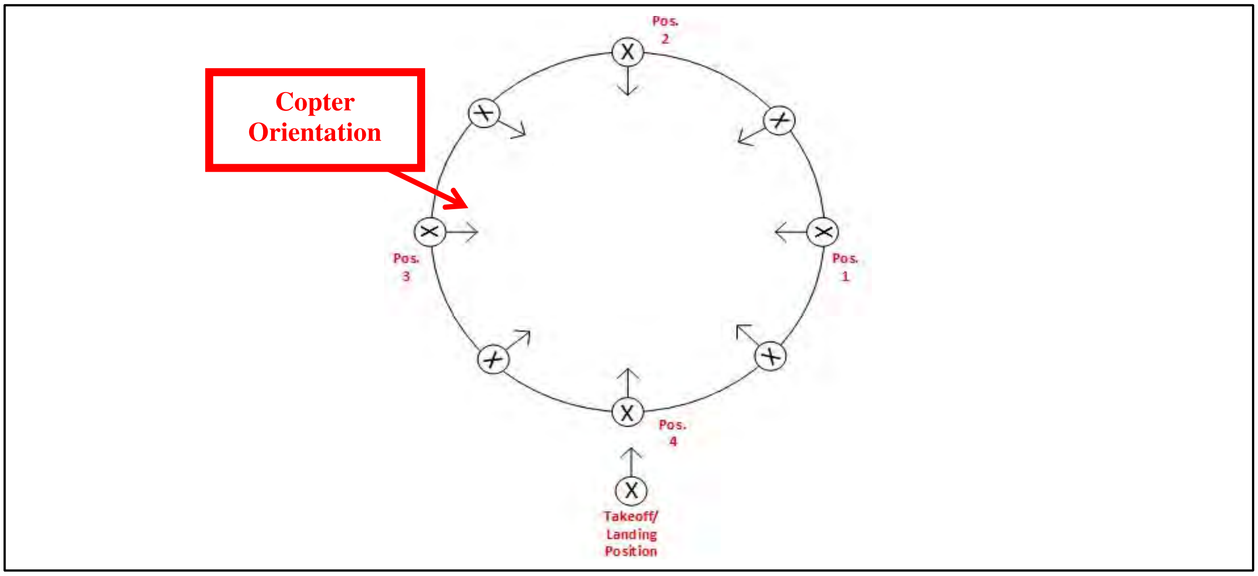

Figure 11-3 Example of a Visual Module Supplement for Training

The training was designed to accommodate different styles of learning by incorporating the following:

- A set of written instructions that a trainee could review
- A one-on-one trainee-trainer open lecture where questions could be individually addressed
- A visual trainer flight demonstration of the module at hand
- A verbal instructional segment where the trainer guided the trainee
- Hands-on performance based tests that a trainee repeated until a satisfactory level of comfort was obtained.

Satisfactory levels of comfort were gauged by how well a trainee was able to operate the training sUAV while conducting various maneuverability activities around pre-defined bounded flight areas (see Figure 11-4a). These areas were marked with wooden stakes of different heights, as depicted in Figure 11-4b.

From the one-on-one training sessions, time data were captured throughout the entire training process. Time data consisted of explanation of tasks, trainer demonstration, trainer-trainee talk-through, and the time it took the trainee to complete test demonstrations. These capture data were used to estimate the time it would take to train an individual to operate and maneuver a basic sUAV.

11.3 Results

Given the limited number of trainees, especially having only four inspectors, the data captured were graphed using a simple technique called *box plots*. This non-parametric technique is a convenient way to graphically depict groups of numerical data through quartiles, and does not make any assumptions regarding underlying statistical distributions. The idea was to determine if any correlation existed between key trainee identifiers and the total training time to successfully complete the program. These key trainee identifiers (i.e., independent variables) were: level of higher education, age, and prior UAV flight experience. Results from these analyses provide a simple way to estimate training duration based on these three parameters.

(a) (b)

Figure 11-4 (a) Training Areas (b) Wooden Stakes Marking Target Points and Boundaries

Figure 11-5 shows the box plot generated based on level of education. The term "Technical Trainee" was used to identify those that possess higher education levels (i.e., past an Associate college degree); otherwise, "Non-Technical Trainee" was used. An Associate college degree was arbitrarily chosen as a threshold between levels due to its commonality in present times. Figure 11-5 can be read by grouped participants along the x-axis and duration in minutes required to train those individuals along the y-axis. In the instance of missing data during training, video data of the training was analyzed to determine the missing time. Similarly, Figure 11-6 and Figure 11-7 show estimated operator training time required based on "Age" and "Prior UAV Experience", respectively.

There were other factors investigated during the training exercises. These factors include:

- Electronic gaming experience
- Wind conditions
- Temperature
- Willingness to learn

Electronic gaming experience was linked to age; therefore, it was considered redundant. Wind conditions varied from 5-15mph during training sessions, and did not have a significant effect on training time. This result can be explained by the relatively small difference of only 10mph between low and high average wind speeds. Moreover, this result can be explained by the fact that the maximum wind speeds were 15mph, which was proven to be an adequate wind condition for sUAV flights via indoor experiments. Temperature had no significant effect on training duration; however, it is recommended that training in extreme heat for an excess of two hours should be broken into segments to avoid personal or equipment fatigue. All of the trainees showed a complete willingness to learn how to fly sUAV systems; therefore, this particular parameter was not used as it had no variation among trainees.

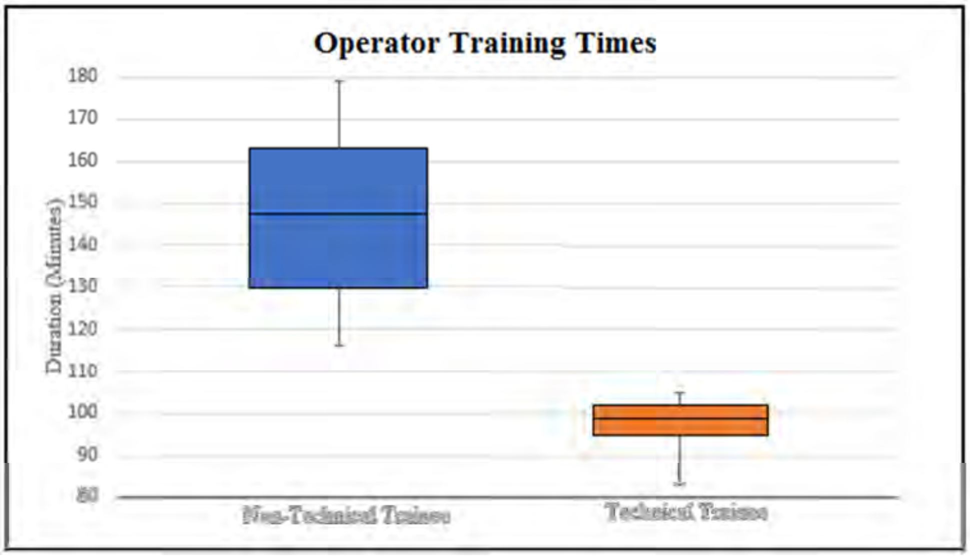

Figure 11-5 Estimated Operator Training Time Required Based on Education

Figure 11-6 Estimated Operator Training Time Required Based on Age

On an objective-based training regimen, it was found that age (which correlates with prior gaming experience) and level of education had that largest effect on sUAV flight training time. While prior UAV experience also showed a strong correlation to required training time, investigating this factor further revealed that in fact the level of previous experience played a larger role on the time required to complete the objective-based training than the existence of prior experience alone.

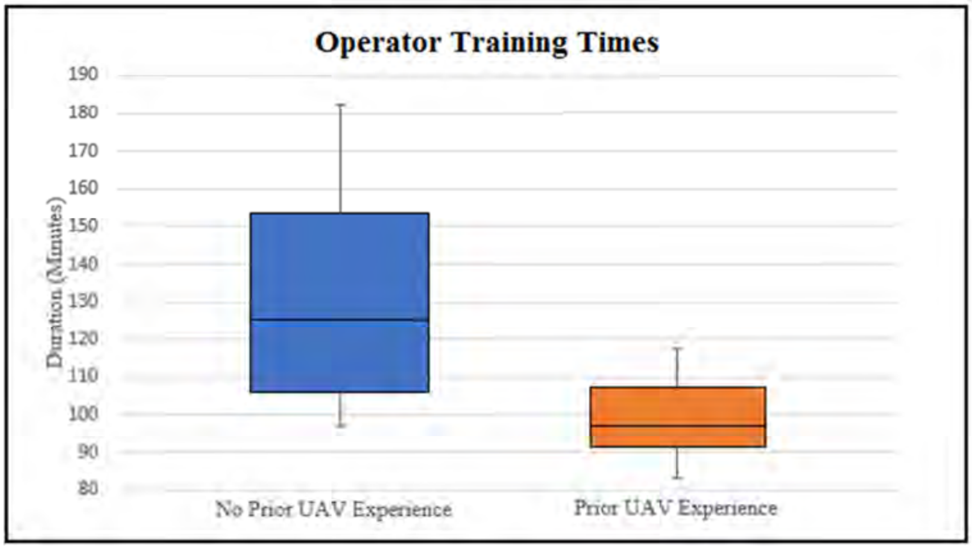

Figure 11-7 Estimated Operator Training Time Required Based on Prior UAV Experience

Accounting for the 75th percentile of the group, the results provide evidence regarding total training times for trainees using an entry-level copter with dedicated fight stabilization software. The maximum amount of training time recorded slightly exceeded 3hrs. That is, the results provide evidence to suggest that training an inspector on basic skills to operate an sUAV for HML inspections should not exceed 3.5hrs. *This total duration time does not account for any specific testing requirement that may be imposed by the FAA in their new set of regulations, which is currently an ongoing process and is expected to be finalized by mid-2016.* Other significant results regarding training times include:

- It took an average of 2.75 hours to successfully complete the basic objective-based sUAV flight training for those fitting the criterion of no prior UAV experience, over the age of 35, or those considered “Non-Technical Trainees”.
- It took an average of 1.75 hours to successfully complete the basic objective-based sUAV flight training for those fitting the criterion of “Technical Trainee”, or under the age of 35, or who have had prior UAV experience.

11.4 sUAV Protective Add-Ons Components

Due to the nature of bridge inspections, and the many differences of environmental factors associated with bridge locations, identifying key safety attributes of which to protect an sUAV is important. Conditions of which to protect the sUAV during inspections include flying over water, sUAV recoverability, and flying in tight quarters. While some commercial equipment exists to tackle these environmental concerns (see Figure 11-8), the level in which they can be modified to suit other needs are very limited.

The current concept of a water resistant design has many drawbacks. Much like previous commercial-off-the-shelf products tested in the Florida Tech research lab, these water resistant systems lack the ability to be customized to meet the unique needs of bridge inspectors. While concepts are being constantly improved, the Florida Tech research team instead focused on protecting key sUAV elements by using protective components in case of an accident. These removable protecting components include waterproof camera housing, floatation devices for the copters, and propeller guards (see Figure 11-9).

Figure 11-8 Examples of Waterproof Quad-Copters

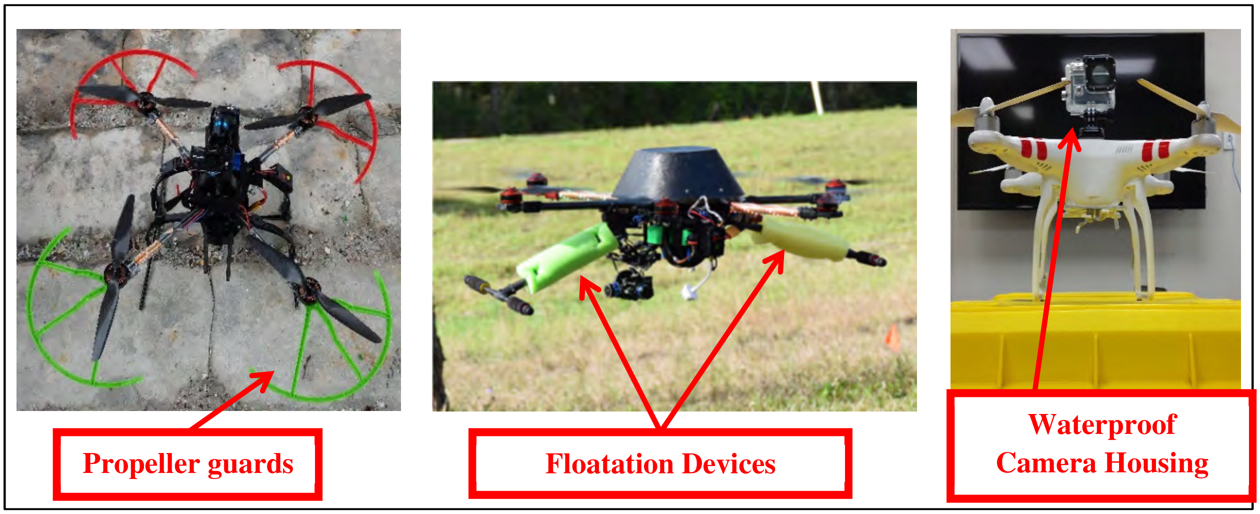

Figure 11-9 Flight-Specific Add-On Protective Components

11.5 CONCLUSION

The training task was reserved for the final quarter of this research project to better refine and understand UAV components and operations. Various purpose-built sUAV systems were up to this point constructed and investigated to better understand their strengths and weaknesses during flight. Indoor and outdoor training locations were also investigated as to their effect on UAV operator control. From these investigations, it was determined that a basic level sUAV with stabilization software was ideal for the initial training.

This chapter describes a basic sUAV flight program developed by the Florida Tech research team to train inspectors in basic theory, operations, and maneuverability of sUAV systems. The results from this training program are used to estimate the time that it would take inspectors to safely operate sUAV systems in open space. The chapter also provides general information regarding sUAV protective components for flights over water or in tight places.

Using a basic level sUAV with stabilization software for training purposes proved to be a useful tool in the introduction to UAV flight. However, it is important to note that ongoing training is needed to retain and improve the skills necessary to perform objective-based maneuvers. Furthermore, once proficiency and mastery of the basic level sUAV is achieved, inspectors should be trained to operate more complex and customized copters that provide better flight performances. These customized sUAV systems are often capable of holding various types of special sensors, which may be needed during special bridge or HML inspections.

CHAPTER 12

ESTIMATE INSPECTION COSTS

12.1 INTRODUCTION

One of the objectives of this proof-of-concept research study was to gain an understanding of expected costs and benefits associated with using an sUAS to visually inspect bridges and HMLs. Expected costs are a function of the type of entity acting as PIC. In the case of structural inspections, either bridge/HML inspectors or contractors can act as PIC of an sUAS. The goal of this chapter is to describe key cost parameters associated with inspectors operating an sUAS during bridge and HML inspections.

This chapter is organized into five sections. Section 12.2 provides a general description of estimated operator costs, including training and data gathering time. Section 12.3 describes estimated equipment costs, including maintenance and repair costs. Section 12.4 provides brief information regarding video editing costs to extract useful still images from video data for report writing. Section 12.5 provides concluding remarks.

12.2 OPERATOR COSTS

Operator costs associated with an inspector acting as PIC are a function of training activities and the time that it takes to complete a mission (i.e., data gathering time). The following subsections describe each of these cost parameters.

12.2.1 OPERATOR TRAINING TIME

A two-stage program to train inspectors to safely operate an sUAS for bridge and HML inspection missions was designed during this research project. Stage 1 considers training operators to safely maneuver simple GPS software-assisted sUAV systems in wide open areas. An estimated time for this basic training, which was described in Chapter 11 of this report, is three hours. In addition, this stage involves 40 hours of supervised and unsupervised flight time as recommended by FAA statistics. FAA procedures state that the first 20 hours should be under supervision of a certified flight instructor (CFI), and the last 20 hours should be solo flight, including at least 10 take-offs and landings. Therefore, the cost for 20 hours of CFI time per trainee needs to be considered. Sources estimate that common average hourly rates for sUAV flight trainers range from \$20-\$30 per hour [54]. The total estimated time for this stage is 43 hours.

Stage 2 is modeled after stage 1, but using a more complex sUAV as aerial training platform. This sUAV will be equipped with advanced features that are necessary to safely and effectively conduct flight missions under bridges. This stage involves familiarizing trainees with more advanced controller features and different flight modes, among other things. Initial training is estimated to be three hours, followed by 70 hours of additional flight time based on national average flight times for sUAV pilot training (e.g., [55], [56]). The total estimated time for this stage is 73 hours. The combined estimated total training time for both stages is 116 hours per trainee. This total training time estimates do not include conducting any supervised training in actual bridge or HML sites.

12.2.2 Data Gathering and Inspection Times

Figure 12-1 shows bridge elements that are considered to estimate data gathering and inspection times. These elements include columns, pier/column caps, and *bays*, which are defined as the space between two girders. The figure also shows portions of a *bridge section*, which is the area composed of a set of bays that spans between two pier/column caps. In this figure, bridge sections include four bays.

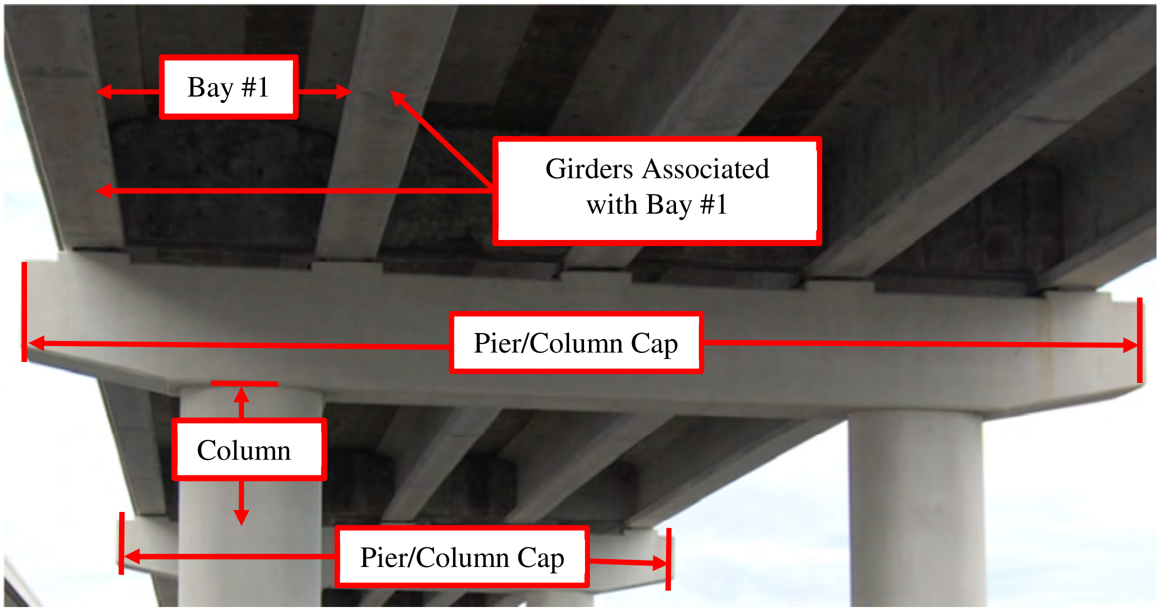

Figure 12-1 Bridge Elements Considered to Estimate Data Gathering and Inspection Times

Figure 12-2 shows a snapshot of a hypothetical bridge inspection site. This figure can be used to describe the parameters presented in Table 12-1 to estimate total data gathering time (TDGT). First, an initial setup time must be considered to account for the time that it takes to conduct activities such as going over safety guidelines, setting up and testing video transmission, installing propellers, verifying wind speeds, setting up FPV systems, and flying the sUAS to a bay area to initiate data collection, among various other activities. The second and most critical parameter to consider is the time that it takes to collect bay, column, and pier/column cap image data associated with a bridge section. This parameter also includes the time that it takes to maneuver the aerial platform between bays. The third parameter to consider is the time that it takes to maneuver the sUAS to ground level to change its battery, and maneuver the aerial platform back to a bay area to continue collecting image data. Equation (1) shows the function to estimate TDGT.

Table 12-1 Parameters for TDGT

No.	Parameter	ID	Description
1	Initial Setup Time	IST	Time to initially set up the equipment (e.g., install propellers, go over safety guidelines and mission plan) and fly the sUAS to the first bridge section.
2	Total Section Time	TST_i	Total time that it takes to maneuver an sUAS to obtain image data of the entire set of bays inside Section$_i$, its associated pier/column cap area(s), and from bay to bay.
3	Battery Change Time	BCT	Time that it takes to maneuver an sUAS from a bay area to a ground location, change its battery, and maneuver the sUAS back into a bay area to continue collecting image data.

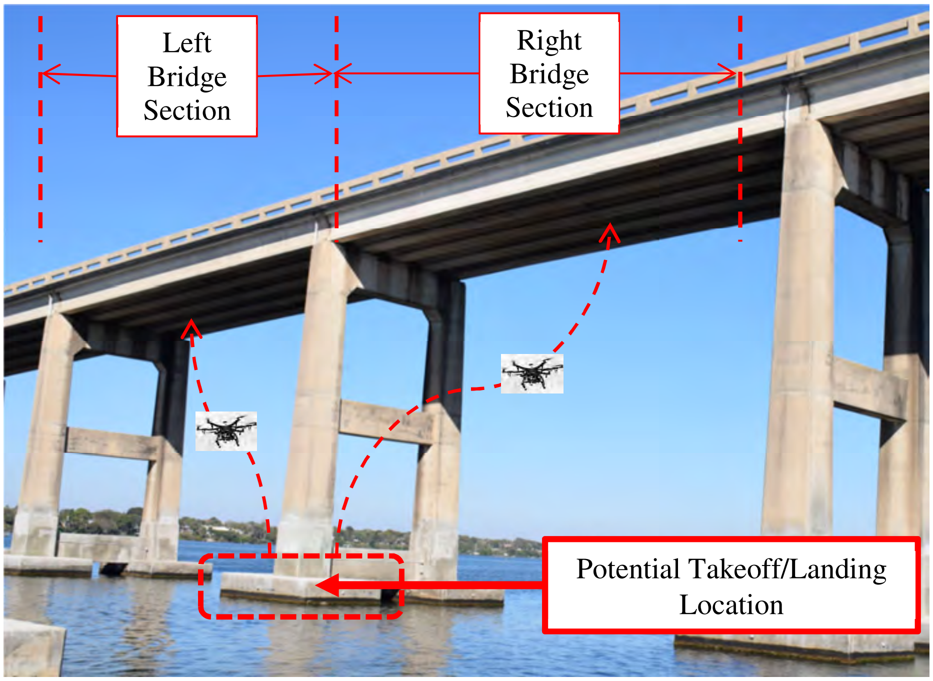

Figure 12-2 Hypothetical Bridge Inspection Site

$$\text{TDGT} = IST + \sum_{i=1}^{n} TST_i + (x * BCT) \quad (1)$$

where,

n = total number of bridge sections

x = number of times that batteries will need to be changed

12.2.3 Preliminary Comparison: Conventional versus sUAS Methods

Figure 9-11 shows an FDOT team consisting of seven people during a routine visual inspection of a concrete girder highway bridge. The total length of this particular bridge is 820 feet, including two 50 feet sections, five 118 feet sections, and a single 130 feet section. Each of these eight bridge sections includes six bays. Underneath the bridge, the figure shows two inspectors and two safety boat operators. A flagging crew of two and a bucket truck (also known as *Inspector 62*) operator are also part of the inspection team. The total visual inspection time incurred by this seven-people crew was 3.5 hours, which is equivalent to 24.5 total man-hours. This bridge can be used as target for a preliminary comparison of visual inspection times between conventional and sUAS methods.

Table 12-2 shows itemized time estimates to come up with an estimated TDGT for using an sUAS as a tool for the inspection of this bridge. Based on previous indoor experiments under controlled wind speeds to understand sUAS maneuverability, an average sUAS flight time of 3ft/sec inside bays is assumed. Other assumptions include maximum battery durations of 20 minutes before starting the sUAS landing process, and mild wind conditions to safely maneuver an sUAS into bay areas underneath the bridge. The estimated TDGT using an sUAS is 5.43 hours (i.e., 326 minutes).

Table 12-2 Estimated TDGT Using an sUAS for an 820ft Bridge Inspection

ID	Parameter	Value
(A)	Flight Time per Foot	3 sec/ft
(B)	Number of Bays per Section	6
(C)	Maximum Flight Time (MFT)	20 min
(D)	Number of 50ft Sections	2
(E)	Number of 118ft Sections	5
(F)	Number of 130ft Sections	1
(ID_1)	**Setup Time**	**15 min**
(ID_2)	Flight Time per 50ft Bay = (A) * 50ft / (60 sec/min)	2.5 min
(ID_3)	Flight Time per 50ft Section = (B) * (ID_2)	15 min
(ID_4)	**Total Time for All 50ft Sections = (D) * (ID_3)**	**30 min**
(ID_5)	Flight Time per 118ft Bay = (A) * 118ft / (60 sec/min)	5.9 min
(ID_6)	Flight Time per 118ft Section = (B) * (ID_5)	35.4 min
(ID_7)	**Total Time for All 118ft Sections = (E) * (ID_6)**	**177 min**
(ID_8)	Flight Time per 130ft Bay = (A) * 130ft / (60 sec/min)	6.5 min
(ID_9)	Flight Time per 130ft Section = (B) * (ID_8)	39 min
(ID_10)	**Total Time for All 130ft Sections = (F) * (ID_9)**	**39 min**
(ID_11)	Number of Times to Change Battery = ((ID_4) + (ID_7) + (ID_10)) / (C)	13
(ID_12)	Time to Fly Down and Change Batteries	5 min
(ID_13)	**Total Battery Change Time = (ID_11) * (ID_12)**	**65 min**
(ID_14)	**Total Data Gathering Time (TDGT) = (ID_1) + (ID_4) + (ID_7) + (ID_10) + (ID_13)**	**326 min**
(ID_15)	**TOTAL INSPECTION TIME = (ID_14) + (C)**	**346 min**

Per ASHTO guidelines, the minimum crack size that inspectors have to include in inspection reports is 0.01 cm. The image sensors being used for this research are capable of recording image data at resolutions under the 0.01cm threshold at a maximum distance of 4ft from its target; however, they can only transmit images wirelessly in near real-time to a base station at a minimum resolution of 0.16cm. Therefore, an inspector must view the recorded data in a separate base station (e.g., laptop) to catch defects that are smaller than 0.16 cm. A proposed approach is to have an inspector on-site to view recorded image data as soon as the sUAS is brought down for its first battery change. That is, during the first battery change, the process would be to remove the storage device (e.g., SD card) from the image sensor and replace it with an empty one. The removed storage device containing previously collected images would then be inserted into a base station for on-site viewing by an inspector. After the first battery change, the process of on-site reviewing of collected data is expected to be executed in parallel to the process of collecting data using the sUAS, except for the last data collected by the aerial system. Therefore, additional time for an inspector to examine the last video data collected by the sUAS must be added to the TDGT. Table 12-2 shows that the estimated maximum flight time (MFT) for a typical sUAS is 20 minutes. That is, every time the sUAS is brought down for landing, the image sensor would have collected MFT minutes of data. Consequently, MFT must be added to TDGT to more accurately estimate total inspection time. The function to estimate total inspection time using an sUAS is presented in Equation (2).

$$\text{Total Inspection Time with sUAS} = \text{TDGT} + \text{MFT} \tag{2}$$

Using a single sUAS, an inspection team consisting of three people would be sufficient to conduct a routine visual inspection of the bridge. The team would have to include a bridge inspector, an sUAS operator (which may be another inspector), and an observer. The total estimated visual inspection time incurred by this three-people crew is 5.77 hours (i.e., 346 minutes), which is equivalent to 17.3 total man-hours. In addition to reduced personnel and man-hours, the sUAS approach to inspect this bridge will not require any maintenance of traffic (MOT) activities, nor an Inspector 62 vehicle, nor additional vehicles to carry traffic cones; therefore, significant cost savings due to less gasoline usage are expected. More importantly, the sUAS approach for bridge inspection will result in no traffic interruptions due to lane closures, which plays a big role in the quality of life of motorists.

12.3 Equipment Costs

Equipment costs involve three major categories: sUAV platforms, sensors, and batteries. The following sections describe each of these categories.

12.3.1 sUAV Cost

Table 12-3 shows estimated initial costs for sUAV platforms. These aerial platforms were selected based on their intended use. The total estimated initial cost for sUAV platforms is $11,300, which includes an sUAV capable of dual operator control, four small training copters, an sUAV with top-mounted controllable sensors, and a small rugged sUAV.

Table 12-3 Estimated Initial Costs for sUAV Platforms

sUAV	Approx. Size - Diagonal Length (in)	Number of sUAVs Needed	sUAV Purpose	Unit Cost	Total sUAV Cost
Dual-Operator Control Capable	22	1	HML	$3,500	$3,500
Training sUAV	14	4	Training	$700	$2,800
sUAV with Top-Mountable Sensors	24	1	Bridge	$3,500	$3,500
Smaller Rugged sUAV	12	1	Bridge	$1,500	$1,500
				Total =	**$11,300**

12.3.2 Sensor and Gimbal Costs

Table 12-4 shows estimated initial costs for imaging sensors and their associated gimbals to be attached to the sUAV platforms. The total estimated initial cost for sensors and gimbals is $4,000. Included in this cost estimate are an imaging sensor with remote optical zooming capabilities (Sensor 1), an ultra-high-definition video sensor (Sensor 2), and respective stabilizing gimbals to affix and steady the sensors on the appropriate sUAV.

Table 12-4 Estimated Initial Costs for Sensors and Gimbals

Item	Unit Cost	Quantity	Total Cost
Sensor 1	$1,300	1	$1,300
Sensor 2	$500	2	$1,000
Gimbal 1	$1,400	1	$1,400
Gimbal 2	$300	1	$300
		Total =	**$4,000**

12.3.3 BATTERY COSTS

Table 12-5 shows estimated initial costs for batteries. The number of batteries associated with each sUAV platform was determined assuming flight time durations of 20 minutes per battery. A typical training duration is two hours; therefore, six batteries for each of the four training sUAV platforms are needed (i.e., 24 batteries). For bridge inspections, the main sUAV expected to be used is one with top mountable sensors. Table 12-2 shows that the expected number of battery changes to inspect an 820 feet bridge is 13. Using 820 feet as a baseline bridge size, and adding a padding of two extra batteries, the expected number of batteries needed is 15. A smaller rugged sUAS is expected to be used no more than one third of the total time of the sUAV with top mountable sensors; therefore, five batteries were estimated for this type of aerial platform. These estimates do not include charging batteries during the inspection process to eliminate any chance of fire hazard risks. The total estimated cost for battery procurement is $9,100.

Table 12-5 Estimated Initial Costs for Batteries

sUAV	sUAV Purpose	Cost Per Battery	Number of Batteries Needed	Total Battery Cost
Dual-Operator Control Capable	HML	$200	10	$2,000
Training sUAV	Training	$150	24	$3,600
sUAV with Top-Mountable Sensors	Bridge	$200	15	$3,000
Smaller Rugged sUAV	Bridge	$100	5	$500
			Total =	**$9,100**

12.3.4 MAINTENANCE AND REPLACEMENT COSTS

Maintenance of sUAS systems involves the following hardware components: motors, ESCs, propellers, airframe, and batteries. Maintenance and inspection activities, which are described in Chapter 10 ("*Develop Maintenance* Procedures"), are estimated to take an average of 45 minutes per mission.

Replacement costs for motors, ESCs, propellers, and batteries are a function of their estimated operational lifespans. Table 12-6 shows estimated battery replacement costs per hour of use for each sUAS type.

These cost estimates are based assuming an average operational lifespan per battery of 75 hours. Table 12-7 shows estimated maintenance replacement costs for motors, ESCs, and propellers. These cost estimates are based assuming an average operational lifespan of 150 hours for each sUAS component.

Table 12-6 Estimated Battery Replacement Costs per Hour

sUAV	sUAV Purpose	Cost Per Battery	Battery Cost per Hour of Use*
Dual-Operator Control Capable	HML	$200	$2.67
Training sUAV	Training	$150	$2.00
sUAV with Top-Mountable Sensors	Bridge	$200	$2.67
Smaller Rugged sUAV	Bridge	$100	$1.33

*Assuming a LiPo battery rated at 300 charging cycles, the operational lifespan per battery is 75 hours.

Table 12-7 Maintenance Replacement Costs of Key Hardware sUAS Components

sUAS Component	Cost per Component	Cost per Hour of Use**
Motors	$60	$0.40
ESCs	$30	$0.20
Propellers	$15	$0.10

**Assuming an operational lifespan of 150 hours for each component.

12.4 Video Editing Costs

Obtaining still pictures from video data to include in bridge reports often requires the use of video editing software. Video data editing can include sniping video segments, zooming, rotating, color correcting, and blurring of objects or people where necessary. An estimated initial cost to purchase a video editing software package is $250. The video editing process may take up to twice as long as the data gathering time.

12.5 Conclusion

This chapter describes key cost parameters that would need to be considered to estimate the total cost for using sUAS systems during bridge and HML inspections. These parameters include operator, equipment, maintenance, repair, and video editing costs. Preliminary results showed potential cost savings in man-hours by using an sUAS approach to conduct visual bridge inspections instead of using conventional methods. These expected cost savings are mainly a function of reduced number of support staff on-site. It is assumed that cost savings from one or two inspections using an sUAS approach will cover initial equipment costs. Additional work is recommended to conduct detailed cost analyses that include, among other parameters, the following:

- Average total inspection time from using an sUAS approach to inspect a set of bridges
- Accurate cost savings related to reduced number of on-site support staff and equipment
- Cost savings related to reduced MOT activities, including safety factors

CHAPTER 13

CONCLUSIONS AND FUTURE RESEARCH

The main objective of this research effort was to conduct a proof-of-concept initial study to develop an understanding of the expected usefulness of sUAV systems for bridge and HML inspections. To this end, a literature review effort was conducted to gain insights into UAV platforms for structural inspections, UAV aircraft control, and different camera configurations. This effort resulted in the following key findings:

- The majority of studies related to understanding the capabilities and feasibility of using UAV systems for transportation systems are in the area of traffic monitoring.
- Studies that involve UAVs for the specific purpose of bridge inspections are very scarce, and for inspection of HML are nonexistent.
- A common issue for using UAV systems in transportation applications was the ability to control the aerial vehicles, particularly in wind speeds higher than 15mph.
- The process of obtaining FAA approval to fly UAVs in transited areas has been a major issue identified by various studies.
- Wireless connectivity and maneuverability are arguably the most significant parameters that make UAVs more useful than other existing methods.
- There is high potential for cost savings in using effective image post-processing algorithms for defect detection and classification.

After completion of the literature review task, weighted factor analyses were employed to select the UAS components needed based on the research objectives. Criteria for selecting each component were established by the research team based on information from various sources (i.e., input information from FAA certified pilots, FDOT's bridge inspectors, and a literature review effort). From the analyses, the final selection of UAS components included a multi-rotor aircraft (based on stability, high level of maneuverability, upgradability, and minimal training time), a GoPro HERO 3 Black edition camera, and a Windows-based tablet PC.

Indoor controlled experiments were conducted to evaluate UAV flight response in various controlled wind conditions, to measure image quality in different flight scenarios, and to determine image quality in low-light conditions. The objective was to define parameters and identify limitations that could help to increase the chance that images captured will serve their intended purpose. Results from these experiments provided evidence that support the potential ability to fly UAVs in high pressure zones, maintain safe flying proximity of 2-3 feet to a target, and the ability to detect crack sizes down to 0.02 inches. These findings, coupled with the ability to maintain adequate resolution under relatively low-light conditions, highlighted the high potential to use UAV systems to assist bridge and HML inspectors during field inspections.

Maintenance procedures and service schedules for key individual sUAV components were also part of this effort. These components include motors, ESCs, propellers, airframe structure, and batteries. Maintenance procedures include pre/post-flight inspection activities, and in some cases, inspection activities that are recommended for every 25 hours of sUAV operation.

Altitude, payload, and maneuverability tests were conducted using quad and hexa-copters to understand performance and limitation parameters that would directly relate to the use of UAVs for transportation infrastructure inspections. Altitude testing results showed that FPV systems provide a pilot the capability to easily detect sUAV orientation up to at least 400ft vertically and 1,500ft horizontally. These tests also showed that the maximum vertical distance to reliably detect sUAV orientation is significantly limited (250ft for the hexa-copter) if relying only on the UAVs' LED lights. Payload testing results showed that carbon fiber propellers can increase flight time by 10 percent. These tests also resulted in a table that shows maximum flight times as a function of battery type, battery configuration, and payload weight. Maneuverability testing results showed that the hexa-copter could be properly operated by a skilled operator at a minimum clearance of 3ft from a target and with constant wind speeds of 15mph. These tests also showed the minimum dimensions required to properly fly the hexa and quad-copters through tight areas, such as in-between girders from a bridge's superstructure that supports the bridge's deck.

In full coordination with FDOT, field tests were conducted to collect image data of HML structures and underside sections of bridges using small aerial systems equipped with high-definition imaging sensors. During field tests, data collection was restricted to only underside bridge images (i.e., bays) from a single bridge section. Visual assessments of collected data (i.e., image and videos) by the research team and FDOT inspectors showed the potential benefits from using sUAV systems for structural inspection purposes. Images collected during field tests were of similar or better quality than those collected by FDOT inspectors during previous inspections.

This research effort also resulted in the development of a basic sUAV flight program to train inspectors in basic theory, operations, and maneuverability of sUAV systems. The results from this training program were used to estimate the time that it would take inspectors to safely operate sUAV systems in open space. Using a basic level sUAV with stabilization software for training purposes proved to be a useful tool in the introduction to UAV flight. However, it is important to note that ongoing training is needed to retain and improve the skills necessary to perform objective-based maneuvers. Furthermore, once proficiency and mastery of the basic level sUAV is achieved, inspectors should be trained to operate more complex and customized copters that provide better flight performances. These customized sUAV systems are often capable of holding various types of special sensors, which may be needed during special bridge or HML inspections. Due to the small sample size of the testers, only general conclusions can be made regarding training time estimates.

This research work described key cost parameters that would need to be considered to estimate the total cost for using sUAS systems during bridge and HML inspections. These parameters include operator, equipment, maintenance, repair, and video editing costs. Preliminary results showed potential cost savings in man-hours by using an sUAS approach to conduct visual bridge inspections instead of using conventional methods. These expected cost savings are mainly a function of reduced number of support staff on-site. It is assumed that cost savings from one or two inspections using an sUAS approach will cover initial equipment costs.

13.1 FUTURE RESEARCH NEEDED

Overall, the results obtained from this proof-of-concept research effort provide evidence that significant benefits can be obtained from the use of UAVs to assist in bridge and HML inspections. However, *there still exist gaps that need to be addressed in order to use these aerial systems safely and effectively in practice*. For example, "flyaway" is a serious problem that causes aerial devices to go rogue and fly off from their users [57]. Flyaways occur when a flight controller malfunctions, resulting in erratic sUAV behavior. Although major companies have claimed that this type of problem has been corrected, it should not have happened in the first place. Therefore, research is needed to overcome problems such as flyaways to significantly reduce mission failure risks and ensure public safety. One potential solution would be to develop safety-critical aerial systems for mission-specific applications. A safety-critical system is one whose “failure could result in loss of life, significant property damage, or damage to the environment” [58]; therefore, these systems are developed using robust systems engineering processes to eliminate risks. Table 13-1 presents areas for future research. In particular, it is highly recommended to conduct further field tests with in-house developed aerial systems to establish more accurate estimations regarding the cost and duration of complete inspections, and develop effective mission-specific training programs. These proposed future research areas would significantly increase the general understanding of sUAS capabilities and benefits from using them as tools during structural inspections, ultimately converting into reality the vision of using these complex systems for structural inspections.

Table 13-1 Future Research Areas

No.	Category	Description
1	Field Tests	Conduct field tests to: • Understand UAV capabilities (and overall mission dynamics) when using them to collect image/video data of entire bridge spans • Develop more accurate estimations regarding the duration of complete inspections using an sUAS
2	Cost Estimation	Develop detailed cost analyses that include, among other parameters: • Average total inspection time from using an sUAS approach to inspect a set of bridges • Accurate cost savings related to reduced number of on-site support staff and equipment • Cost savings related to reduced MOT activities, including safety factors
3	sUAV Training	• Develop mission-specific training programs • Conduct mission-specific training sessions to collect and analyze data for accurate estimation of training times
4	sUAV Technology	• Develop safety-critical sUAV systems to ensure that flight areas are restricted to predetermined boundaries (i.e., elevation and coverage areas) • Develop more effective approaches to UAV control and navigation
5	Remote Sensing	Conduct research to understand the capabilities of other sensors, mounted on small UAV systems, for structural inspection purposes (e.g., LiDAR, hyperspectral, thermal)
6	Information System	Design and develop an information system to: • Provide a user-friendly interface that allows inspectors to, among other things, zoom into areas of interest within a video, annotate them, and store them for future use • Develop digital libraries that can eventually be used for post analyses

REFERENCES

[1] A. S. of C. Engineers, "2013 Report card for America's infrastructure," 2013. .

[2] S. Chase and M. Edwards, "Developing a Tele-Robotic Platform for Bridge Inspection," 2011.

[3] Y. Dong, R. Song, and H. Liu, "Bridges Structural Health Monitoring and Deterioration Detection-Synthesis of Knowledge and Technology," Citeseer, 2010.

[4] M. C. Isola and R. L. McCrum, "Inspection and Repair of High-Mast Luminaires (HML)," 1996.

[5] P. (NYDOT) Weykamp, "Best Practices in Bridge Management Decision-Making," New York, 2010.

[6] B. Kitchenham, "Procedures for Performing Systematic Reviews," 2004.

[7] P. S. Moller, "CALTRANS Bridge Inspection Aerial Robot," 2008.

[8] S. L. Barfuss, A. Jensen, and S. Clemens, "EVALUATION AND DEVELOPMENT OF (UAV) FOR UDOT NEEDS Prepared For : Utah Department of Transportation Submitted By : Authored By :," 2012.

[9] W. S. Hart and N. G. Gharaibeh, "Use of Micro Unmanned Aerial Vehicles for Roadside Condition Assessment," Southwest Region University Transportation Center, Texas Transportation Institute, Texas A & M University System, 2010.

[10] E. D. McCormack and T. Trepanier, "The Use of Small Unmanned Aircraft by the Washington State Department of Transportation," Washington State Department of Transportation, 2008.

[11] B. Coifman, M. McCord, M. Mishalani, and K. Redmill, "Surface Transportation Surveillance from Unmanned Aerial Vehicles," in *Proc. of the 83rd Annual Meeting of the Transportation Research Board*, 2004.

[12] P. Farradine, "Use of Unmanned Aerial Vehicles in Traffic Surveillance and Traffic Management," Technical Memorandum Prepared for: Florida Department of Transportation, 2005.

[13] K. Ro, J.-S. Oh, and L. Dong, "Lessons Learned: Application of Small uav for Urban Highway Traffic Monitoring," in *45th AIAA Aerospace Sciences Meeting and Exhibit*, 2007, pp. 2007–2596.

[14] K. Kanistras, G. Martins, M. J. Rutherford, and K. P. Valavanis, "Survey of Unmanned Aerial Vehicles (UAVs) for Traffic Monitoring," in *Handbook of Unmanned Aerial Vehicles*, Springer, 2014, pp. 2643–2666.

[15] A. Puri, K. P. Valavanis, and M. Kontitsis, "Statistical Profile Generation for Traffic Monitoring using Real-Time UAV Based Video Data," in *Control & Automation, 2007. MED'07. Mediterranean Conference on*, 2007, pp. 1–6.

[16] F. Heintz, P. Rudol, and P. Doherty, "From Images to Traffic Behavior - A Uav Tracking and Monitoring Application," in *Information Fusion, 2007 10th International Conference on*, 2007, pp. 1–8.

[17] P. Cheng, G. Zhou, and Z. Zheng, "Detecting and Counting Vehicles from Small Low-Cost UAV Images," in *ASPRS 2009 Annual Conference, Baltimore*, 2009, vol. 3, pp. 9–13.

[18] Z. Yin, "A Quadcopter with Heterogeneous Sensors for Autonomous Bridge Inspections," 2014.

[19] Z. Yin, "Develop a UAV Platform for Automated Bridge Inspection." 2013.

[20] C. Brooks, "Evaluating the Use of Unmanned Aerial Vehicles for Transportation Purposes (Michigan DOT)," 2013.

[21] S. Siskowski and T. Frierson, "Use of Unmanned Aerial Vehicles for AHTD Application." 2012.

[22] N. Metni and T. Hamel, "A UAV for Bridge Inspection: Visual Servoing Control Law with Orientation Limits," *Autom. Constr.*, vol. 17, no. 1, pp. 3–10, 2007.

[23] S. Rathinam, P. Almeida, Z. Kim, S. Jackson, A. Tinka, W. Grossman, and R. Sengupta, "Autonomous searching and tracking of a river using an UAV," in *American Control Conference, 2007. ACC'07*, 2007, pp. 359–364.

[24] P. E. I. Pounds, D. R. Bersak, and A. M. Dollar, "Stability of Small-Scale UAV Helicopters and Quadrotors with Added Payload Mass under PID Control," *Auton. Robots*, vol. 33, no. 1–2, pp. 129–142, 2012.

[25] J. J. G. Ramos, S. M. Maeta, L. G. B. Mirisola, S. S. Bueno, M. Bergerman, B. G. Faria, G. E. M. Pinto, and A. H. Bruciapaglia, "Internet-Based Solutions in the Development and Operation of an Unmanned Robotic Airship," in *Proceedings of the IEEE*, 2003, vol. 91, no. 3, pp. 463–474.

[26] R. R. Nidamanuri and B. Zbell, "Use of FieldRreflectance Data for Crop Mapping Using Airborne Hyperspectral Image," *ISPRS J. Photogramm. Remote Sens.*, vol. 66, no. 5, pp. 683–691, 2011.

[27] J. E. Krajewski, "Bridge Inspection and Interferometry (Worchester Polytechnic Institute)," Worcester Polytechnic Institute., 2006.

[28] (GPO) Government Publishing Office, "Electronic Code of Federal Regulations (eCFR) - Title 14 Part 1," 2015. [Online]. Available: http://www.ecfr.gov/cgi-bin/text-idx?rgn=div8&node=14:1.0.1.1.1.0.1.1.

[29] (FAA) Federal Aviation Administration, "Special Operations - FAA JO 7610.4," 2014. [Online]. Available: http://www.faa.gov/air_traffic/publications/spec_ops/.

[30] K. D. Davis, "Interim Operational Approval Guidance 08-01 - Unmanned Aircraft Systems Operations in the US National Airspace System," 2008.

[31] K. D. Sabatini, "Federal Registry FAA-2006-27614."

[32] F. P. Paskiewicz, "Airworthiness Certification of Unmanned Aircraft Systems - FAA Order 8130.34."

[33] A. R. (FAA) Foxx, "Operation and Certification of Small Unmanned Aircraft Systems - Notice of proposed rulemaking (NPRM)," 2015.

[34] (FAA) Federal Aviation Administration, "Aircraft Registry - Register an Aircraft," 2013. [Online]. Available: https://www.faa.gov/licenses_certificates/aircraft_certification/aircraft_registry/register_aircraft/.

[35] (FAA) Federal Aviation Administration, "Public Operations," 2015. .

[36] (FAA) Federal Aviation Administration, "Online COA Application System," 2015. [Online]. Available: https://ioeaaa.faa.gov/oeaaa/Welcome.jsp.

[37] (FAA) Federal Aviation Administration, "Sample COA Application," 2008. [Online]. Available: https://www.faa.gov/about/office_org/headquarters_offices/ato/service_units/systemops/aaim/organizations/uas/media/COA Sample Application v 1-1.pdf.

[38] (FAA) Federal Aviation Administration, "Freedom of Information Act Responses," 2015. [Online]. Available: http://www.faa.gov/uas/public_operations/foia_responses/.

[39] (FAA) Federal Aviation Administration, "Section 333," 2015. [Online]. Available: https://www.faa.gov/uas/legislative_programs/section_333/.

[40] J. L. Mica, "H.R.658 - FAA Modernization and Reform Act of 2012," 2012. [Online]. Available: https://www.congress.gov/bill/112th-congress/house-bill/658.

[41] (FAA) Federal Aviation Administration, "Petitioning for Exemption under Section 333," 2015. [Online]. Available: https://www.faa.gov/uas/legislative_programs/section_333/how_to_file_a_petition/.

[42] (FAA) Federal Aviation Administration, "Guidelines for Submitting a Petition for Exemption," 2015.

[43] (FAA) Federal Aviation Administration, "How to Send Your Petition for Exemption or Rulemaking," 2015. [Online]. Available: https://www.faa.gov/uas/legislative_programs/section_333/how_to_file_a_petition/media/How_to_Send_Your_Petition_for_Exemption_or_Rulemaking.pdf.

[44] (FAA) Federal Aviation Administration, "Section 333 Public Guidance," 2015. [Online]. Available: https://www.faa.gov/uas/legislative_programs/section_333/how_to_file_a_petition/media/section333_public_guidance.pdf.

[45] (GPO) Government Publishing Office, "Electronic Code of Federal Regulations Title 14 Chapter 1 Subchapter D," 2015. [Online]. Available: http://www.ecfr.gov/cgi-bin/text-idx?SID=f7e44c14be30648081e08ff2535a25ae&tpl=/ecfrbrowse/Title14/14cfrv2_02.tpl#0.

[46] (GPO) Government Publishing Office, “Title 14 Aeronautics and Space,” 2015. [Online]. Available: http://www.ecfr.gov/cgi-bin/text-idx?SID=f7e44c14be30648081e08ff2535a25ae&tpl=/ecfrbrowse/Title14/14tab_02.tpl.

[47] (FAA) Federal Aviation Administration, “FAA-8083-30 Chapter 12,” 2015. [Online]. Available: https://www.faa.gov/regulations_policies/handbooks_manuals/aircraft/amt_handbook/media/FAA-8083-30_Ch12.pdf.

[48] (FAA) Federal Aviation Administration, “sUAS Summary,” 2015. [Online]. Available: http://www.faa.gov/regulations_policies/rulemaking/media/021515_suas_summary.pdf.

[49] (FAA) Federal Aviation Administration, “Operation and Certification of Small Unmanned Aircraft Systems (sUAS),” 2015. [Online]. Available: https://www.federalregister.gov/articles/2015/02/23/2015-03544/operation-and-certification-of-small-unmanned-aircraft-systems.

[50] F. Senate, “The 2014 Florida Statutes,” 2014. [Online]. Available: http://www.leg.state.fl.us/Statutes/index.cfm?App_mode=Display_Statute&Search_String=&URL=0300-0399/0379/Sections/0379.411.html.

[51] FWC, “Threatened Endangered Species,” 2013. [Online]. Available: http://myfwc.com/media/1515251/threatened_endangered_species.pdf.

[52] N. T. S. Board, “Collapse of I-35W Highway Bridge Minneapolis, Minnesota,” *National Transportation Safety Board: Washington DC*, 2008. [Online]. Available: http://www.ntsb.gov/news/events/Pages/Collapse_of_I-35W_Highway_Bridge_Minneapolis_Minnesota_August_1_2007.aspx.

[53] K. W. Gee, “Inspection of Gusset Plates Using Non-Destructive Evaluation Technologies,” Federal Highway Administration (FHWA), 2010.

[54] (AOPA) Aircraft Owners and Pilots Association, “Let’s Go Flying: Career Options,” 2014. [Online]. Available: http://www.aopa.org/letsgoflying/dream/whyfly/careers.html.

[55] (AOPA) Aircraft Owners and Pilots Association, “Let’s Go Flying: Pilot Certificate Options and Timeline,” 2014. [Online]. Available: http://www.aopa.org/letsgoflying/ready/time/options.html.

[56] “UAV Pilot Training Certificate - Unmanned Vehicle University,” 2015. [Online]. Available: http://www.uxvuniversity.com/uav-pilot-training-certificate/.

[57] J. Nicas, “What Happens When Your Drone Escapes,” 2014. [Online]. Available: http://www.wsj.com/articles/what-happens-when-your-drone-escapes-1418086281.

[58] J. C. Knight, “Safety critical systems: challenges and directions,” in *Software Engineering, 2002. ICSE 2002. Proceedings of the 24rd International Conference on*, 2002, pp. 547–550.

Appendix A SNAPSHOTS OF WEATHERING STEEL HML


(a)


(b)

Figure A - 1 Zoomed-in Potential Crack (a) Bottom (b) Top

(a)


(b)

Figure A - 2 SJ 1 (a) South Face (b) West Face

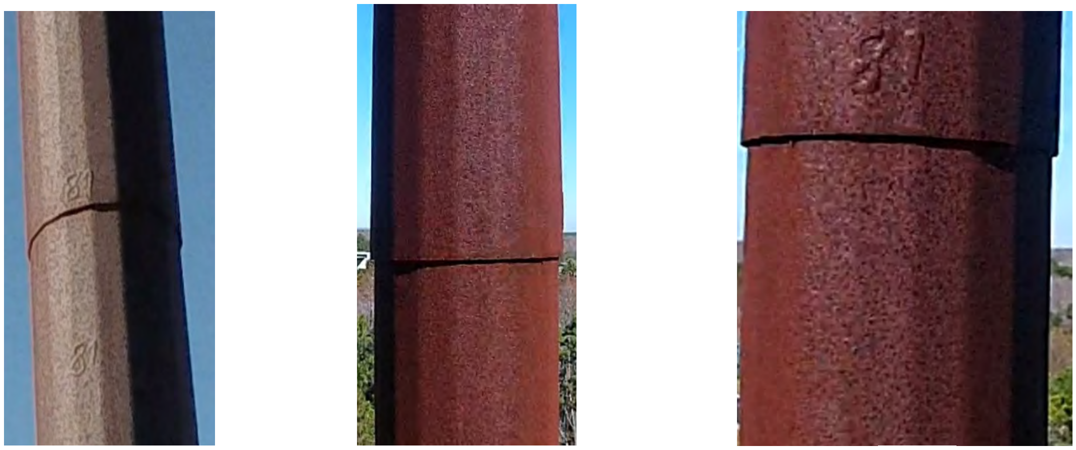

(a) (b) (c)

Figure A - 3 (a) SJ 2 South Face (b) SJ 3 West Face (c) SJ 3 South Face

(a) (b)

Figure A - 4 Light Structure (a) South Face (b) East Face

(a) (b)

Figure A - 5 Light Structure (a) North Face (b) West Face

Figure A - 6 Light Structure South-West Face

Appendix B SNAPSHOTS OF GALVANIZED PIVOT MOUNT HML

(a) (b) (c)

Figure B - 1 (a) Back (b) Bottom and (c) Top View of East Light Fixture

(a) (b) (c)

Figure B - 2 (a) Back (b) Bottom and (c) Top View of North Light Fixture

(a) (b) (c)

Figure B - 3 (a) Back (b) Bottom and (c) Top View of South Light Fixture

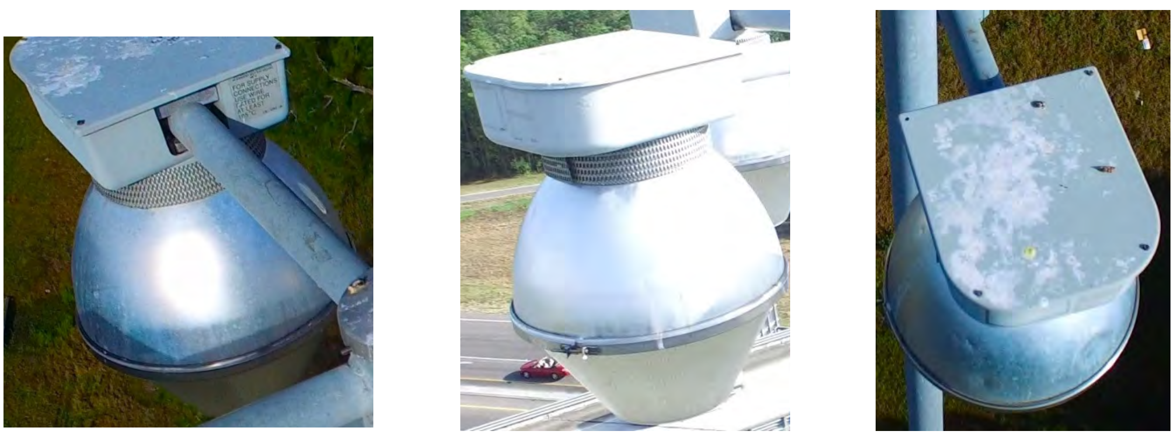

(a) (b) (c)

Figure B - 4 (a) Back (b) Bottom and (c) Top View of West Light Fixture

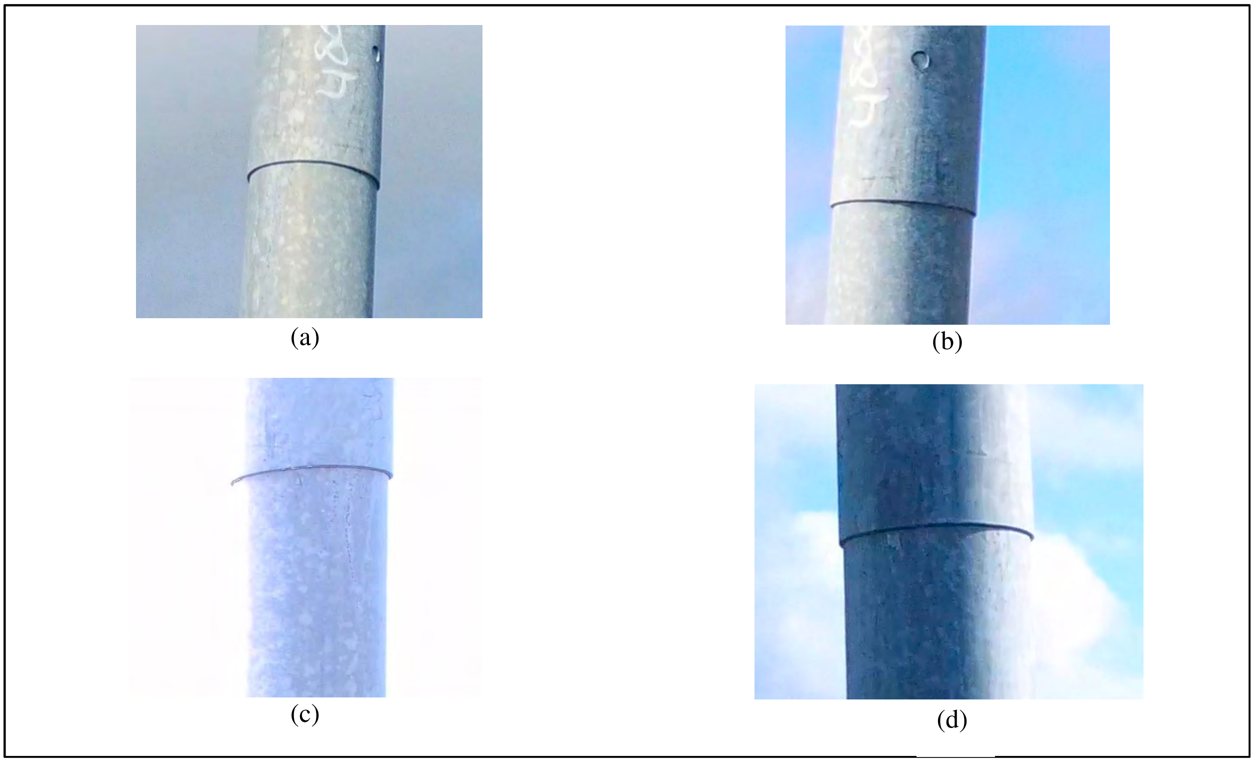

Figure B - 5 (a) East (b) North (c) South, and (d) West Face of SJ3

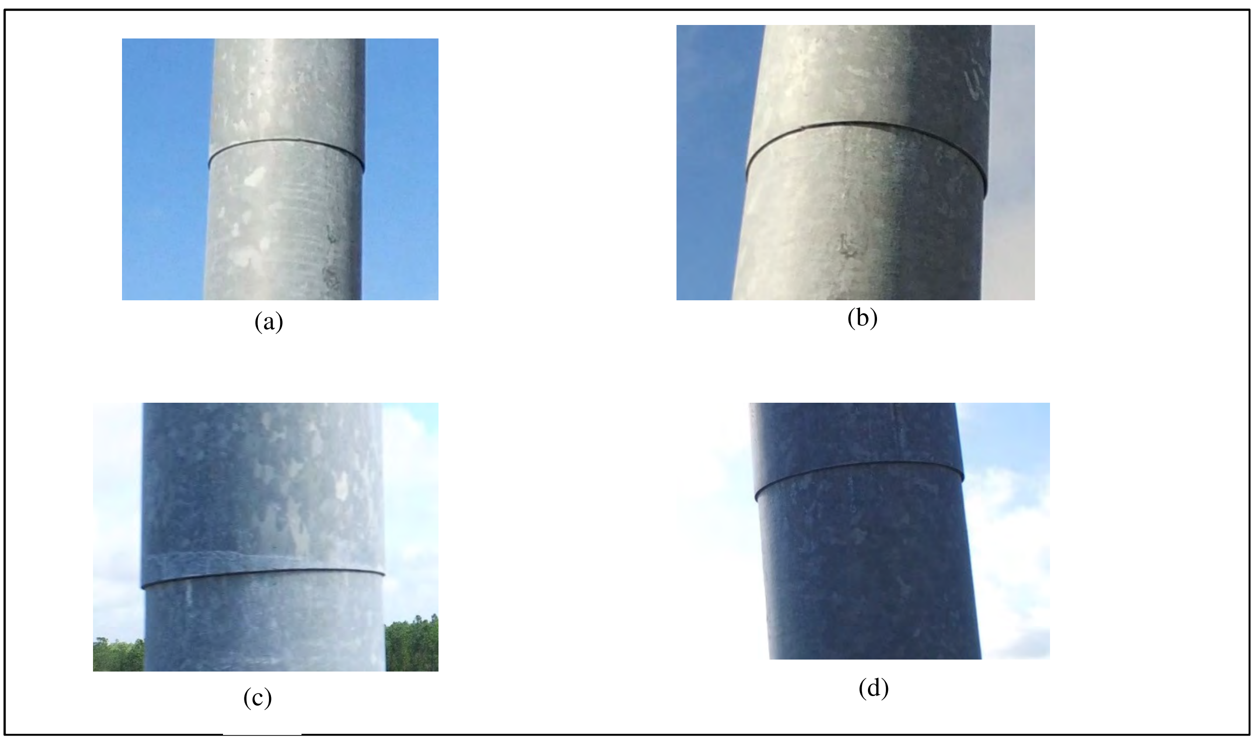

Figure B - 6 (a) East (b) North (c) South, and (d) West Face of SJ2

Appendix C SNAPSHOTS FROM STEEL RAILWAY DRAWBRIDGE

The photos in this appendix are labeled according to their relative position of the bridge components in order from south to north. Gusset plates throughout the bridge are listed as follows:

- 'T' for *top-side of the bridge*
- 'U' for *upper portion of the main diagonal members*
- 'C' for *top-center on the X-bracing on the top of the bridge*
- 'MRC' for *moment resisting connection splices*

An 'E' indicates an image corresponding to the east portion of the bridge. In instances where more than one image was collected of a particular gusset plate, a number in parenthesis '(#)' is used to identify the particular image capture.

Figure C - 1 T1C

Figure C - 2 T2C

Figure C - 3 T3C

Figure C - 4 T1E

Figure C - 5 T2

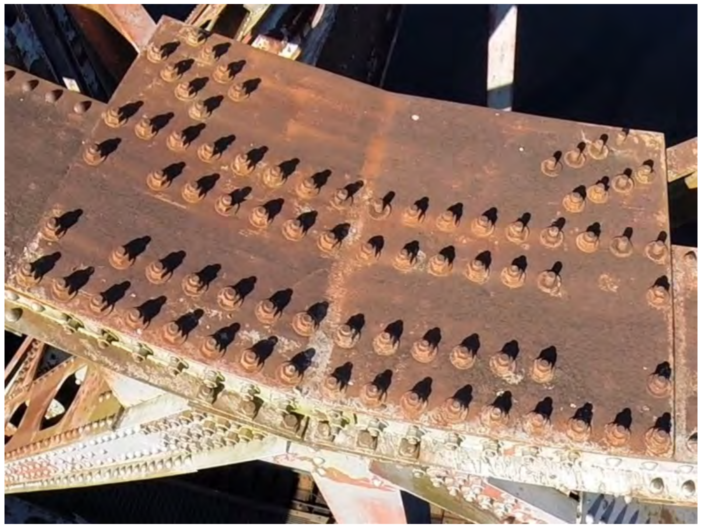

Figure C - 6 T3E

Figure C - 7 T3E (2)

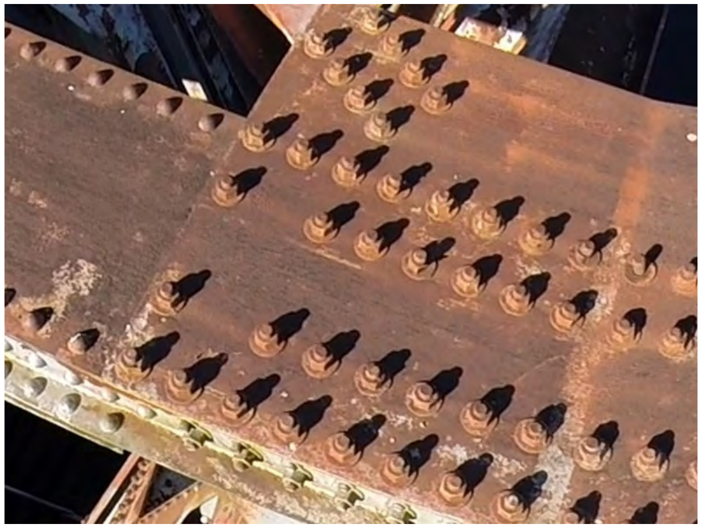

Figure C - 8 T3E (3)

Figure C - 9 T3E (4)

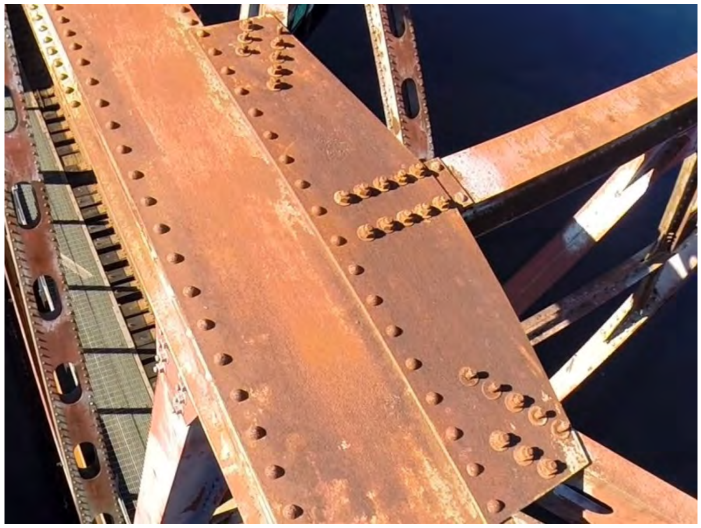

Figure C - 10 T4E

Figure C - 11 T4E (2)

Figure C - 12 T4E (3)

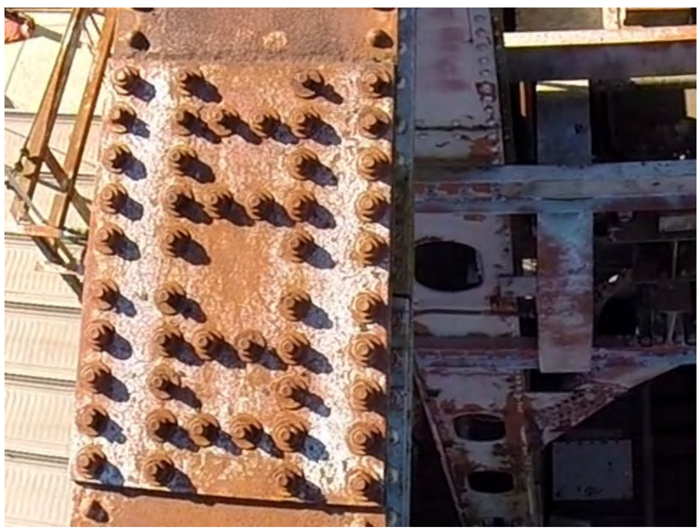

Figure C - 13 TMRC1E

Figure C - 14 UMRC1E

Figure C - 15 U1E

Figure C - 16 U1E (2)

Figure C - 17 U1E (3)

Figure C - 18 U2E

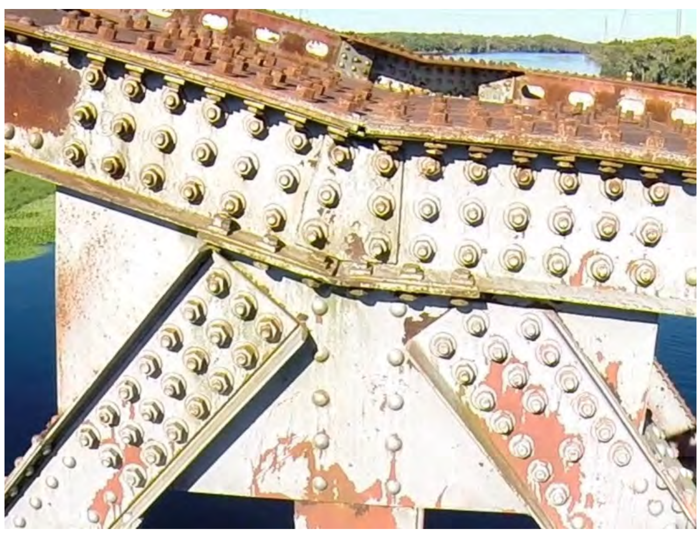

Figure C - 19 U2E (2)

Figure C - 20 U3E

Figure C - 21 U4E

Figure C - 22 U4E (2)

Appendix D TRAINING FLIGHT GUIDES

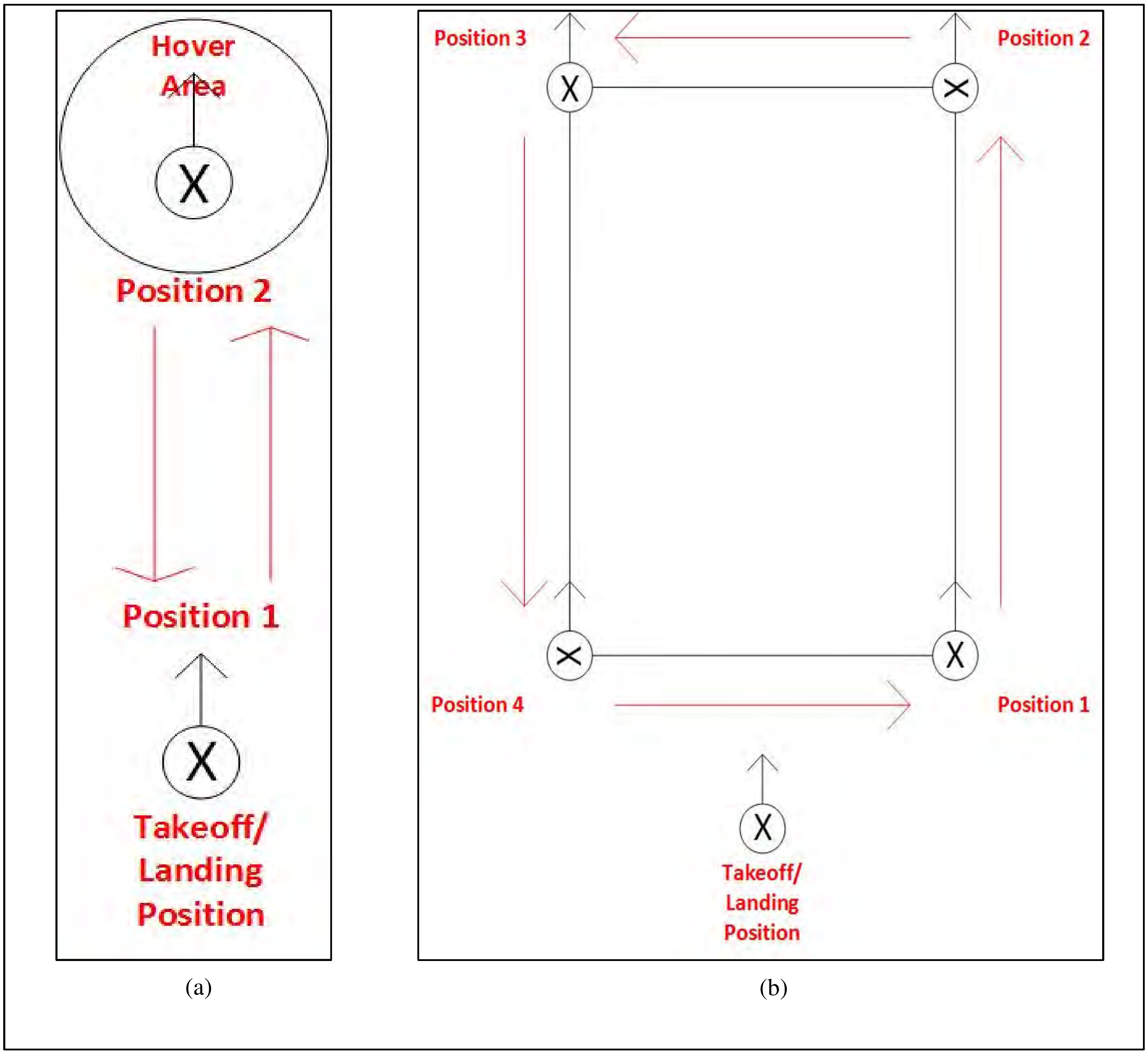

Figure D - 1 (a) Phase 1 Module 1 (b) Phase 2 Module 1

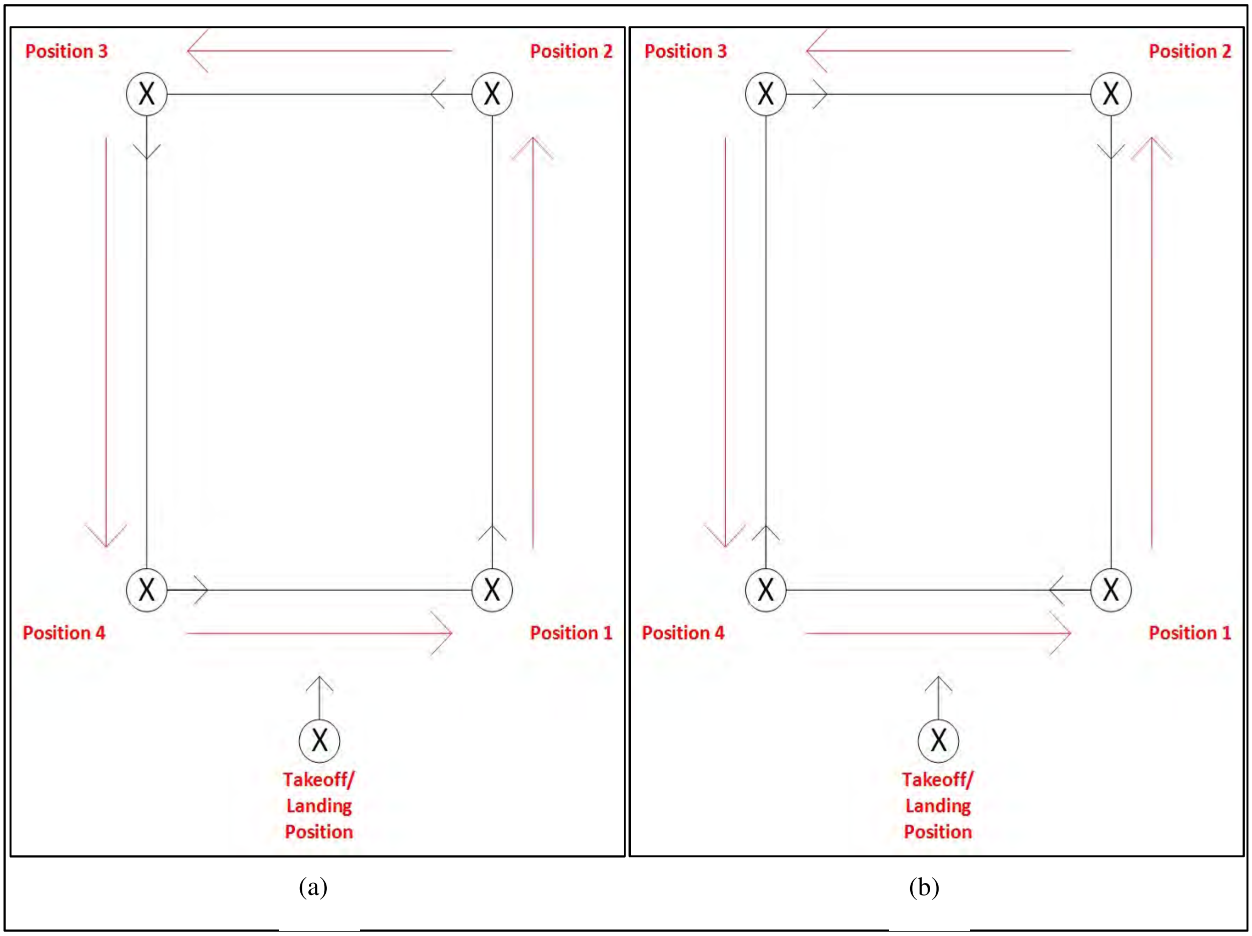

Figure D - 2 (a) Phase 2 Module 2 (b) Phase 2 Module 3

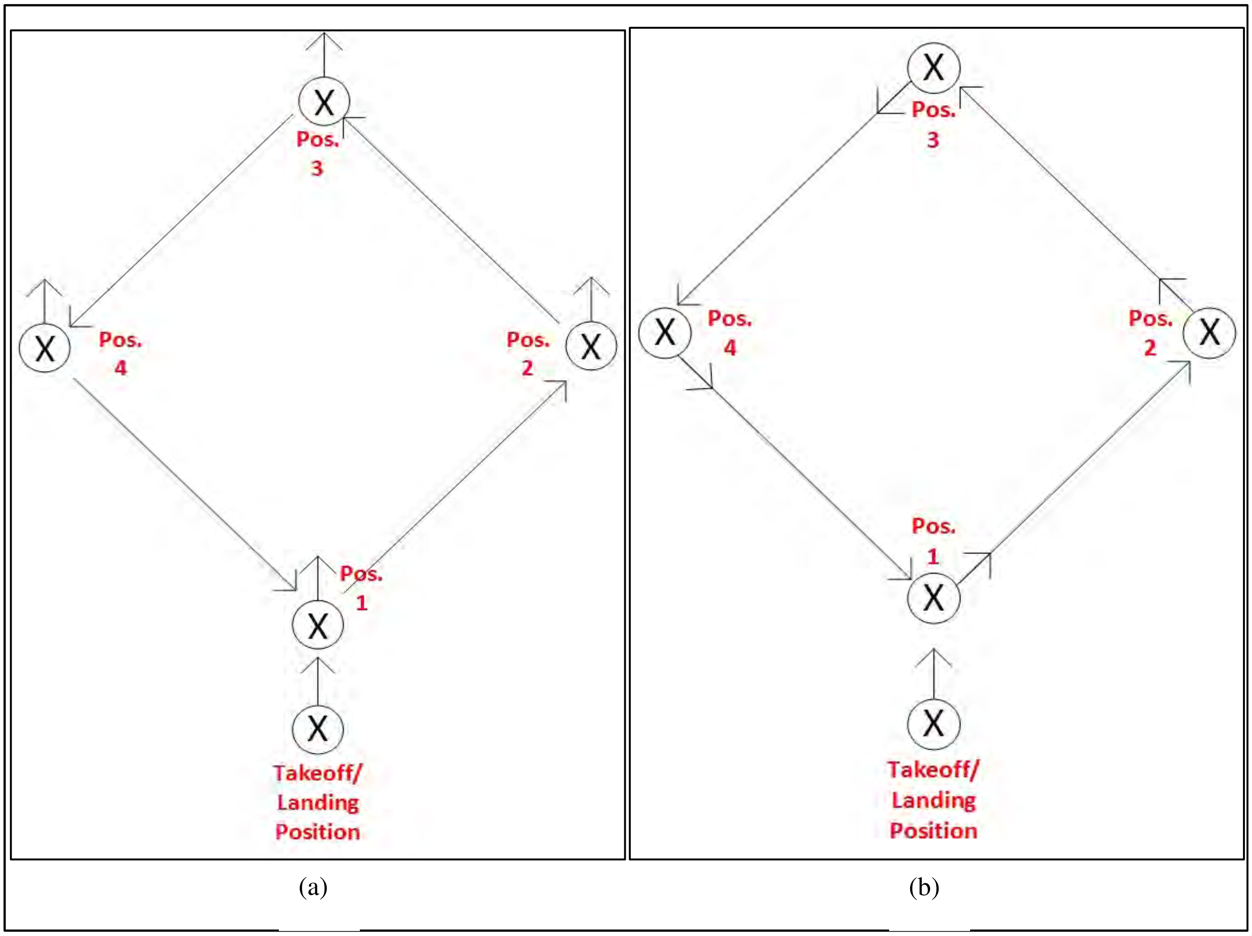

Figure D - 3 (a) Phase 3 Module 1 (b) Phase 3 Module 2

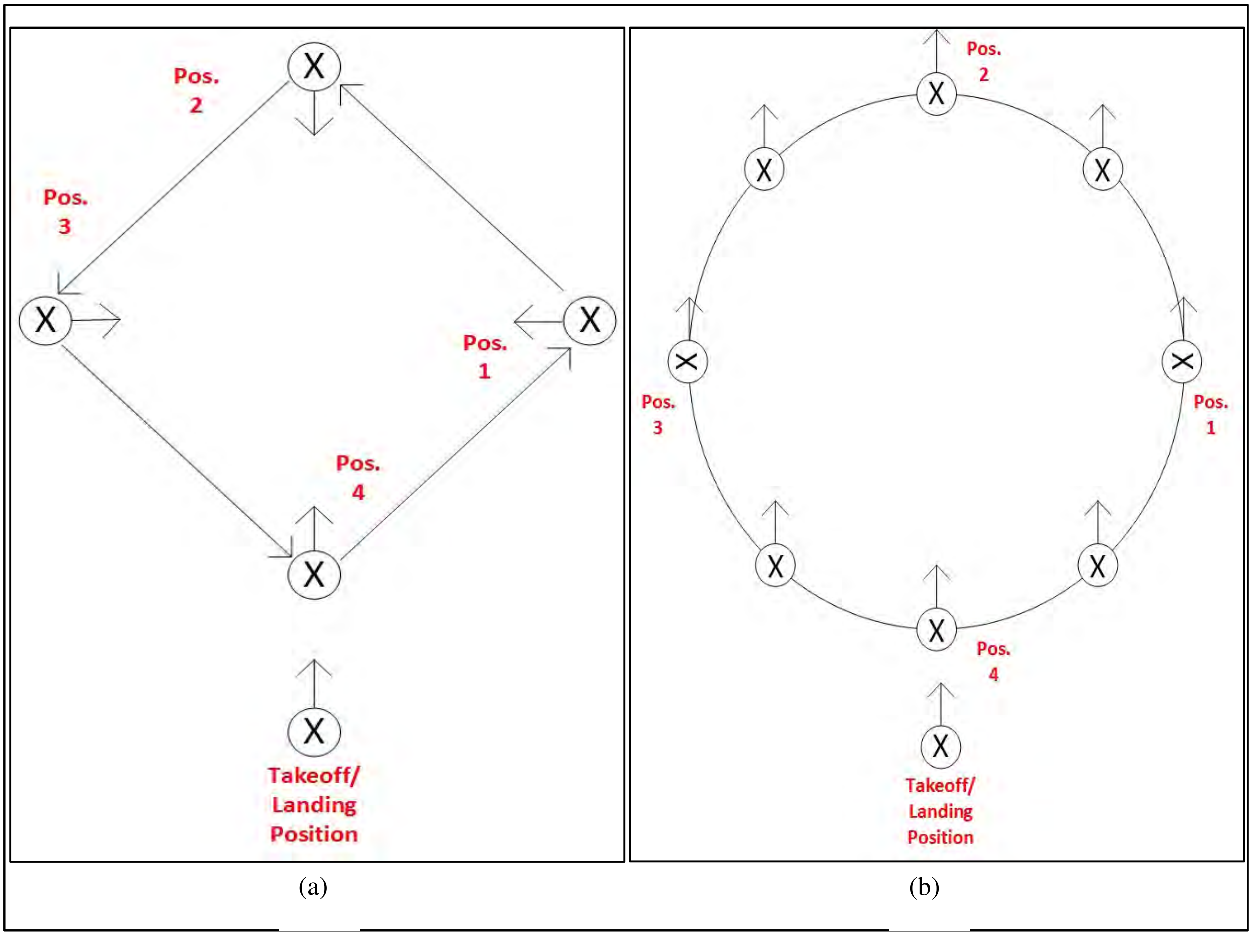

Figure D - 4 (a) Phase 3 Module 3 (b) Phase 4 Module 1

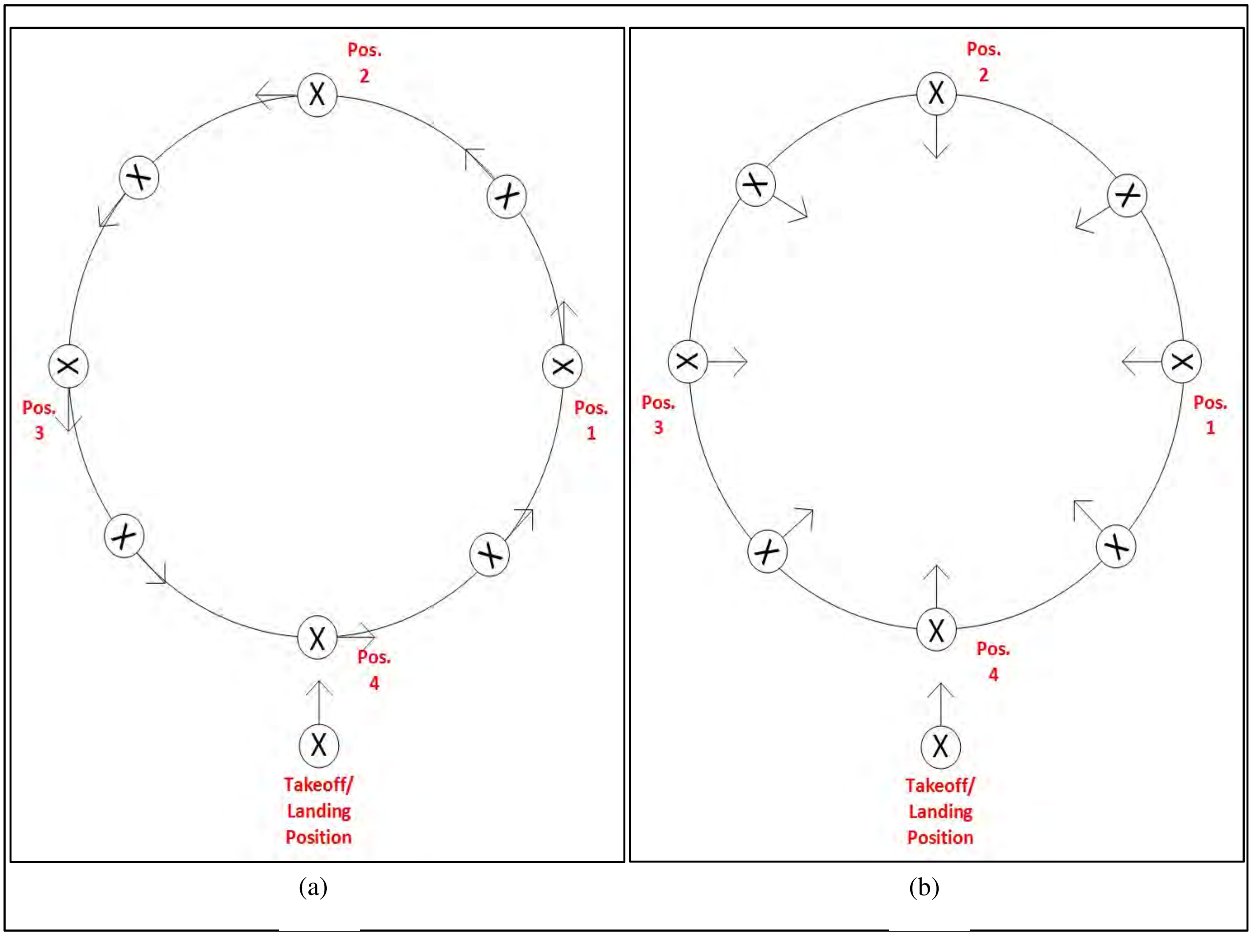

Figure D - 5 (a) Phase 4 Module 2 (b) Phase 4 Module 3